

**Qianjiangping Landslide near Three Gorges
Reservoir: Coupled analysis of Seepage and Slope
stability**

by

PAK KAM IN

Final Year Project Report submitted in partial fulfillment
of the requirement of the Degree of

Bachelor of Science in Civil Engineering

2020/2021



**Faculty of Science and Technology
University of Macau**

DECLARATION

I declare that the project report here submitted is original except for the source materials explicitly acknowledged and that this report as a whole, or any part of this report has not been previously and concurrently submitted for any other degree or award at the University of Macau or other institutions.

I also acknowledge that I am aware of the Rules on Handling Student Academic Dishonesty and the Regulations of the Student Discipline of the University of Macau.

Signature : PAK KAM IN

Name : PAK KAM IN

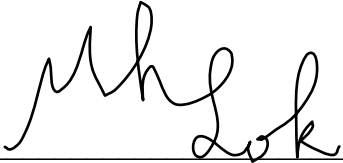
Student ID : DB725088

Date : 28/05/2021

APPROVAL FOR SUBMISSION

This project report entitled “**Qianjiangping Landslide near Three Gorges Reservoir: Coupled analysis of Seepage and Slope stability**” was prepared by PAK KAM IN in partial fulfillment of the requirements for the degree of Bachelor of Science in Civil Engineering at the University of Macau.

Endorsed by,

Signature : _____

Supervisor : Prof. Lok Man Hoi

ACKNOWLEDGEMENTS

First of all, I would like to thank Prof. Lok Man Hoi, my supervisor. Thank you for your tireless teachings during the four years of university study. The suggestions you gave played a key role in the completion of this report. Without your firm support, I could not have overcome the difficulties throughout the whole process and this report could never have reached its present form.

Also, I would like to thank Marc from the GEOSLOPE support team. Because I encountered some difficulties when I started running the program, it was with the assistance of Marc that I could get these analysis results.

Finally, I sincerely thank my family and fiancée for supporting, encouraging in life. Thank you for giving me confidence and encouragement throughout these years.

ABSTRACT

The Qianjiangping landslide occurred on July 14, 2003, near the Three Gorges Reservoir in China. The accident was a large planar rockslide. In order to deeply understand the mechanism and failure process of the landslide, Geo-Studio software was used to simulate and analyze the accident site. The results show that the landslide was caused by the rise of the water level and continuous rainfall. By adding several monitoring points, it was found that the change of pore water pressure in different positions of the slope will be different. The change of water level has a more obvious effect on the pore water pressure at the bottom of the slope while rainfall has a greater impact on the change of pore water on the slope surface. In addition, the results show the impact of rainfall on slope stability is not immediate, because it takes some time for infiltration water to transfer to the bottom of the slope.

For soil slope, the influence of different rainfall patterns on slope stability was different. Therefore, the effects of four rainfall patterns (delayed, uniform, normal and advanced) and different rainfall intensities on slope stability are analyzed. The results show that under the influence of an "advanced" rainfall pattern, the cumulative rainfall rate was the fastest. Therefore, the factor of safety of slope decreases the fastest. The cumulative rainfall rate of "normal" and "uniform" patterns was slightly slower than that of advanced patterns, so the time of slope landslide was also slightly later. The accumulated rainfall of the "delayed" pattern was the slowest among the four, and the occurrence time of landslide was also the latest. Finally, by increasing the rainfall intensity, it is found that the rainfall intensity has an important impact on the slope stability, and the total rainfall is proportional to the pore water pressure.

TABLE OF CONTENTS

DECLARATION	I
APPROVAL FOR SUBMISSION	II
ACKNOWLEDGEMENTS	III
ABSTRACT	IV
TABLE OF CONTENTS	V
LIST OF FIGURES	VIII
LIST OF TABLES	XI
CHAPTER 1 INTRODUCTION	1
1.1 Background	1
1.2 Qianjiangping landslide	2
1.3 Research object and purpose	3
1.4 Outline of the Study	4
CHAPTER 2 LITERATURE REVIEW	5
2.1 Rainfall-induced slope failures	5
2.1.1 Mechanisms of rainfall-induced slope failures	5
2.1.2 Slope stability analysis	6
2.1.2.1 Limit equilibrium analysis	6
2.1.2.2 Coupled hydro-mechanical analysis	7
2.1.3 SLOPE/W program	8
2.1.4 Rainfall infiltration analysis	9
2.1.5 SEEP/W program	9
2.2 Types of rainfall patterns	10
2.3 Study on unsaturated soil	11
2.3.1 Properties of unsaturated soil	11
2.3.2 Effect of unsaturated soil mechanics in slope stabilization	12

2.3.3 Introduction of soil-water characteristic curve (SWCC)	13
2.4 Factors causing the landslide in Qianjiangping	15
2.4.1 The structural problems of the slope	15
2.4.2 Previous rupture surface	17
2.4.3 Rising water level and continuous rainfall	17
2.5 Case study on the Qingning landslide	18
2.5.1 Background	18
2.5.2 Investigation	19
Chapter 3 METHODOLOGY	22
3.1 Research methods and procedures	22
3.2 Geo-studio program	23
3.3 Theory and Equation	23
3.3.1 Morgenstern-Price Method	23
3.3.2 Governing differential equation for seepage analysis	25
3.4 Rock and soil parameters, SWCC and Hydraulic conductivity	25
3.5 Simulation model	27
3.5.1 Geometry for SEEP/W and SLOPE/W	27
3.5.2 Define material properties	28
3.5.3 Analysis type and slip surface	29
3.5.4 Boundary condition for first research purpose	30
3.5.6 Boundary condition for second and third research purpose	32
3.5.7 Summary	35
3.6 Monitoring Points	37
Chapter 4 ANALYSIS RESULTS AND DISCUSSION	39
4.1 Results for the first research purpose (research on Qianjiangping landslide)	39
4.1.1 Results from SEEP/W	39
4.1.1.1 SEEP/W result analysis	47

4.1.2 Results from SLOPE/W	52
4.1.2.1 First step results of SLOPE/W analysis	53
4.1.2.2 Second step results of SLOPE/W analysis.....	53
4.1.2.3 Third step results of SLOPE/W analysis.....	55
4.1.2.4 Final step results of SLOPE/W analysis	57
4.1.2.5 Summary for the results of SLOPE/W.....	59
4.1.3 Discussion.....	60
4.2 Results for the second research purpose (rainfall patterns analysis).....	62
4.2.1 Results for the pattern of “Delayed”	62
4.2.2 Results for the pattern of “Advanced”	65
4.2.3 Results for the pattern of “Uniform”	68
4.2.4 Results for the pattern of “Normal”	71
4.2.5 Results summary.....	74
4.3 Results for the third research purpose (rainfall intensity analysis)	77
4.3.1 Results summary.....	80
Chapter 5 CONCLUSION&FUTURE STUDY	84
5.1 Conclusion of this study	84
5.2 Future study.....	85
REFERENCES.....	86

LIST OF FIGURES

Figure 1-1 Qianjiangping landslide at 2003 (Wang et al., 2004).....	3
Figure 1-2 Failure Mechanism of the Qianjiangping slope (Jian et al., 2014).....	3
Figure 2-1 Definition sketch for infinite slope stability for planar failures (Sidle et al., 1985).....	7
Figure 2-2 Definition sketch for the method of slices stability analysis for rotational failures (Sidle et al., 1985)	7
Figure 2-3 Slope/W modules in Geo-Studio	8
Figure 2-4 SEEP/W modules in Geo-Studio.....	10
Figure 2-5 Types of rainfall patterns: a. Advanced b. Uniform c. Normal d. Delayed (Li et al., 2020).....	11
Figure 2-6 Typical desorption of soil-water characteristic curve (Fredlund & Rahardjo, 1993).....	14
Figure 2-7 Zones corresponding to the soil-water characteristic curve (López-Acosta & Mendoza-Promotor, 2016)	14
Figure 2-8 Soil-water characteristic curves (SWCC) for different soil types (Fredlund & Xing, 1994)	15
Figure 2-9 Geological profile of the Qianjiangping landslide (Jian et al., 2014)	16
Figure 2-10 Geological map of Qianjiangping landslide (Jian et al., 2014)	16
Figure 2-11 the water level variation and rainfall condition (Jian et al., 2014)	18
Figure 2-12 Topographic map of the Qingning landslide (Zhang et al., 2015)	19
Figure 2-13 Daily rainfall and factor of safety of the Qingning landslide (Zhang et al., 2015).....	20
Figure 2-14 simulated seepage field on June 18, 2007 (Zhang et al., 2015).....	21
Figure 2-15 simulated seepage field on June 27, 2007 (Zhang et al., 2015).....	21
Figure 2-16 simulated seepage field on July 7, 2007 (Zhang et al., 2015)	21
Figure 3-1 Static scheme of Morgenstern-Price method (Duncan. et al., 2014).....	24
Figure 3-2 volumetric water content function (Jian et al., 2014).....	26
Figure 3-3 Hydraulic conductivity function (Jian et al., 2014).....	27
Figure 3-4 Geometry shape of the soil slope.....	28
Figure 3-5 Defined material properties for SEEP/W analysis	28
Figure 3-6 Defined material properties for SLOPE/W analysis	29

Figure 3-7 Slip surface setting for SLOPE/W analysis	30
Figure 3-8 Change in water total head versus time for SEEP/W analysis.....	31
Figure 3-9 Daily rainfall versus time for SEEP/W analysis	31
Figure 3-10 Boundary condition setting for SEEP/W analysis	32
Figure 3-11 “Delayed” rainfall pattern	33
Figure 3-12 “Advanced” rainfall pattern	33
Figure 3-13 “Uniform” rainfall pattern.....	34
Figure 3-14 “Normal” rainfall pattern	34
Figure 3-15 rainfall setting for rainfall intensity study	35
Figure 3-16 final models in SEEP/W module.....	38
Figure 3-17 final models in SLOPE/W module.....	38
Figure 4-1-1 SEEP/W first step results (Initial).....	41
Figure 4-1-2 SEEP/W second step results (day1).....	41
Figure 4-1-3 SEEP/W second step results (day3).....	41
Figure 4-1-4 SEEP/W second step results (day5).....	41
Figure 4-1-5 SEEP/W second step results (day7).....	41
Figure 4-1-6 SEEP/W second step results (day9).....	41
Figure 4-1-7 SEEP/W second step results (day10).....	42
Figure 4-1-8 SEEP/W third step results (day11)	42
Figure 4-1-9 SEEP/W third step results (day13)	42
Figure 4-1-10 SEEP/W third step results (day15)	42
Figure 4-1-11 SEEP/W third step results (day17)	42
Figure 4-1-12 SEEP/W third step results (day19)	42
Figure 4-1-13 SEEP/W third step results (day20)	43
Figure 4-1-14 SEEP/W final step results (day21).....	44
Figure 4-1-15 SEEP/W final step results (day23).....	44
Figure 4-1-16 SEEP/W final step results (day25).....	44
Figure 4-1-17 SEEP/W final step results (day27).....	44
Figure 4-1-18 SEEP/W final step results (day29).....	45
Figure 4-1-19 SEEP/W final step results (day31).....	45
Figure 4-1-20 SEEP/W final step results (day33).....	45
Figure 4-1-21 SEEP/W final step results (day35).....	45
Figure 4-1-22 SEEP/W final step results (day37).....	46
Figure 4-1-23 SEEP/W final step results (day39).....	46

Figure 4-1-24 SEEP/W final step results (day41)	46
Figure 4-1-25 SEEP/W final step results (day43)	46
Figure 4-2 the change of PWP monitored by Point A and C over time	49
Figure 4-3 the change of PWP vs Rainfall (monitored by Point B).....	51
Figure 4-4 SLOPE/W first step results (Initial State)	53
Figure 4-5 SLOPE/W second step results (day10).....	53
Figure 4-6 SLOPE/W second step results	54
Figure 4-7 SLOPE/W third step results (day20)	55
Figure 4-8 SLOPE/W third step results.....	56
Figure 4-9 SLOPE/W final step results (day43)	57
Figure 4-10 SLOPE/W final step results.....	58
Figure 4-11 Amount of PWP change (Point A & C) vs Factor of safety.....	60
Figure 4-12 Rainfall vs Factor of safety over time	61
Figure 4-13 Amount of PWP change (Point B) vs Factor of safety over time	61
Figure 4-14 Daily rainfall and accumulated rainfall over time (Delayed)	63
Figure 4-15 Accumulated rainfall verse factor of safety over time (Delayed)	64
Figure 4-16 Daily rainfall and accumulated rainfall over time (Advanced)	66
Figure 4-17 Accumulated rainfall verse factor of safety over time (Advanced)	67
Figure 4-18 Daily rainfall and accumulated rainfall over time (Uniform)	69
Figure 4-19 Accumulated rainfall verse factor of safety over time (Uniform)	70
Figure 4-20 Daily rainfall and accumulated rainfall over time (Normal)	72
Figure 4-21 Accumulated rainfall verse factor of safety over time (Normal)	73
Figure 4-22 Accumulated rainfall for four patterns	75
Figure 4-23 Factor of safety changes over time (for four rainfall patterns).....	76
Figure 4-24 Location of observation points D	77
Figure 4-25 rainfall setting for rainfall intensity analysis	78
Figure 4-26 Amount of PWP change verse factor of safety for rainfall intensity = 50mm/d.....	78
Figure 4-27 Amount of PWP change verse factor of safety for rainfall intensity = 75mm/d.....	79
Figure 4-28 Amount of PWP change verse factor of safety for rainfall intensity = 100mm/d.....	79
Figure 4-29 the change of PWP monitored by Point D over time	81
Figure 4-30 Factor of safety changes over time for three situations	82

LIST OF TABLES

Table 3-1 Geotechnical parameters (Jian et al., 2014).....	26
Table 3-2 Analysis process for the first research purpose	35
Table 3-3 Analysis process for the second research purpose (Delayed).....	36
Table 3-4 Analysis process for the second research purpose (Advanced).....	36
Table 3-5 Analysis process for the second research purpose (Uniform)	36
Table 3-6 Analysis process for the second research purpose (Normal).....	36
Table 3-7 Analysis process for the second research purpose (rainfall intensity analysis)	37
Table 4-1 Phenomena in different stages and days.....	39
Table 4-2 Amount of PWP change detected by Point A.....	48
Table 4-3 Amount of PWP change detected by Point C.....	49
Table 4-4 Amount of PWP change detected by Point B.....	51
Table 4-5 SLOPE/W second step results	54
Table 4-6 SLOPE/W third step results.....	55
Table 4-7 SLOPE/W final step results.....	57
Table 4-8 Daily rainfall and accumulated rainfall for pattern “Delayed”	63
Table 4-9 Factor of Safety results for rainfall pattern “Delayed”	64
Table 4-10 Daily rainfall and accumulated rainfall for pattern “Advanced”	66
Table 4-11 Factor of Safety results for rainfall pattern “Advanced”	67
Table 4-12 Daily rainfall and accumulated rainfall for pattern “Uniform”	69
Table 4-13 Factor of Safety results for rainfall pattern “Uniform”	70
Table 4-14 Daily rainfall and accumulated rainfall for pattern “Normal”	72
Table 4-15 Factor of Safety results for rainfall pattern “Normal”	73
Table 4-16 Accumulated rainfall for four rainfall patterns.....	74
Table 4-17 Factor of Safety results for four rainfall patterns	75
Table 4-18 The PWP changes observed by point D for three rainfall conditions	80
Table 4-19 Factor of Safety results for three rainfall conditions	81

CHAPTER 1 INTRODUCTION

1.1 Background

Slope stability was triggered by many factors, mainly including geomorphic features, rock and soil types, and properties, geological structure, water, earthquakes, etc. The factors mentioned above, such as geomorphic features, rock, and soil types and properties, and geological structure, can control the form and scale of slope deformation and failure, and control slope stability. In addition, factors such as water and earthquake can promote the occurrence and development of slope deformation and failure and become the triggering factor of slope deformation and failure.

Many practical projects have proven that rainfall is the most important and common environmental factor that affects slope stability and causes slope instability, whether in rainy subtropical and tropical areas or cold and arid areas. At the same time, it is also the most critical triggering factor for shallow slope damage. A large number of research results show that the infiltration of rainwater leads to a decrease in the suction in the slope soil (Ng et al., 1998), which in turn leads to a reduction in the shear strength of the unsaturated soil on the potential sliding surface (Fredlund & Rahardjo, 1993). When the shear strength of the soil is insufficient to maintain the stability of the slope, it will lose stability. Before analyzing the slope stability, it is essential to thoroughly and systematically study the change law of the seepage field in the slope caused by rainfall. In previous studies, most scholars used numerical simulation or rainfall infiltration model tests to analyze the impact of rainfall intensity, rainfall duration, the saturated permeability coefficient of soil, and initial water content on slope seepage field and stability (Chen et al., 2009). This type of research

is carried out under the same rainfall pattern, and rarely involves the study of the variation of the slope seepage field under different rainfall patterns. The existing literature shows that the slope instability caused by rainfall is related to the rainfall pattern (Zhang et al., 2018). For soil slope, the influence of rainfall on its seepage field under different rainfall modes is bound to be different. In this study, Geo-studio software will be used to analyze the case of Qianjiangping. Through the saturated-unsaturated seepage finite element method, the influence of rainwater infiltration on the slope is analyzed, and the change of seepage field and the change of a factor of safety are obtained. On this basis, the influence of four typical rainfall patterns and different rainfall amounts on slope stability was analyzed.

1.2 Qianjiangping landslide

Qianjiangping was a large flat rock landslide occurred in 2003. The landslide caused a lot of damage, killing 24 people and destroying the homes of more than 1,200 people. The investigation showed that the impoundment of the Three Gorges Reservoir and subsequent continuous rainfall were the main cause of the landslide. Also considering the previous ruptures and structural problems of the slope, the landslide was finally triggered. The occurrence of the accident has a certain relationship with the geological structure of the site (Wang et al., 2004). Before the accident, people generally believed that this slope was very safe because of its simple geological conditions. In addition, during the on-site investigation, no traces of landslides were found on the slope. Therefore, people did not expect that there would be such a large landslide area because there was no ground deformation around the slope.



Figure 1-1 Qianjiangping landslide at 2003 (Wang et al., 2004)

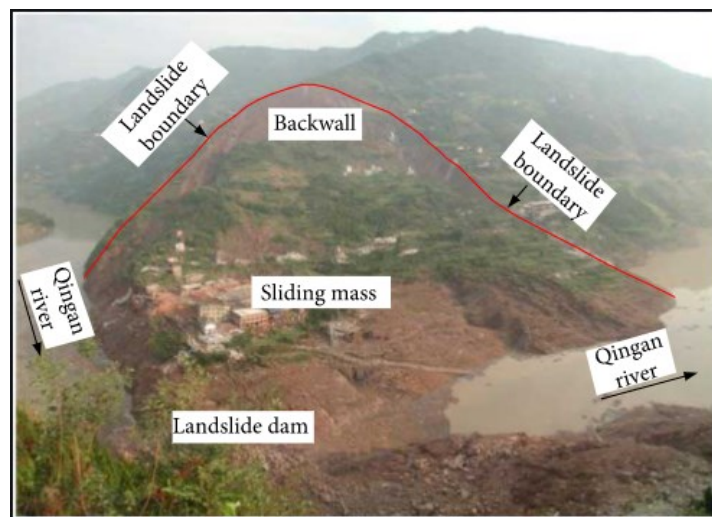


Figure 1-2 Failure Mechanism of the Qianjiangping slope (Jian et al., 2014)

1.3 Research object and purpose

The object of this research is Qianjiangping mentioned above. The reason for choosing it is that some information has been obtained in some research, such as material properties, SWCC, etc. There is also mention of changes in water levels and rainfall. This information helps to build models.

There are three main purposes of this study: First, it is hoped to be able to explore the mechanism and failure process of landslides and to simulate the failure of

slopes and changes in pore water pressure. After obtaining the results, some internal mechanisms can be discovered. In addition, the simulation results can be compared with the actual situation to prove whether the results are reasonable. The second purpose is to study the influence of different rainfall methods on the seepage field. The four rainfall modes mentioned in Chapter 2.2 will be used to test which mode has the greatest impact on the research object. The research method is similar to the previous research purpose, and the results can be obtained by changing the rainfall pattern. For the first research purpose, the model can be built smoothly by integrating known information. For the second research purpose, it is necessary to assume that the four different rainfall patterns have the same rainfall intensity, rainfall duration, soil saturation permeability coefficient, and initial water level. In this way, the results obtained can be used to understand which rainfall method will have the greatest impact on the safety of the research object. The last research purpose is to study the influence of rainfall intensity on slope stability. By increasing the area of one of the rainfall patterns (which means that the total amount of rainfall will increase), the influence of rainfall intensity on slope stability can be obtained.

1.4 Outline of the Study

This study will be divided into five chapters. The first chapter will list the motivation and goals of this research while the second chapter will review some related articles, and the third chapter will list some definitions, formulas, tools, and methods used in this research. In addition, the fourth chapter will list the results of the analysis and discuss the results, and the fifth chapter is the summary of the whole study.

CHAPTER 2 LITERATURE REVIEW

2.1 Rainfall-induced slope failures

2.1.1 Mechanisms of rainfall-induced slope failures

Slope instability aroused by rainfall has attracted more and more attention around the world. In general, it is believed that slope failures triggered by rainfall are aroused by the variation in seepage force and the pore water pressure (Gerscovich et al., 2006; Zhu & Anderson, 1998). Precisely speaking, there are two types of failure mechanisms.

For the first type of failure mechanism, consider the influencing of rainfall, positive pore water pressure will continue to be generated, this will lead to rainfall-induced slope failure (Collins & Znidarcic, 2004). The local collapse of the material is aroused by the continuous increment of positive pore water pressure (Chen et al., 2004). During the failure process, the sliding surface will be liquefied due to the loss of shear strength and excess pore water pressure. This is the fundamental mechanism that causes continuous movement (Chen et al., 2004). On the other hand, high infiltration rates and coarse-grained soil will promote the increment of positive pore water pressure, and seepage force within the slope will cause failure (Collins & Znidarcic, 2004).

For the second type of failure mechanism, considering that the reduction of suction will affect the effective normal stress of the failure surface and thereby the value of shear strength will decrease. Therefore, the reduction of matrix suction will affect the shear strength, which is the cause of slope damage caused by rainfall (Au,

1998; Chen et al., 2004; Collins & Znidarcic, 2004). It is observed that the reduction of matrix suction after a rainstorm is related to the initial matrix suction before a rainstorm (Lim et al., 1996). Some scholars found that the failure of fine-grained soils is more caused by the decrease in shear strength caused by suction loss (Collins & Znidarcic, 2004).

2.1.2 Slope stability analysis

Generally speaking, there are two main analysis methods. One is limit equilibrium analysis and the other is coupled hydro-mechanical analysis. The first method can be further divided into infinite slope stability analysis method (1D) and method of slices (2D or 3D). Zhang et al. (2011a) have conducted a comprehensive review of slope stability analysis:

2.1.2.1 Limit equilibrium analysis

The infinite slope stability model is suitable for shallow slope failure and is widely used due to its simplicity. Its sliding surface depth is much smaller than plain dimensions. The sliding surface is considered that to be paralleled to the ground surface. The failure mechanism of an infinite slope is characterized by two parts, one of them is resisting basal Coulomb friction, and another of them is the gravitationally induced downslope basal driving stress. The ratio between these two values is called the factor of safety (Hsu & Liu, 2019). The stability analysis of infinite slope is uncomplicated. However, the sliding surface is circular in many cases, it is impossible to fully describe the failure of the slope. Therefore, the slicing method is also widely used. For the method of slices, there are currently many different methods. The main difference between the different methods is the static equations considered, the

interlayer normal and shear forces included, and the assumed correlation between the internal interlayer forces (Krahn, 2003). Figure 2-2 is an example of the method of slices, where forces act on the slice. The actual number of slices used is based on the geometry and contour of the slope fill (Duncan. et al., 2014).

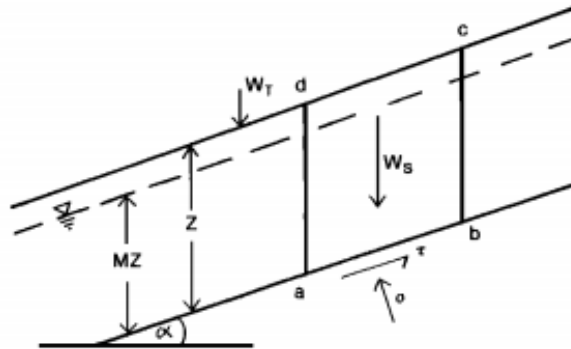


Figure 2-1 Definition sketch for infinite slope stability for planar failures (Sidle et al., 1985)

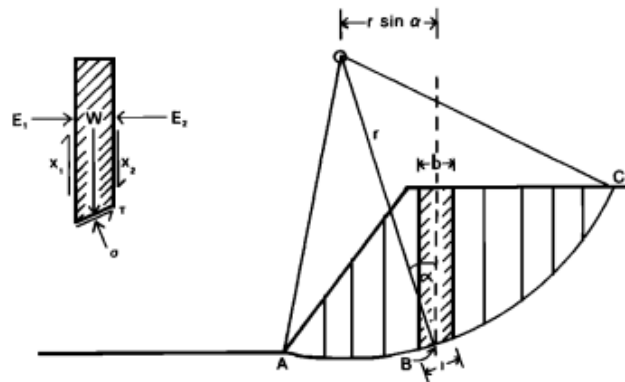


Figure 2-2 Definition sketch for the method of slices stability analysis for rotational failures (Sidle et al., 1985)

2.1.2.2 Coupled hydro-mechanical analysis

In the Limit equilibrium analysis, the deformation of the slope has not been considered. Alternatively, the FEM (Finite Element Method) can be used for a realistic analysis of slope deformation (Duncan, 1996; Griffiths & Lane, 1999; Potts &

Zdravković, 2001). In fact, not only the distribution of pore water pressure but also the stress state of the soil itself will significantly affect the stability of the slope. The seepage process will affect the stress state of the soil, thus affecting the deformation of the slope. On the contrary, the deformation of the slope will seriously affect the seepage process, because hydraulic parameters (such as porosity and permeability) are greatly affected by the stress state. Therefore, the problems of seepage and stress deformation in unsaturated soils are highly correlated under rainfall conditions (Zhang et al., 2011).

In SLOPE/W, the limit equilibrium method is mainly used to analyze slope stability. One of them is called the method of slices, which is used to analyze slope stability and calculate the factor of safety. The results obtained from SEEP/W analysis can be used for more accurate analysis. The parameters needed for slope stability analysis are soil unit weight, cohesion, and friction angle. This module also contains a variety of analysis methods, including Morgenstern price, bishop, Janbu, and so on. People usually use the Morgenstern price method because of its higher accuracy. Moreover, this module can set the non-slip surface and the known sliding surface according to the distribution of the soil layer.

Figure 2-3 Slope/W modules in Geo-Studio

2.1.4 Rainfall infiltration analysis

Regarding the slope failures caused by rainfall, the influence of permeability cannot be ignored because it can be used to calculate the distribution of pore water pressure. In the theoretical basis of infiltration numerical simulation, Darcy's law combined with the conservation of flow mass describes pore water pressure profile and the infiltration process. In fact, there may be unsaturation in the soil. Therefore, it is better to use the Richards equation in order to consider the most realistic situation. The Richards equation is based on Darcy's law and the conservation of water mass and can be used to describe the three-dimensional water flow in unsaturated soils (Richards, 1931). The formula is as follows:

$$\frac{\partial}{\partial x} \left[k(\theta_w) \frac{\partial H_t}{\partial x} \right] + \frac{\partial}{\partial y} \left[k(\theta_w) \frac{\partial H_t}{\partial y} \right] + \frac{\partial}{\partial z} \left[k(\theta_w) \frac{\partial H_t}{\partial z} \right] = -\frac{\partial \theta_w}{\partial t} \quad (2.1)$$

From the equation above, where θ_w is the volumetric water content; k is the permeability, which is a function of θ_w ; H_t is the total head.

2.1.5 SEEP/W program

There are two analysis modes of SEEP/W: steady-state and transient analysis. The steady-state analysis is the state of groundwater level over a long period of time, while transient analysis is used to perform a specific time analysis. In this module, the influence of rainfall on infiltration can be obtained by inputting rainfall data. Since the calculation of grids and nodes is considered in the analysis, it is necessary to have SWCC, soil saturated permeability coefficient, and other conditions in order to simulate the pressure head and volumetric water content of the soil in a saturated or unsaturated state under rainfall conditions.

The boundary conditions of SEEP/W are mainly divided into five types, and the total head and unit discharge are usually used for analysis. In the steady-state model, the head is mainly used to analyze the long-term groundwater level distribution. In transient mode, various function modes can be used to input the change of rainfall or water head for each event. The results of the analysis can also be displayed in different ways.

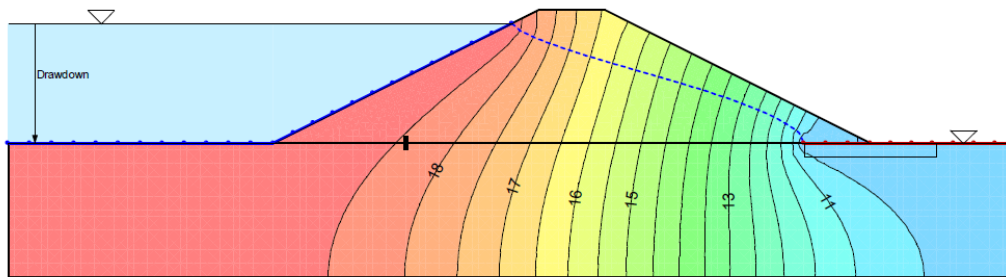


Figure 2-4 SEEP/W modules in Geo-Studio

2.2 Types of rainfall patterns

A large number of scholars have done a lot of research on the impact of rainfall-induced landslides and achieved many results. Rainfall infiltration is a dynamic process that changes with time and space. The amount of infiltration is affected by factors such as rainfall intensity, rainfall duration, soil physical properties, roughness, and vegetation conditions (Chen et al., 2009). Therefore, the slope instability caused by rainfall is related to the rainfall pattern (Zhang et al., 2018), and the influence of rainfall on the seepage field on the oblique surface must be different under different rainfall patterns. It is of great significance to study the rules of rainfall infiltration and stability changes of soil slopes under different rainfall patterns. By studying the variation of pore water pressure at each position of the slope and the change of the factor of safety under different rainfall patterns, the slope pore water pressure (that is, the change of matrix suction) and the slope instability

process can be obtained. Generally speaking, there are four rainfall modes: Advanced, Normal, Delayed, and Uniform (Wu et al., 2017).

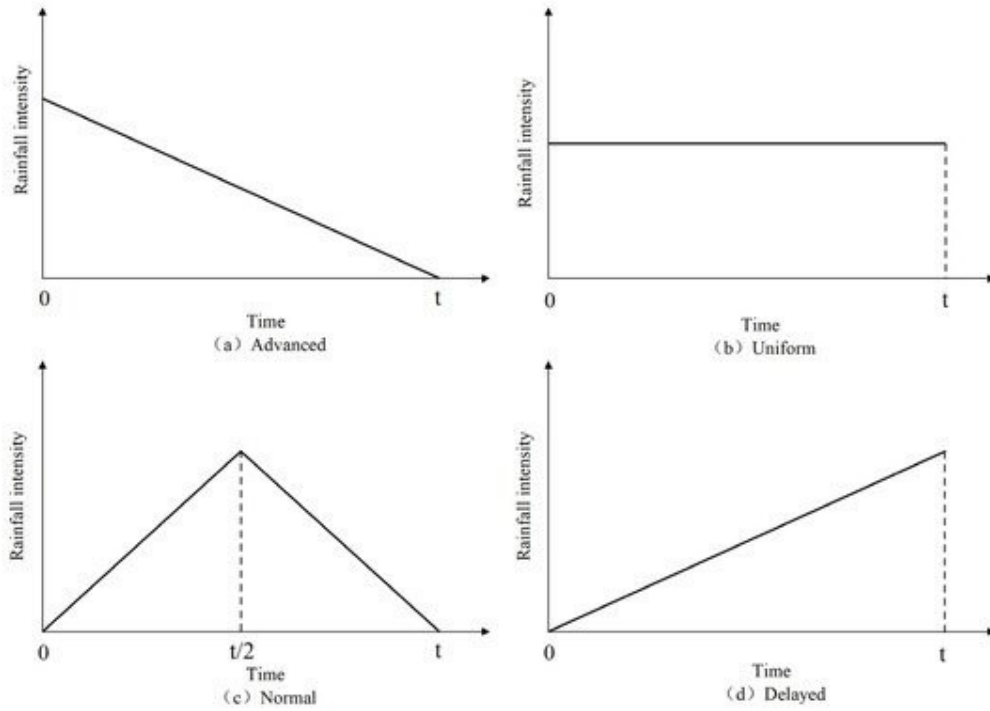


Figure 2-5 Types of rainfall patterns: a. Advanced b. Uniform c. Normal d. Delayed (Li et al., 2020)

2.3 Study on unsaturated soil

2.3.1 Properties of unsaturated soil

Generally, people use the limit equilibrium method in most cases when analyzing slopes. This is because the results obtained in most practical situations are more reliable. In this analysis method, the shear strength of the soil is an important parameter. According to the Mohr-Coulomb failure criterion and Terzaghi's concept of effective stress (Terzaghi, 1943), the shear strength of saturated soil is defined as:

$$\tau_f = c' + (\sigma_n - \mu_w) \tan \phi' \quad (2.2)$$

where τ_f is the shear strength at failure; c' is the effective cohesion, $(\sigma_n - \mu_w)$ is the effective stress, and ϕ' is the effective friction angle.

However, for unsaturated soils, when referring to the pore volume, there is not only considering the water, but also the air. Therefore, the definition of the effective normal stress will be the main difference between the shear strength of saturated soil and unsaturated soil. In order to better quantify the shear strength of the unsaturated soil, the soil-water characteristic curve and effective shear strength parameters can be used. Vanapalli proposed the following estimation equation (Vanapalli, 2009):

$$\tau = c' + (\sigma - u_a) \tan \phi' + (u_a - u_w) \tan \phi^b \quad (2.3)$$

where τ is shear strength of unsaturated soil, c' is effective cohesion, ϕ' is effective friction angle of frictional resistance for a saturated soil, ϕ^b is angle of frictional resistance related to the change of soil suction, $(\sigma - u_a)$ is net normal stress, u_a is pore air pressure, u_w is pore water pressure, $(u_a - u_w)$ is matric suction.

2.3.2 Effect of unsaturated soil mechanics in slope stabilization

Rainfall is one of the factors affecting the stability of saturated unsaturated soil slope (Mahmood et al., 2016). Some examples of landslides are due to the deep groundwater level of the slope, so rainwater infiltration will increase the groundwater level and reduce the matric suction (Rahardjo et al., 2019). Therefore, the negative pore water pressure or matrix suction is the key to affect slope stability. The total suction of soil is conceptually defined as the ability of unsaturated soil to attract or retain water (Jindal et al., 2016), expressed as pressure or head. It is caused by the interaction between soil, water, and air. This complex state will produce negative

pore water pressure. Therefore, suction is also defined as the energy required to extract a unit volume of water from a given soil. The analysis of unsaturated soil slope needs extensive and detailed seepage analysis because the failure of unsaturated soil slope is closely related to heavy rainfall and infiltration (Yeh et al., 2008). The hydraulic conductivity and matric suction can affect the permeability; increase the water pressure in slope, the change rate of volume, the decreasing rate of shear strength, and the change of FS (Mahmood et al., 2013).

2.3.3 Introduction of soil-water characteristic curve (SWCC)

SWCC is mainly used to describe the relationship between water content and suction in the soil (Fredlund et al., 2012). It plays an important role while determining the property function of unsaturated soil. Generally speaking, it can be divided into three zones. In Figure 2-6 and 2-7, from top to bottom, they are boundary effect zone (or capillary zone), transition zone, and residual zone. In the region between air-entry value (AEV) and residual (θ_r), the change rate of soil suction is the largest. Therefore, the shear strength in the transition zone changes significantly with respect to the soil suction. To have a good estimation of the shear strength of unsaturated soil; it is first necessary to well define AEV and residual soil suction. Theoretically, if the soil suction of unsaturated soil is less than AEV, it will then be regarded as saturated soil. In addition, the soil-water characteristic curves for different types of soils are also very different (Fredlund & Xing, 1994). For example, SWCC of sand, silt, and clay are listed in Figure 2-8. Due to the different characteristics of soil, there are great differences between them.

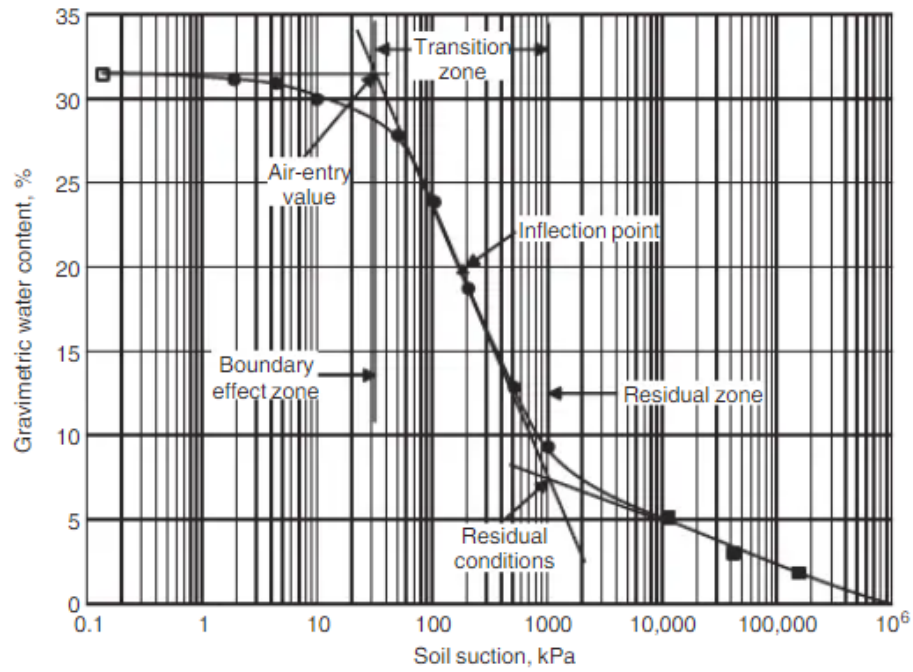


Figure 2-6 Typical desorption of soil-water characteristic curve (Fredlund & Rahardjo, 1993)

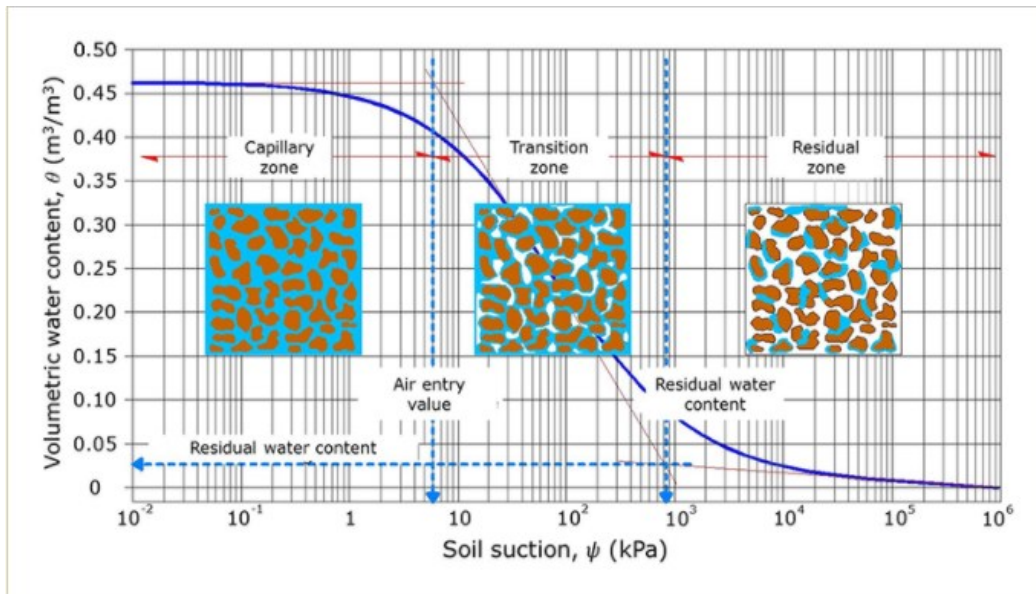


Figure 2-7 Zones corresponding to the soil-water characteristic curve (López-Acosta & Mendoza-Promotor, 2016)

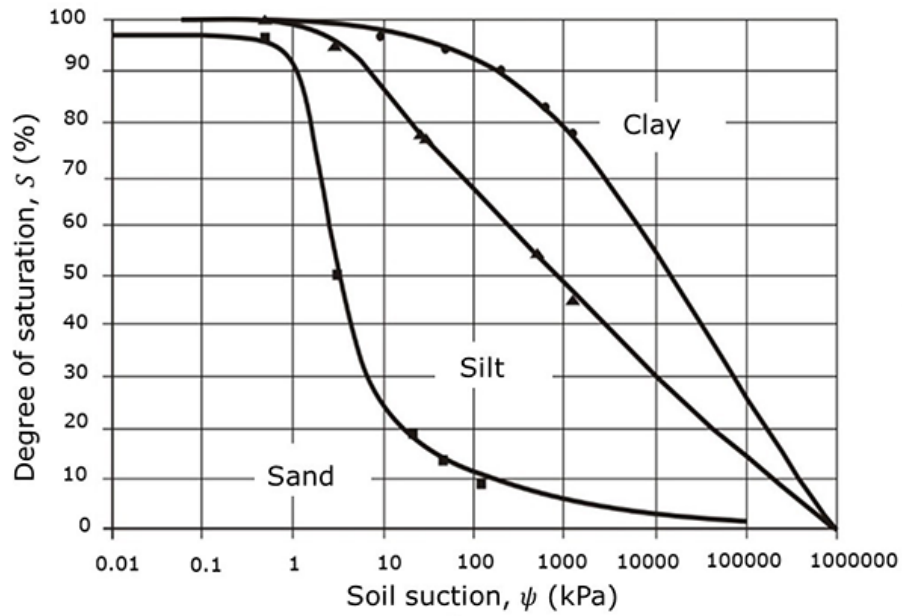


Figure 2-8 Soil-water characteristic curves (SWCC) for different soil types (Fredlund & Xing, 1994)

2.4 Factors causing the landslide in Qianjiangping

2.4.1 The structural problems of the slope

Field investigations show that the bedding planes of the strata in the site dip out of the slope surface. Furthermore, the dip direction of the stratum is listed in Figure 2-9, and the dip range is from 15 degrees to 30 degrees. It is not difficult to find that the dip angle of the upper part of the slope is greater than that of the lower part of the slope, and the average dip angle is about 24 degrees, which meets the landslide condition. On the other hand, it can be seen from Figure 1-2 that the Qinggan-he River made a big curve in front of the slope, eroding the toes of the hillside and removing the support of the toes. The stratum of the slope is composed of continuous intercalation of siltstone and carbonaceous shale, which plays an important role in slope instability.

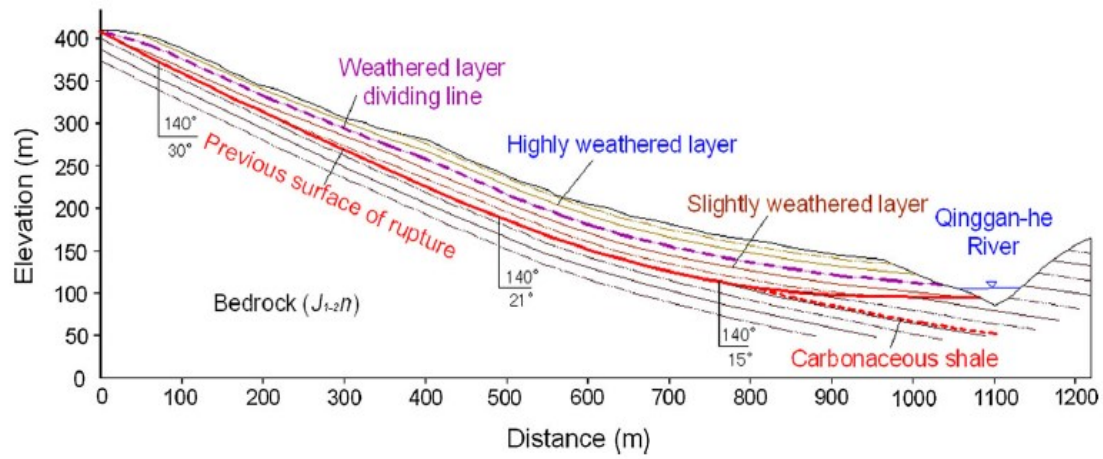


Figure 2-9 Geological profile of the Qianjiangping landslide (Jian et al., 2014)

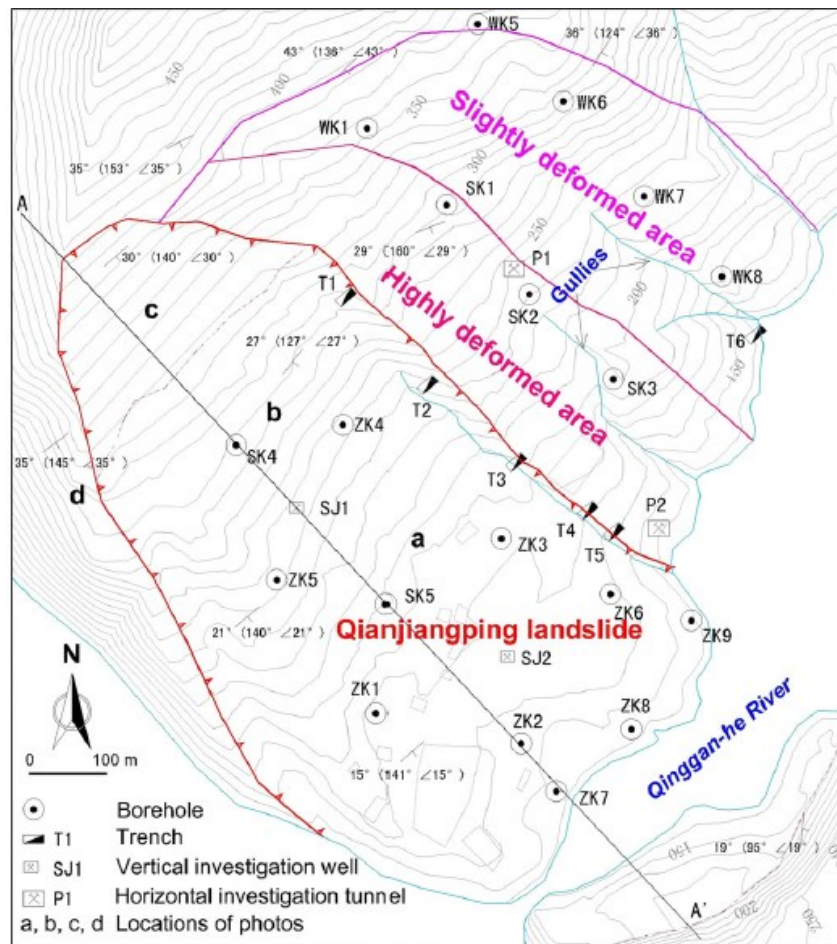


Figure 2-10 Geological map of Qianjiangping landslide (Jian et al., 2014)

2.4.2 Previous rupture surface

In the follow-up investigation and research, it was discovered that this mountain slope was not the first time to have cracked. In the highly deformed area which can be found in Figure 2-10, two rupture surface areas composed of silt and clay were found, with a thickness of about 40 cm. These two areas are the black calcite gravel silt layer, which is regarded as yellow clay. By comparing the percentages of fine particles in the two regions, the result shows that the yellow clay region is the previous rupture surface (Wang et al., 2008). This is because the percentage of fine particles is larger. Many crashed calcite were found in that layer. So far, it is believed that the black layer was produced in the latest landslide. The existence of the previous surface of rupture is also one of the factors that caused this landslide.

2.4.3 Rising water level and continuous rainfall

Rising water levels and continuous rainfall are considered to be the main causes of this landslide. From Figure 2-11, the change of water level and daily rainfall can be obtained. First, the reason for the rising water level is due to continuous water storage. The rise of the water level will cause the decline of the shear strength of the soil and rock. In addition, the upward pressure will increase. Secondly, continuous rainfall will greatly reduce the shear strength of shale. This is due to the fact that water penetrates the shale through the cracks, causing high hydrostatic pressure in the cracks. Under the combined action of rising pressure and hydrostatic pressure, landslides occur.

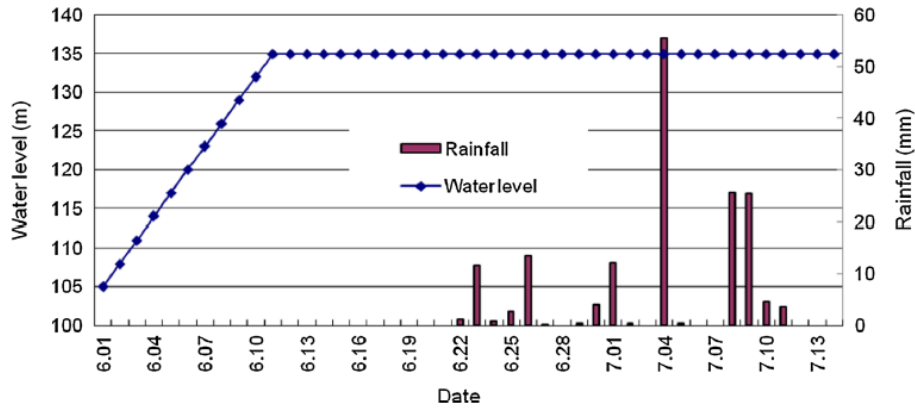


Figure 2-11 the water level variation and rainfall condition (Jian et al., 2014)

2.5 Case study on the Qingning landslide

2.5.1 Background

The Qingning landslide occurred on July 7, 2007. Fortunately, the local government issued a timely warning of the landslide, so no casualties were reported. It can be seen from Figure 2-12 that the area where the landslide accident occurred can be subdivided into three sub-areas, including deformation, sliding and debris flow areas (Zhang et al., 2015). The total area of the three sub-regions is approximately 1.81 km² and the altitude ranges from 500 meters to 788 meters. According to the follow-up investigation, it can be concluded that the average thickness of the slider is about 6 m. After obtaining the thickness, it can be concluded that the total volume of the accident site is approximately $1.1 \times 10^7 \text{ m}^3$.

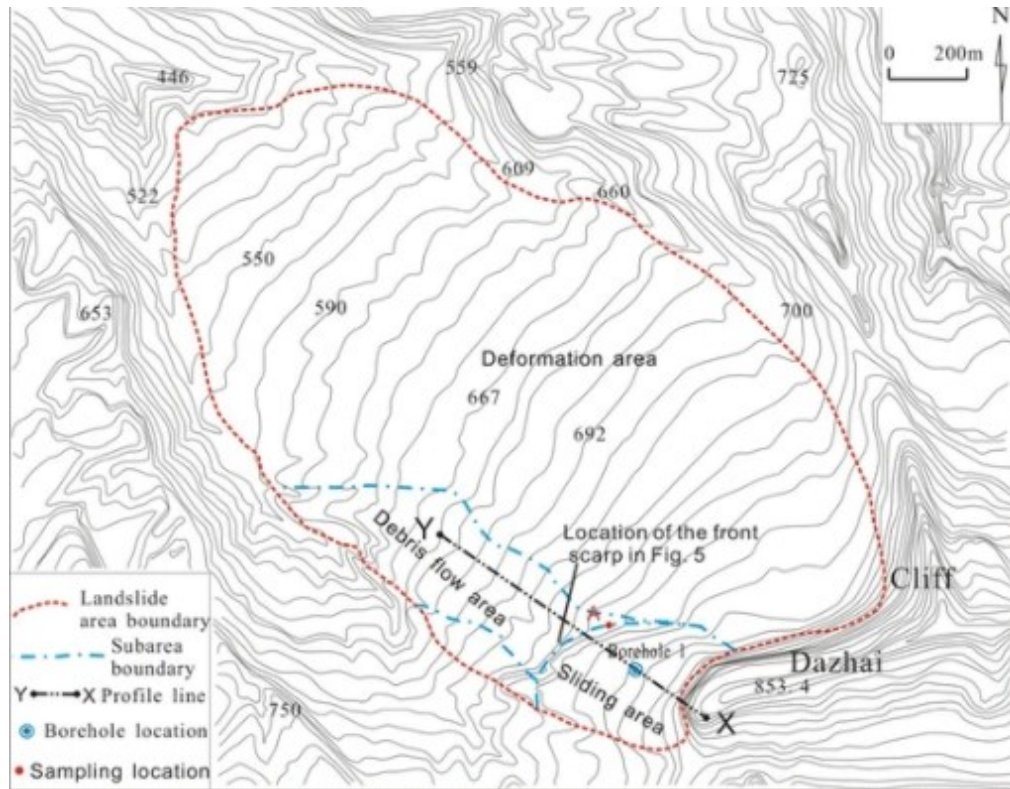


Figure 2-12 Topographic map of the Qingning landslide (Zhang et al., 2015)

2.5.2 Investigation

After the landslide incident, the local government investigated the landslide site immediately. The results show that under the influence of rainfall, the effective stress of the failure surface becomes one of the key factors for the stability of the landslide (Matsushi et al., 2006; Rahardjo et al., 2013; Tsao et al., 2005). It can be seen from Figure 2-13 that the landslide area experienced heavy rain before the landslide occurred. Among them, it can be found that the daily rainfall on July 5 and 6 is about 76 and 64 mm, respectively. Therefore, the heavy rain caused catastrophic damage on the morning of July 7. In the figure, it can be found that there was a greater daily rainfall in mid-June. However, the landslide occurred three weeks after the heavy rain. Through the Geo-studio software, the seepage field, water pressure distribution, and the factor of safety of the slope before and after the accident can be

simulated. The simulation results showed that the heavy rain in mid-June was not enough to fully saturate the seepage field under the soil in the sliding zone, and the water pressure was insufficient, so the landslide did not occur. However, on the day of the accident, it can be found that the seepage field under the soil in the slip zone is completely saturated, and the hydrostatic pressure in the landslide area has increased. Therefore, under the influence of horizontal stress, the effective stress of the failure surface is reduced. This is the reason for the sharp drop in the factor of safety and caused the landslide.

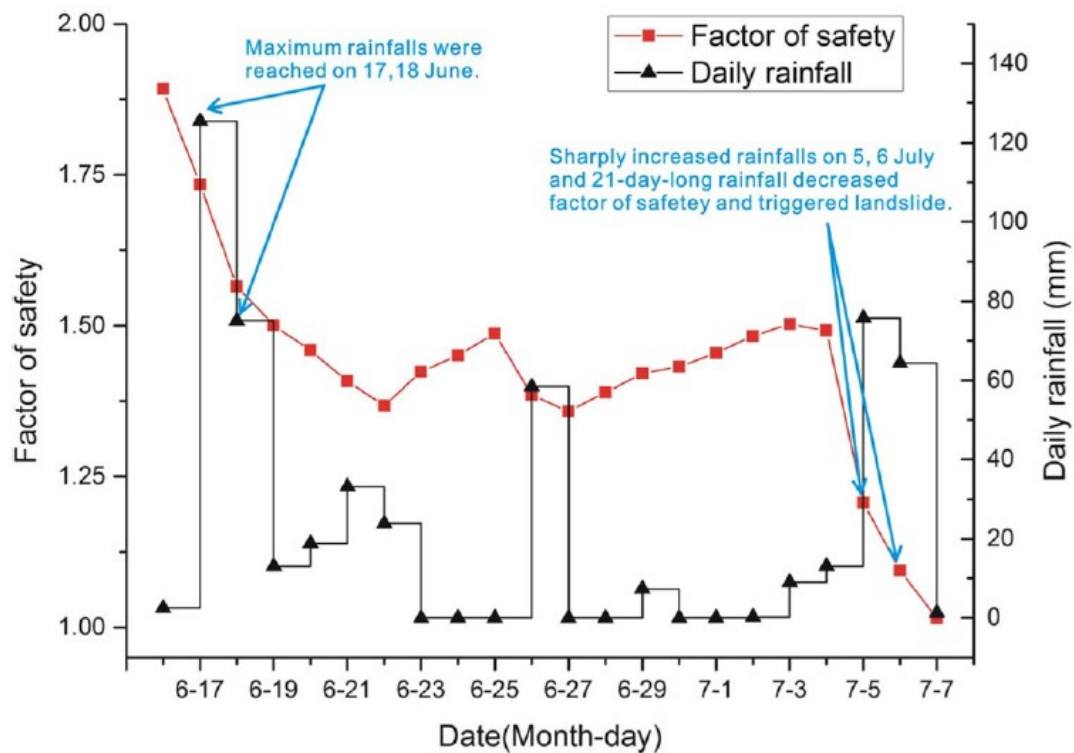


Figure 2-13 Daily rainfall and factor of safety of the Qingning landslide (Zhang et al., 2015)

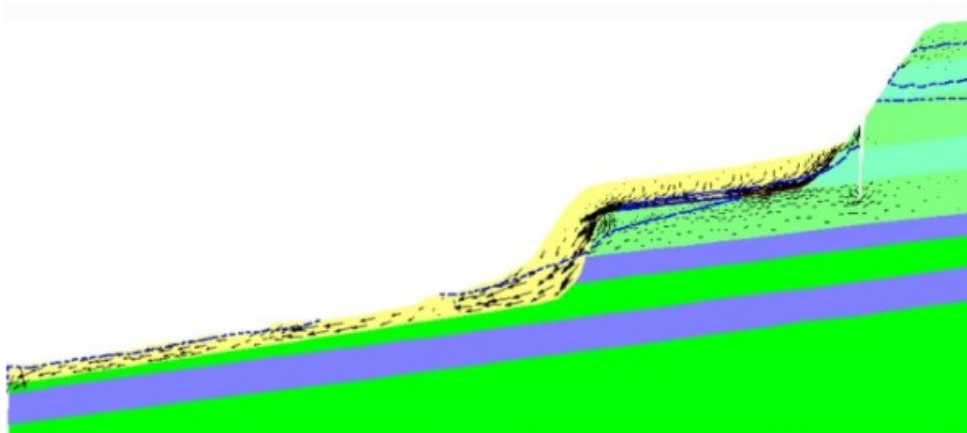


Figure 2-14 simulated seepage field on June 18, 2007 (Zhang et al., 2015)

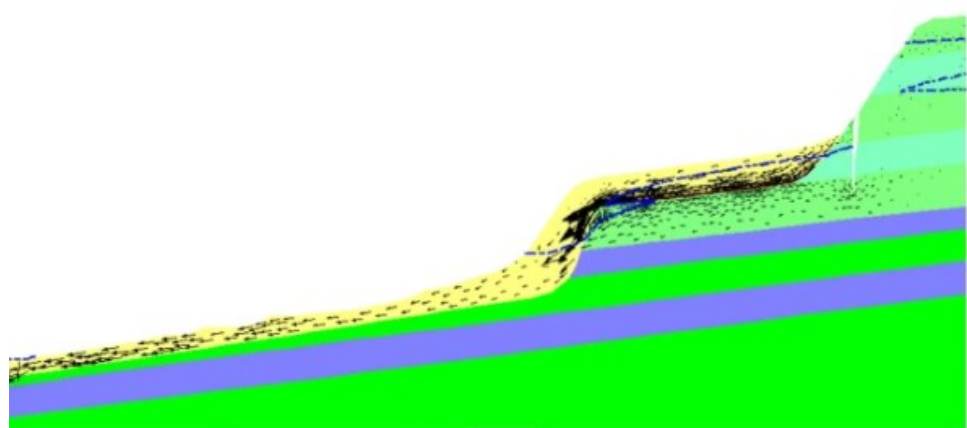


Figure 2-15 simulated seepage field on June 27, 2007 (Zhang et al., 2015)

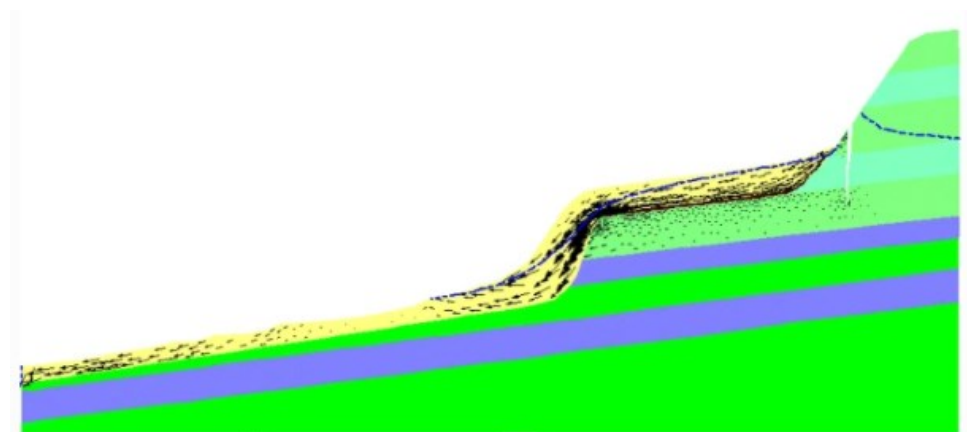


Figure 2-16 simulated seepage field on July 7, 2007 (Zhang et al., 2015)

Figures 2-14 to 2-16 are the results of the simulation in SEEP/W. Through this module, the changes in the seepage field can be obtained.

Chapter 3 METHODOLOGY

3.1 Research methods and procedures

In this study, Geo-studio was used to analyze the seepage field and slope stability. The formulas and theorems used in the analysis will be mentioned in the section below. Since it was going to create two different modules, SEEP/W and SLOPEW, it is necessary to strictly follow the following steps (detailed instructions will be mentioned in the section below). For the SEEP/W module, transient analysis is selected. Firstly, it is important to define the geometric shape of the soil slope. This is the first step for building a model. After the geometric shape of the soil slope is defined, the next steps can be carried out. The next part was defining the material, which includes defining SWCC and conductivity and selecting the type of saturated/unsaturated. After that, by setting the boundary condition, the change of the water level and the amount of rainfall can be simulated. At this point, the setting of SEEP/W has been completed. For the SLOPE/W module, the geometry in the SEEP/W module is directly imported without redefining the geometry. The next step is to define the materials. Some rock and soil parameters are used, which will be listed below. Next is to define the slip surface. After defining the slip surface, the results of SEEP/W are imported to SLOPE/W (set SEEP/W as a parent analysis, and perform slope stability analysis according to the seepage field in SEEP/W). Therefore, the variation of groundwater level, pore water pressure, and factor of safety can be obtained gradually.

The steps mentioned above are for the first research purpose, and for the second research purpose, most of the steps are the same. The only requirement is to change the rainfall method in the boundary condition to get the result.

3.2 Geo-studio program

In this research, the geotechnical software Geo-studio developed by Calgary University in 1998 would be used. An outstanding advantage of Geo-Studio is that all its software can be run under the same interface, which means that users only need to build a geometric model. It can be used in all analyses so that comprehensive geotechnical problems such as seepage, stability, stress and deformation, dynamic effects, water and gas two-phase flow, and pollutant migration can be analyzed at the same time. This study will use SEEP/W to simulate changes in the internal pore water pressure and groundwater level of Qianjiangping during rainfall and water level rise. And also simulate the influence of different rainfall patterns on slope stability. The results obtained in SEEP/W can be applied to SLOPE/W for more in-depth slope stability analysis.

3.3 Theory and Equation

3.3.1 Morgenstern-Price Method

The method of slices is the most commonly used method due to its ability to handle complex geometries and variable soil and water pressure conditions (Terzaghi et al., 1996). Morgenstern-Price is one of the limit equilibrium methods, which is a general method of slices developed on the basis of the original (Atashband, 2015). The slices are created by dividing the soil above the sliding surface by the plane. The factor of safety of the Morgenstern-Price method is determined at the point where the two curves intersect. At this point, both the moment equilibrium and the force equilibrium are satisfied.

To sum up, this method has the following characteristics: consider both shear and normal inter-slice forces, satisfy both moment and force equilibrium, and allow for a variety of user-selected inter-slice force functions (Morgenstern & Price, 1965).

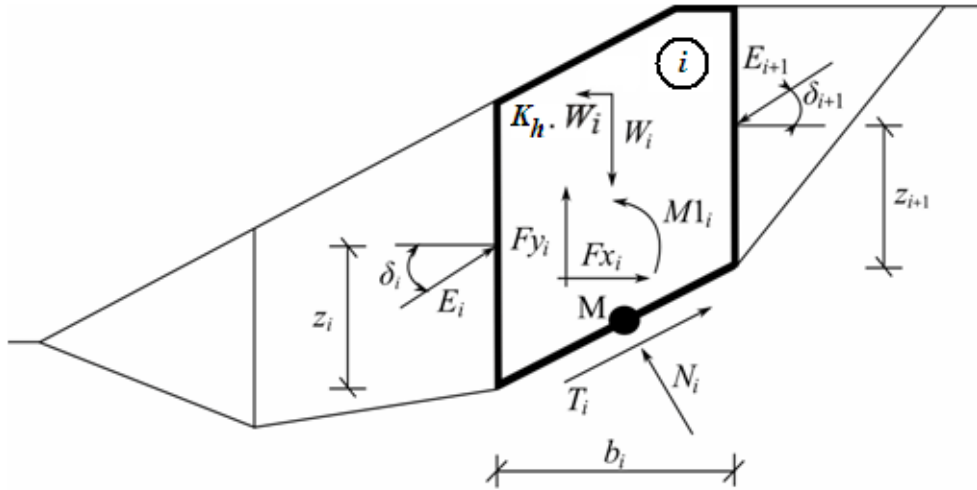


Figure 3-1 Static scheme of Morgenstern-Price method (Duncan. et al., 2014)

In this method, the following assumptions are introduced to calculate the limit equilibrium of forces and moments on each block (Morgenstern & Price, 1965):

1. Dividing planes between blocks are always vertical (see Figure 3-1).
2. The line of action of the weight of block W_i passes through the center of the i^{th} segment of slip surface represented by point M.
3. The normal force N_i is acting in the center of the i^{th} segment of slip surface, at point M.
4. The inclination of forces E_i acting between blocks is different on each block (δ_i) at slip surface end points is $\delta = 0$.

3.3.2 Governing differential equation for seepage analysis

In the two-dimensional analysis of SEEP/W, the following equation will be used. The general governing differential equation of two-dimensional seepage flow can be expressed as:

$$\frac{\partial}{\partial x} \left[k_x \frac{\partial H}{\partial x} \right] + \frac{\partial}{\partial y} \left[k_y \frac{\partial H}{\partial y} \right] + Q = \frac{\partial \theta}{\partial t} \quad (3.1)$$

where H is the water total head, k_x and k_y corresponds to the hydraulic conductivity of the x or y-axis, Q is the applied boundary flux, θ is the volumetric water content and t is the time

This equation shows that the difference between the flows (flux) in and out of the element volume at a certain point in time is equal to the change in the storage capacity of the soil system. Fundamentally, it means that the sum of the rate of change of flow in the x and y directions and the externally applied flux is equal to the rate of change of volumetric water content with respect to time.

3.4 Rock and soil parameters, SWCC and Hydraulic conductivity

Table 3-1 summarizes the rock and soil parameters (Jian et al., 2014). It contains some data such as unit weight, cohesion, friction, etc. These data are obtained through some tests or experiments in the laboratory, and they can be used while performing slope stability analysis. The data of the soil-water characteristic curve are measured in the laboratory (Fredlund et al., 2012). The volumetric water content function can be obtained by the Van Genuchten estimation model (Jian et al., 2014). Once the volumetric water content function is specified, the saturated hydraulic conductivity can be derived. Assuming that both are defined, the software can be used to simulate the seepage field. It can be seen from Figure 3-3 that the maximum values

of conductivity of both highly weathered layer and slightly weathered layer are greater than the negative fifth power of 10. Therefore, these two layers can be considered as high conductivity soil.

Table 3-1 Geotechnical parameters (Jian et al., 2014)

	Highly weathered layer	Slightly weathered layer	Zone of rupture surface	Bedrock
Unit weight (kN/m ³)	22.5	24.5	16.3	25.0
Saturated unit weight (kN/m ³)	23.5	25.5	20	26.0
Bulk modulus (Pa)	6.94×10^8	1.11×10^{10}	4.17×10^7	2.03×10^{10}
Shear modulus (Pa)	1.81×10^8	4.55×10^9	1.92×10^7	1.16×10^{10}
Cohesion (kPa)	100	150	22	4,000
Friction angle (°)	30	40	15	42
Tension strength (Pa)	2.0×10^6	4.0×10^6	2.0×10^5	2.0×10^7

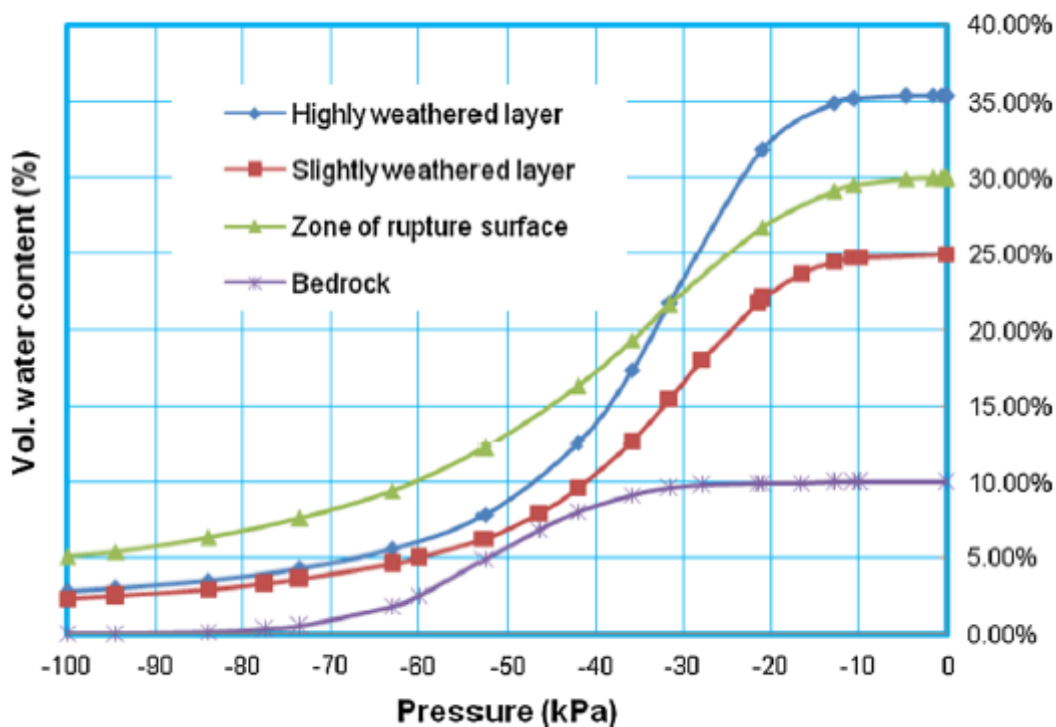


Figure 3-2 volumetric water content function (Jian et al., 2014)

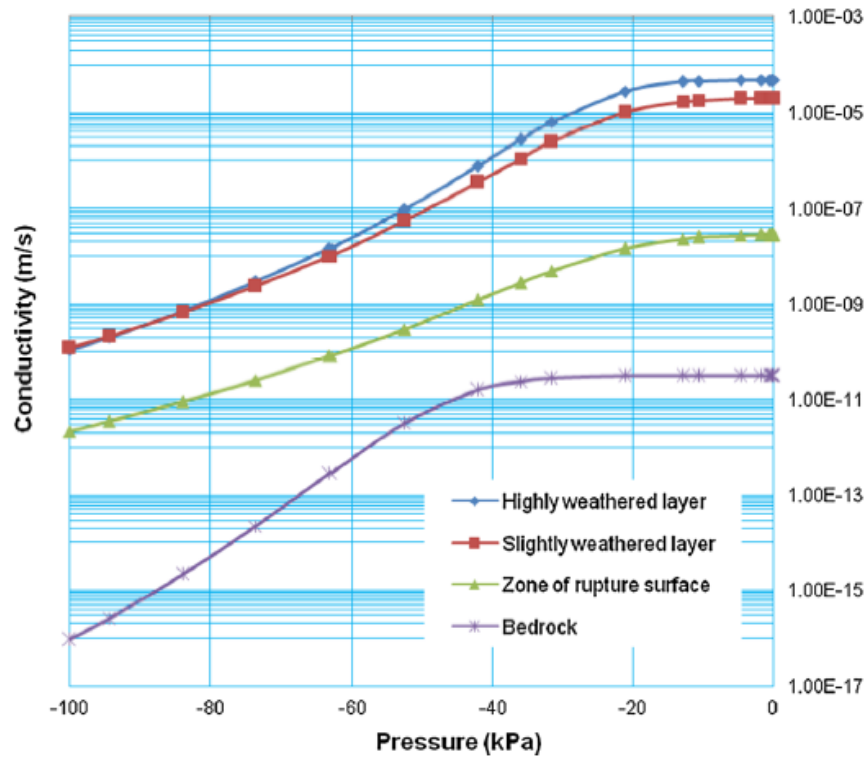


Figure 3-3 Hydraulic conductivity function (Jian et al., 2014)

3.5 Simulation model

3.5.1 Geometry for SEEP/W and SLOPE/W

In the first step of building the model, the geometry of the soil slope should be defined. In Figure 2-3, the length and height of the slope are roughly shown, and it is divided into four layers. There is a very thin layer in the middle, which is the previous rupture surface. According to the above conditions, a 2D slope model is defined for seepage field and slope stability analysis. Finally, the length is 1130 meters, and the height is 420 meters. It is divided into four layers and decomposed into 1716 nodes and 1558 elements. This step is very important, and the geometry of the slope will have a significant impact on the results. After completing this step, this geometric shape can be directly applied to two modules at the same time.

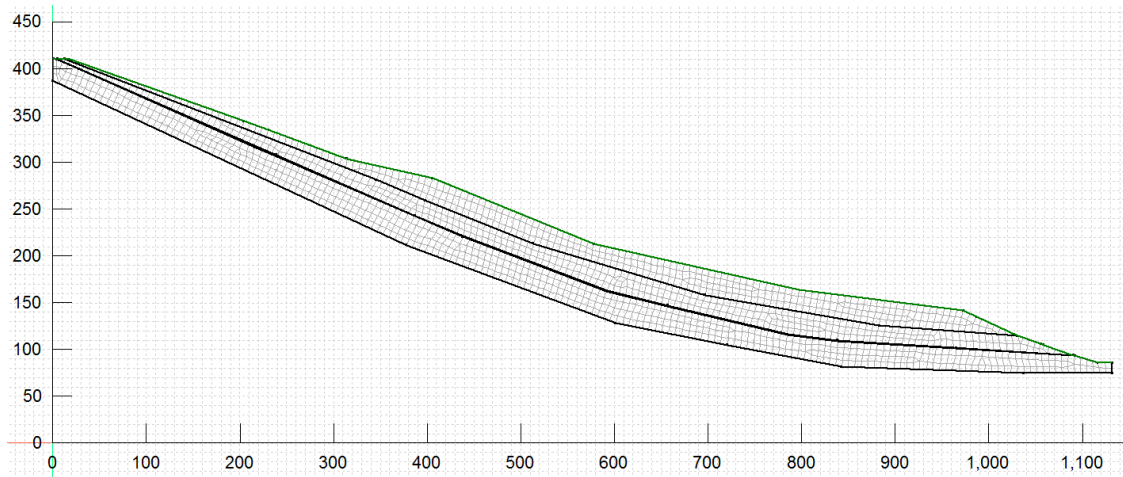


Figure 3-4 Geometry shape of the soil slope

3.5.2 Define material properties

In chapter 3.4.1, conditions such as SWCC and soil saturated permeability coefficient are mentioned. Therefore, these can be directly used to define materials in SEEP/W analysis. The conventional material model will choose Saturated/Unsaturated. In Table 3-1, the parameters of different layers are also integrated. These can also be directly used in the analysis of Slope/W; the parameters that need to be used are unit weight, cohesion, friction angle. In the material model selection of SLOPE/W, the bedrock can be directly defined as a non-sliding layer. The rest of the layers can choose Mohr-Coulomb as their material model.

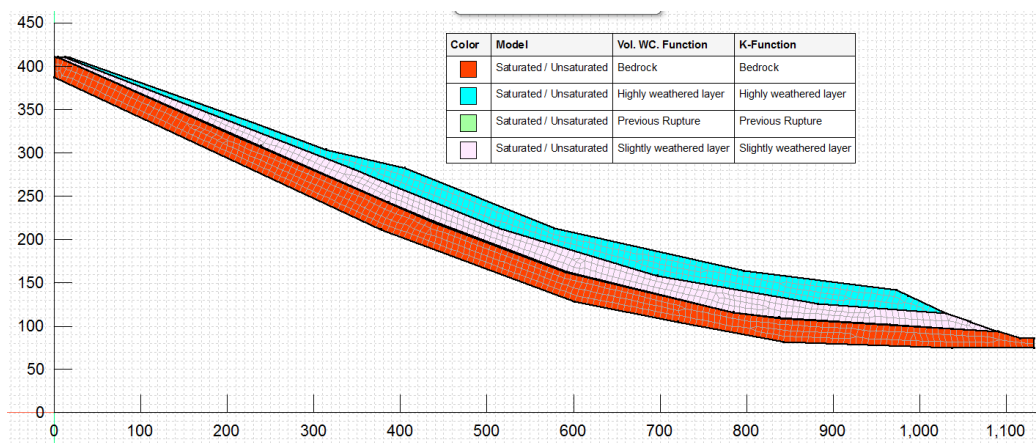


Figure 3-5 Defined material properties for SEEP/W analysis

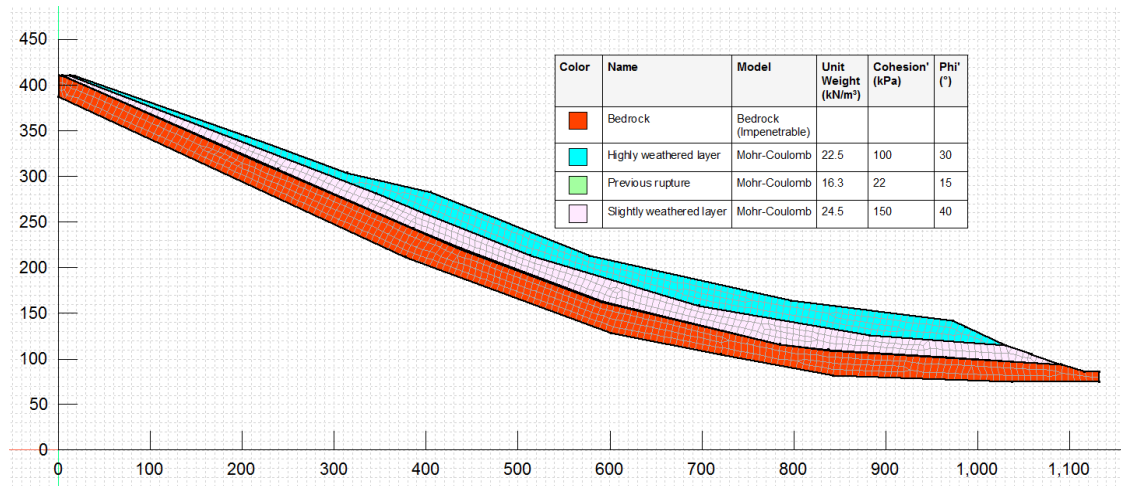


Figure 3-6 Defined material properties for SLOPE/W analysis

3.5.3 Analysis type and slip surface

For SEEP/W, hydraulic conditions will change over time. Therefore, for the first research purpose, to accurately grasp the daily situation, the transient analysis in SEEP/W can be used so that the daily results from June 1 to July 14 can be grasped. The analysis method chosen in SLOPE/W is Morgenstern-Price since it is more popular. When considering the initial hydraulic conditions, by directly applying the result of SEEP/W to SLOPE/W. The daily critical factor of safety and failure surfaces verse time can be determined. In the setting of the sliding surface, first, the direction of sliding may be chosen as “from left to right”, and then choose “entry and exit” in the options. Finally, the entrance and exit slip surface lines are added to the model. This slip surface line should cover most of the locations as much as possible in order to obtain more accurate results. After these steps are completed, the program could be run.

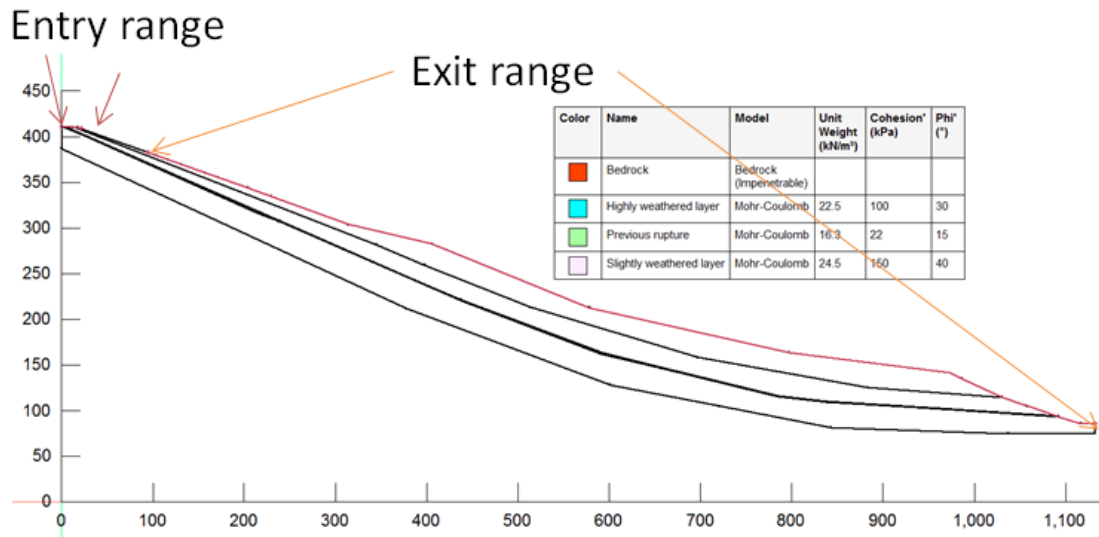


Figure 3-7 Slip surface setting for SLOPE/W analysis

3.5.4 Boundary condition for first research purpose

For the first research purpose: In SEEP/W, boundary condition needs to be added to apply hydraulic conditions to the program. In Figure 2-10, changes in groundwater level and rainfall are mentioned. Therefore, these data must be converted into boundary conditions to be added to the model. For the rise of the water level, it is only necessary to set the total water pressure as a function of time. For rainfall, it will be added to the model in the form of water flux. One thing to note here is that the definition of rainfall is the depth of rain falling on a horizontal surface in a certain period. Therefore, it is necessary to convert the rainfall value to water flux before adding it to the model. By comparing the values of soil conductivity and water flux, it can be found that the value of soil conductivity is larger than that of water flux. Therefore, the rainfall can completely infiltrate into the soil. For the second research purpose, the boundary conditions will be mentioned in the following section.

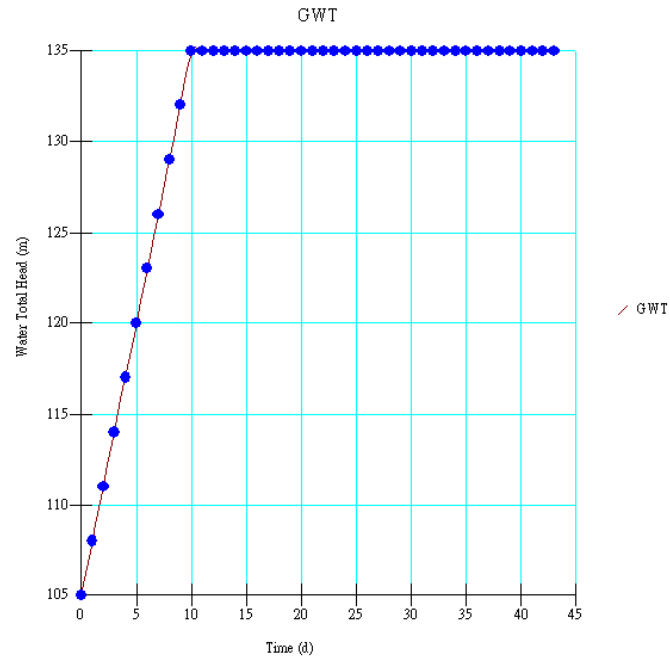


Figure 3-8 Change in water total head versus time for SEEP/W analysis

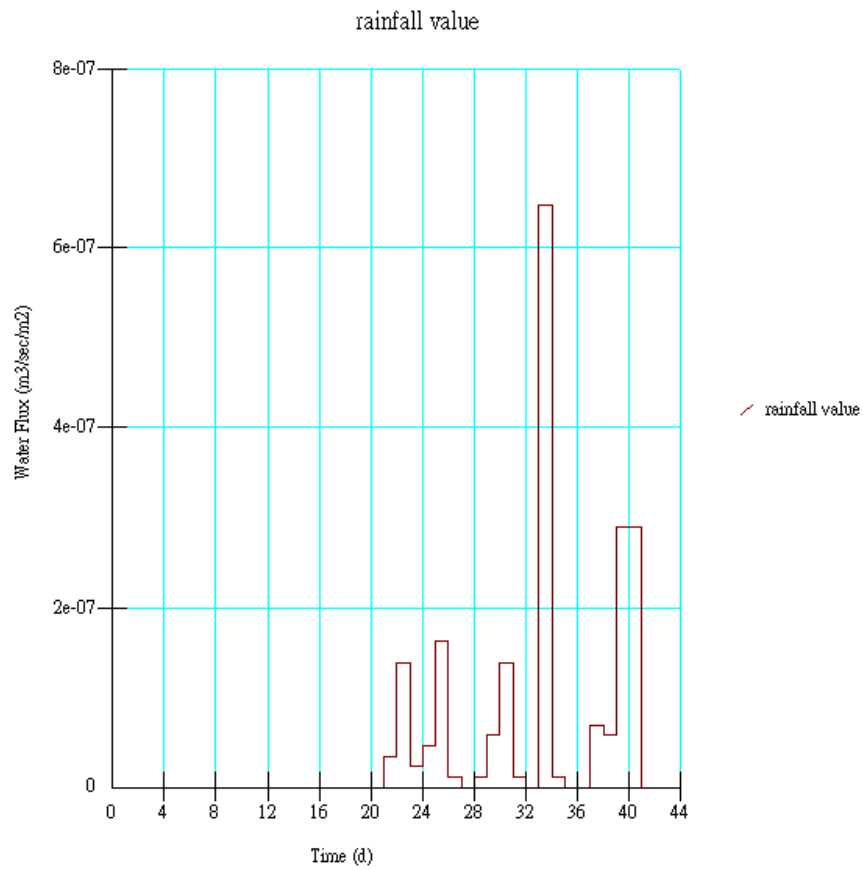


Figure 3-9 Daily rainfall versus time for SEEP/W analysis

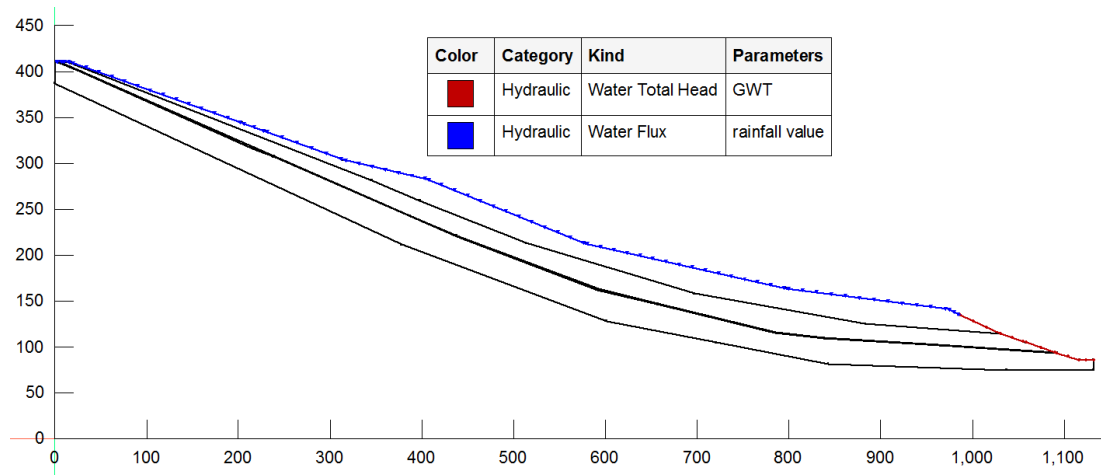


Figure 3-10 Boundary condition setting for SEEP/W analysis

3.5.6 Boundary condition for second and third research purpose

For the second purpose, the content of the boundary condition needs to be adjusted. In Chapter 2.2, four rainfall patterns are mentioned: advanced, normal, delayed, and uniform rainfall. It was assumed that the four rainfall patterns (shown in Table 3-1) have the same rainfall intensity, rainfall duration, permeability coefficient, and initial groundwater level. Therefore, the first 20 days of the previous analysis are used as the same initial state. Then, the geometry and material remain unchanged. Finally, four rainfall models are applied to the model to find out their different impacts. The simulation process includes nine days of rainfall, the maximum rainfall is 100 mm (the average value is 50 mm), so the duration and rainfall intensity of the four conditions are the same. After nine days of rainfall, another nine days will be analyzed to observe its effects.

In addition, in order to study the influence of rainfall intensity on slope stability. As shown in Figure 3-15, the "uniform" rainfall pattern is improved by changing the boundary conditions. For comparison, the daily rainfall will increase

from 50 mm to 75 mm and 100 mm. Through the three sets of results, it can be determined whether the total amount of rainfall will affect the results.

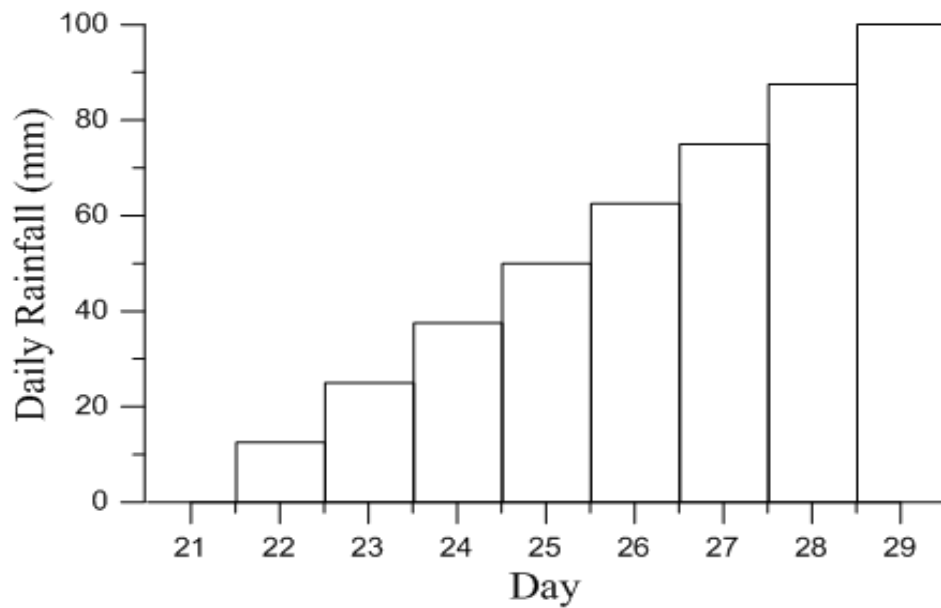


Figure 3-11 “Delayed” rainfall pattern

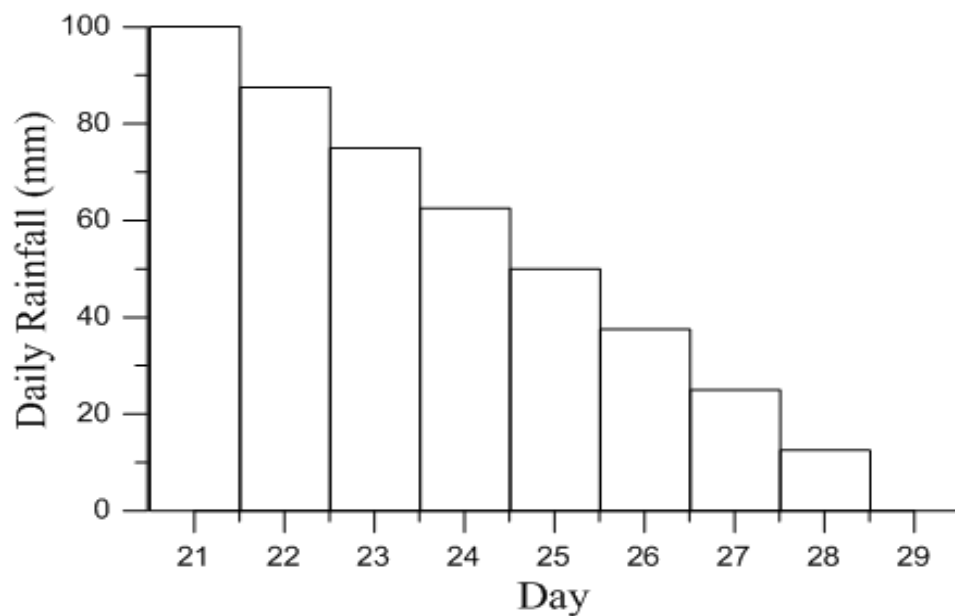


Figure 3-12 “Advanced” rainfall pattern

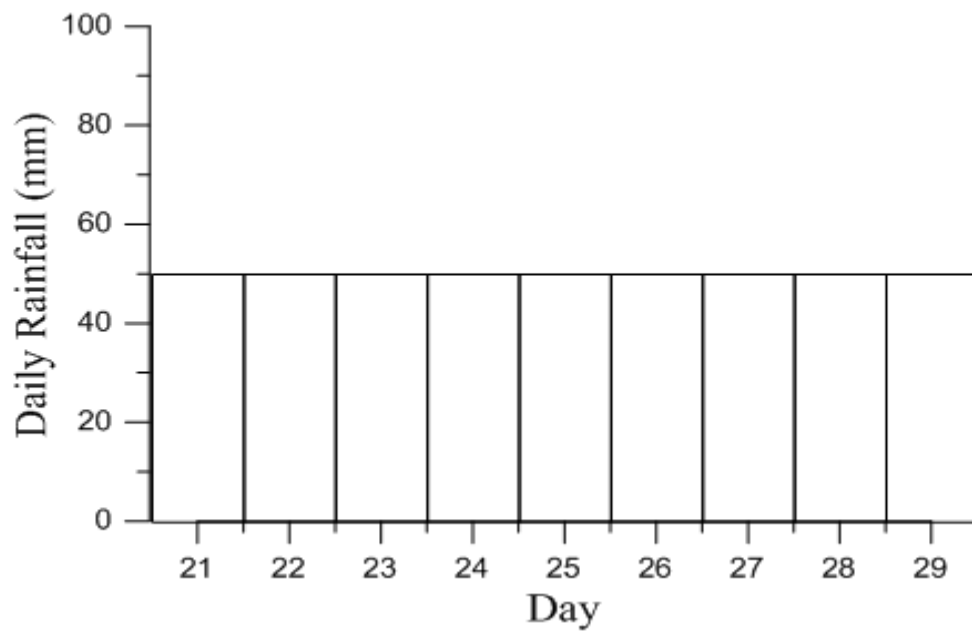


Figure 3-13 “Uniform” rainfall pattern

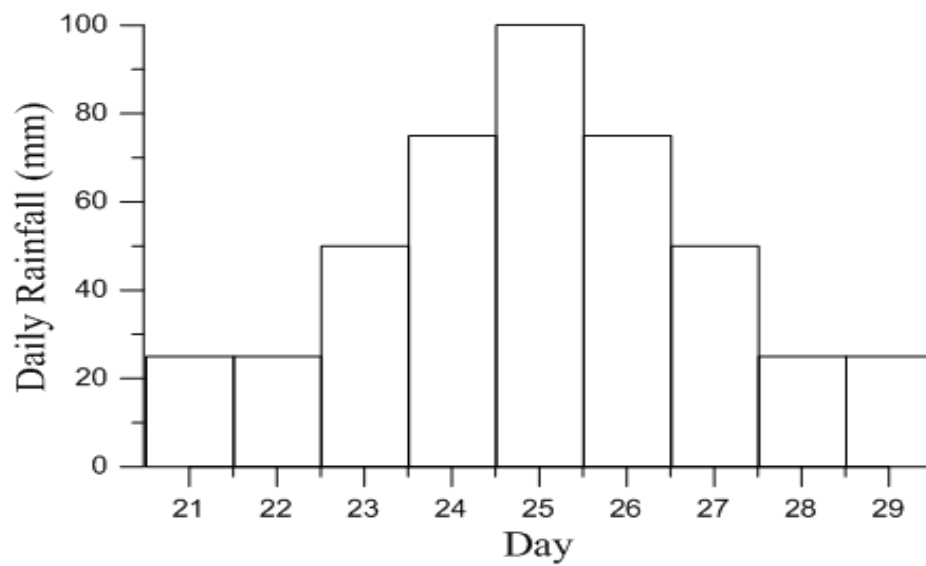


Figure 3-14 “Normal” rainfall pattern

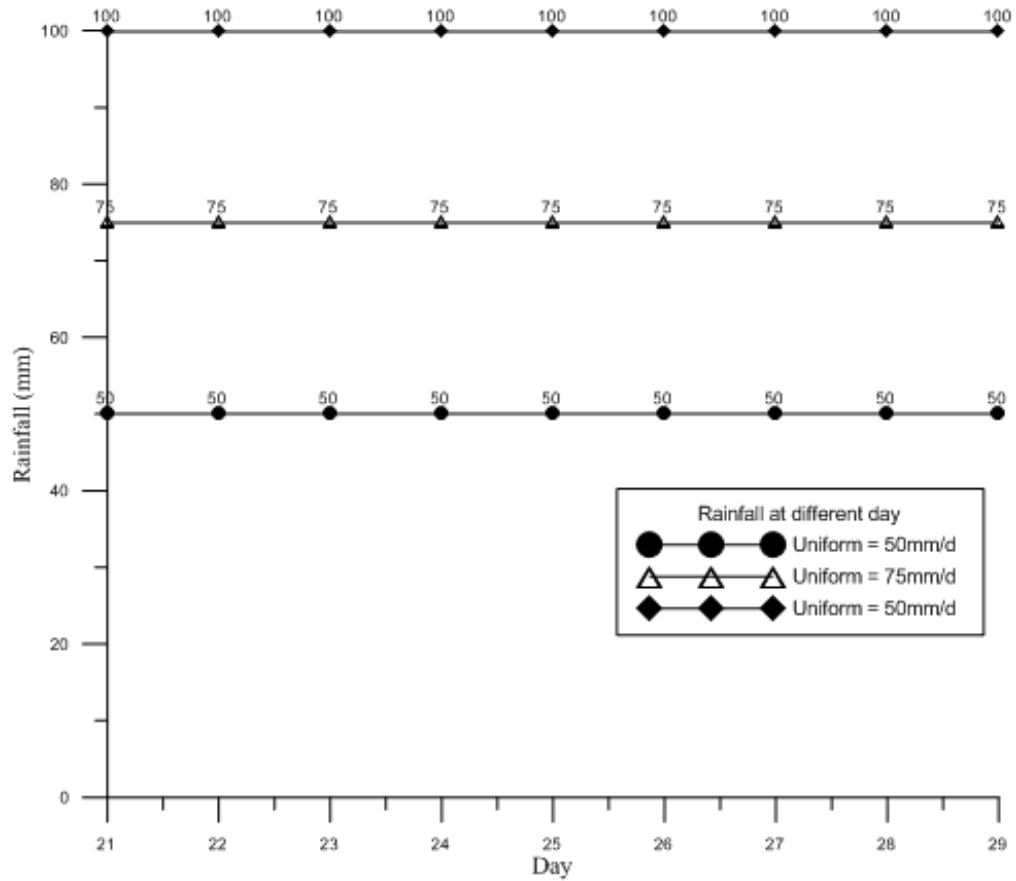


Figure 3-15 rainfall setting for rainfall intensity study

3.5.7 Summary

Summary of the analysis process for the first research purpose:

Table 3-2 Analysis process for the first research purpose

	Time	Phenomenon
STEP1	Initial state	WL=105m
STEP2	Day1 to 10	The water level rises by 3 meters/day
STEP3	Day11 to 20	WL=135m
STEP4	Day21 to 43	Continuous rainfall

Summary of the analysis process for the second research purpose:

Table 3-3 Analysis process for the second research purpose (Delayed)

	Time	Phenomenon
STEP1	Initial state	WL=105m
STEP2	Day1 to 10	The water level rises by 3 meters/day
STEP3	Day11 to 20	WL=135m
STEP4	Day21 to 38	Pattern: Delayed

Table 3-4 Analysis process for the second research purpose (Advanced)

	Time	Phenomenon
STEP1	Initial state	WL=105m
STEP2	Day1 to 10	The water level rises by 3 meters/day
STEP3	Day11 to 20	WL=135m
STEP4	Day21 to 38	Pattern: Advanced

Table 3-5 Analysis process for the second research purpose (Uniform)

	Time	Phenomenon
STEP1	Initial state	WL=105m
STEP2	Day1 to 10	The water level rises by 3 meters/day
STEP3	Day11 to 20	WL=135m
STEP4	Day21 to 38	Pattern: Uniform

Table 3-6 Analysis process for the second research purpose (Normal)

	Time	Phenomenon
STEP1	Initial state	WL=105m
STEP2	Day1 to 10	The water level rises by 3 meters/day
STEP3	Day11 to 20	WL=135m
STEP4	Day21 to 38	Pattern: Normal

Summary of the analysis process for the third research purpose:

Table 3-7 Analysis process for the second research purpose (rainfall intensity analysis)

	Time	Phenomenon
STEP1	Initial state	WL=105m
STEP2	Day1 to 10	The water level rises by 3 meters/day
STEP3	Day11 to 20	WL=135m
STEP4	Day21 to 38	Pattern: Uniform(50mm, 75mm,100mm)

3.6 Monitoring Points

After completing the above steps, the final model will be able to run and get the results. The model in Figure 3-16 will be used for seep / W analysis, and the model in Figure 3-17 will be used for slope / W analysis. For the first purpose, it is necessary to add points A, B, and C to the seep / W model to monitor the change of pore water pressure. Point B is located on the slope surface and its main function is to monitor the impact of rainfall. Points A and C are located at the bottom of the slope and are mainly used to monitor the impact of water level changes. These data are of great help to find out the mechanism and cause of the landslide. For the SLOPE/W model, the factor of safety is calculated directly by using the method of limit equilibrium, so it is not necessary to add some monitoring points to observe its changes.

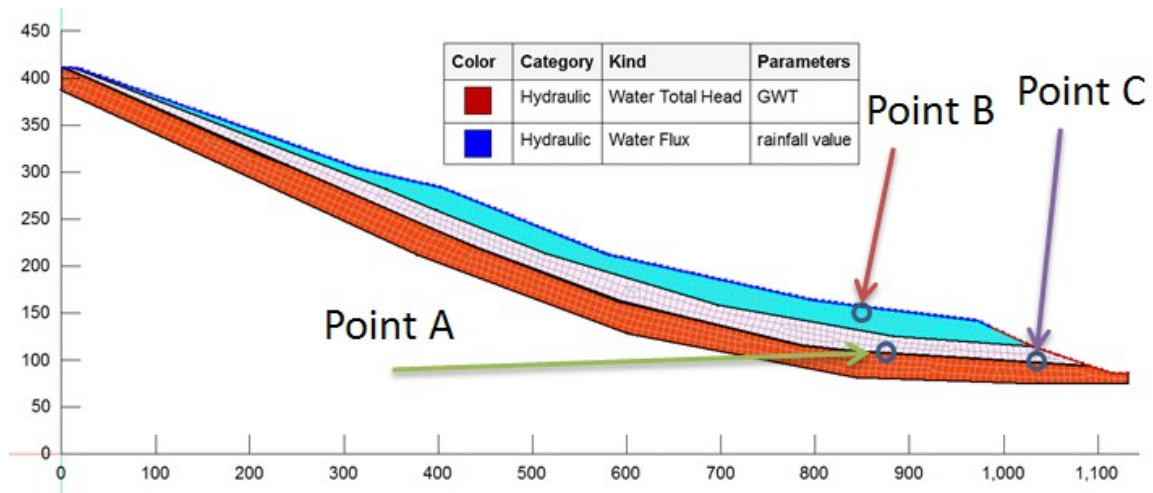


Figure 3-16 final models in SEEP/W module

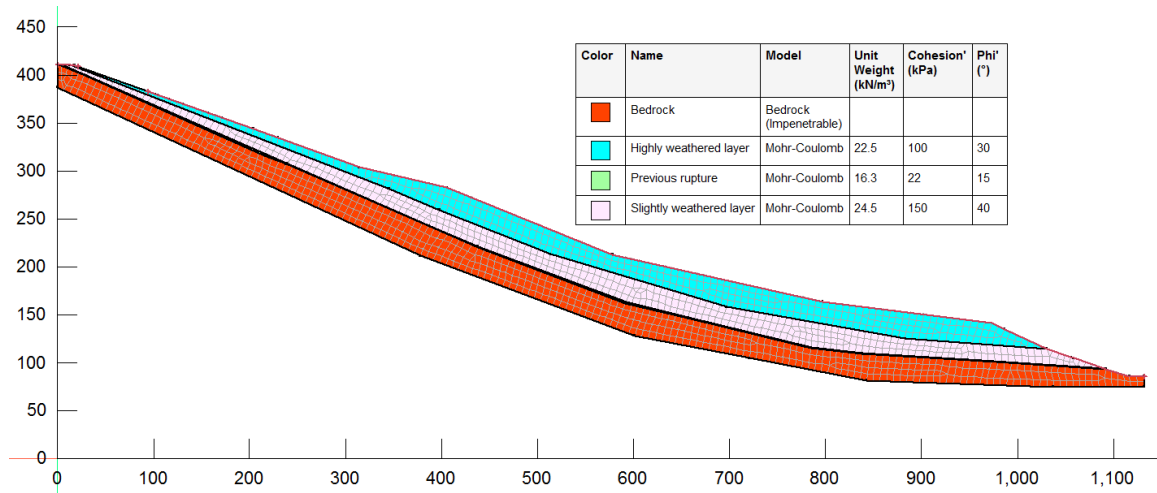


Figure 3-17 final models in SLOPE/W module

Chapter 4 ANALYSIS RESULTS AND DISCUSSION

4.1 Results for the first research purpose (research on Qianjiangping landslide)

In order to express the date more conveniently, the whole event is divided into four steps. Step one is to maintain WL=105m unchanged, which is a steady-state analysis. The second step is to ascend WL from 105m to 135m for ten days and 3 meters per day. Step three is to maintain the water level at 135m for ten days. The final step is to consider 23 days of rainfall. The following will show the results of these four steps in SEEP/W and SLOPE/W.

4.1.1 Results from SEEP/W

From Figure 4-1-1 to 4-1-23, there will be a large number of similar photos, which are derived from our SEEP/W analysis. In order to make it easier to understand the results, a table will be provided below to express the phenomena that occurred on different days.

Table 4-1 Phenomena in different stages and days

	Step	Day	Phenomenon
Figure 4-1-1	1	Initial state	The groundwater level is almost horizontal
Figure 4-1-2	2	1	The water level is constantly rising, and because of the low hydraulic conductivity of the slope, the groundwater level seems to slope downward.
Figure 4-1-3	2	3	
Figure 4-1-4	2	5	
Figure 4-1-5	2	7	
Figure 4-1-6	2	9	
Figure 4-1-7	2	10	

Figure 4-1-8	3	11	The groundwater level gradually tends to be flat. This is because the hydraulic gradient is reduced, and the water flows more slowly into the slope.
Figure 4-1-9	3	13	
Figure 4-1-10	3	15	
Figure 4-1-11	3	17	
Figure 4-1-12	3	19	
Figure 4-1-13	3	20	
Figure 4-1-14	4	21	Less rainfall, coupled with slow water infiltration, and therefore no significant changes.
Figure 4-1-15	4	23	
Figure 4-1-16	4	25	
Figure 4-1-17	4	27	Rainwater infiltration began to appear above the slope.
Figure 4-1-18	4	29	
Figure 4-1-19	4	31	Due to continuous rainfall, the saturation zone on the slope surface is increasing.
Figure 4-1-20	4	33	
Figure 4-1-21	4	35	
Figure 4-1-22	4	37	
Figure 4-1-23	4	39	There is a small amount of rainfall, and the saturated zone above the slope is shifting to the bottom of the slope
Figure 4-1-24	4	41	
Figure 4-1-25	4	43	

The results of the first three steps of the analysis are listed below. Figure 4-1-1 is the result of the first step, Figure 4-1-2 to 4-1-7 are the result of the second step, and Figure 4-1-8 to 4-1-13 are the third The results of the steps, and Figures 4-1-14 to 4-1-25 are the results of the last step.

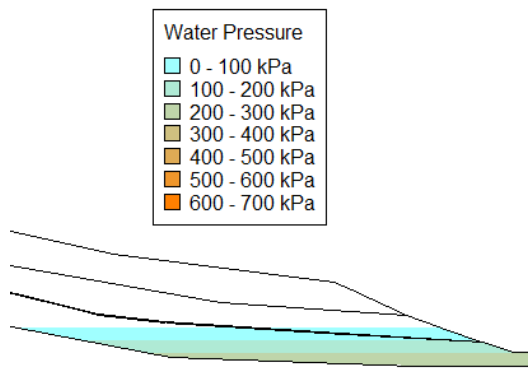


Figure 4-1-1 SEEP/W first step results (Initial)

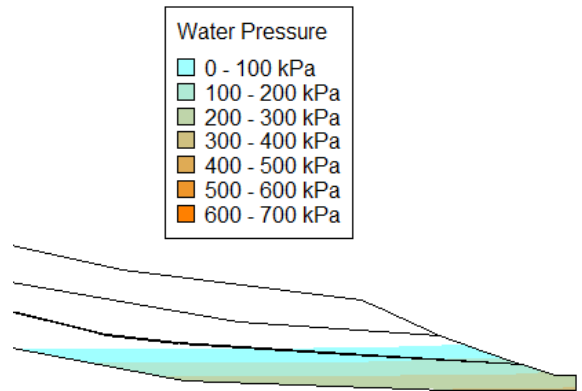


Figure 4-1-2 SEEP/W second step results (day1)

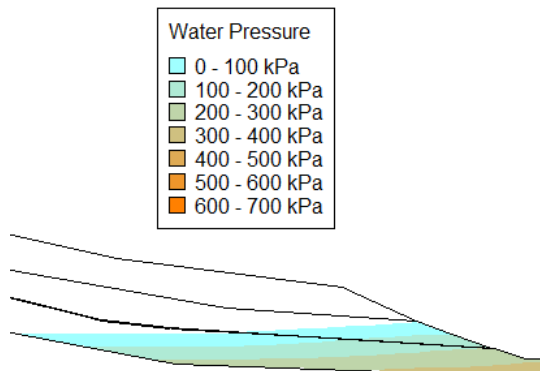


Figure 4-1-3 SEEP/W second step results (day3)

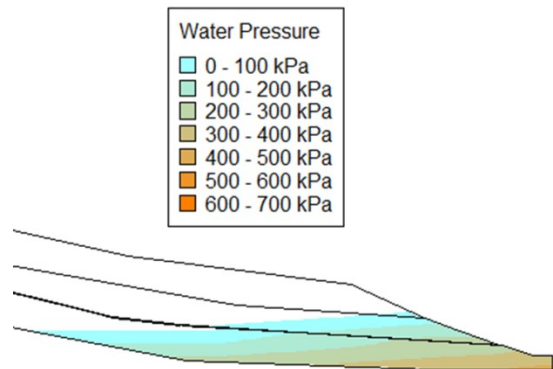


Figure 4-1-4 SEEP/W second step results (day5)

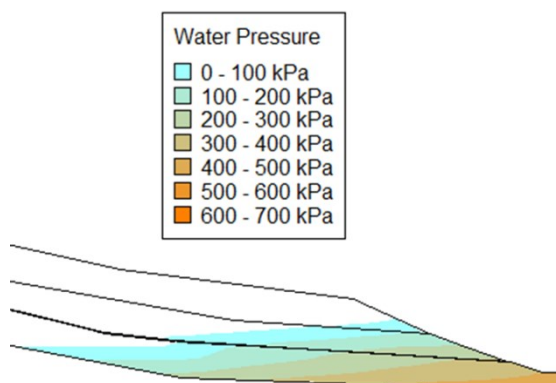


Figure 4-1-5 SEEP/W second step results (day7)

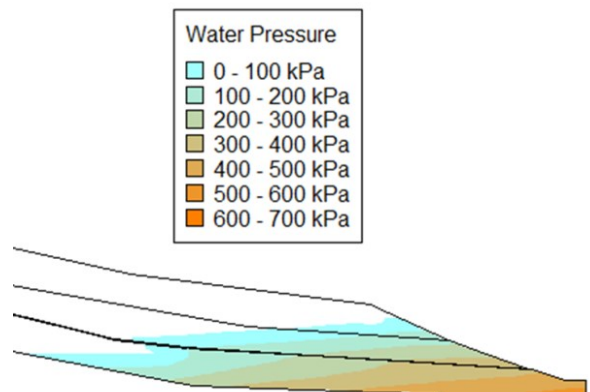


Figure 4-1-6 SEEP/W second step results (day9)

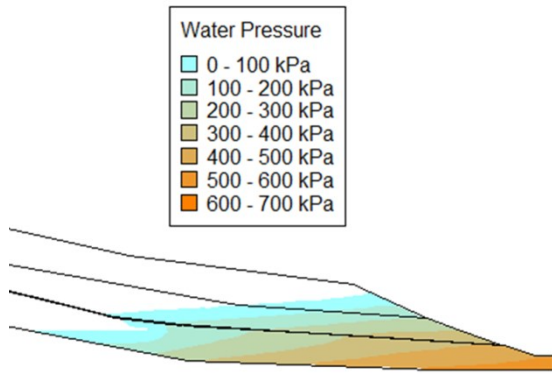


Figure 4-1-7 SEEP/W second step results (day10)

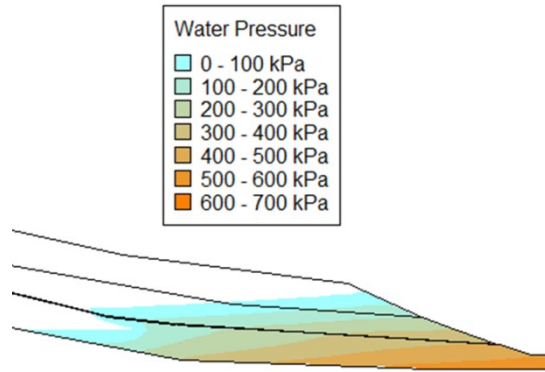


Figure 4-1-8 SEEP/W third step results (day11)

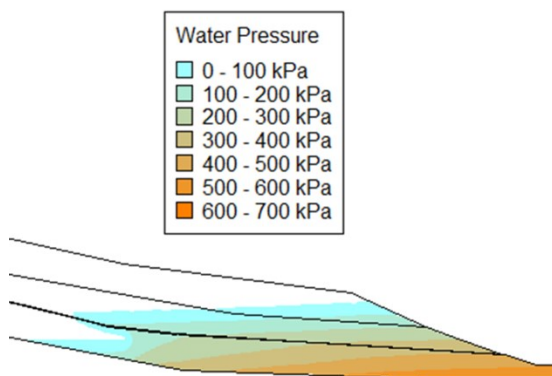


Figure 4-1-9 SEEP/W third step results (day13)

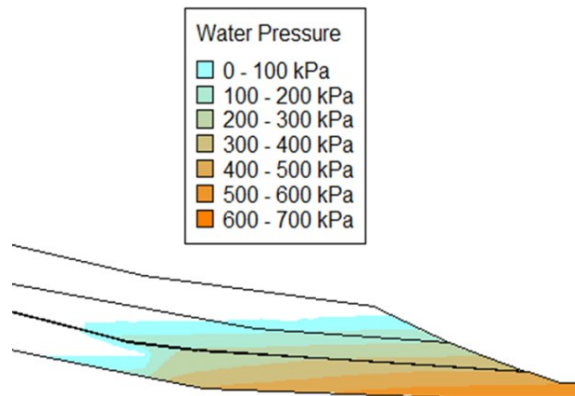


Figure 4-1-10 SEEP/W third step results (day15)

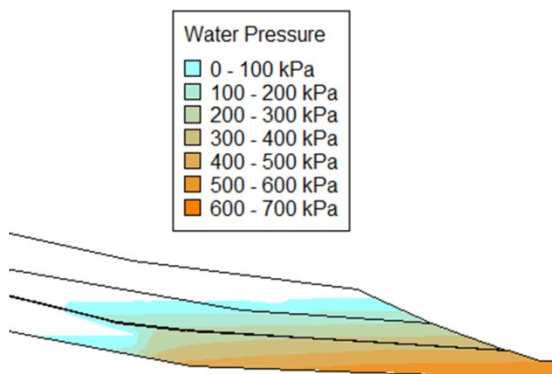


Figure 4-1-11 SEEP/W third step results (day17)

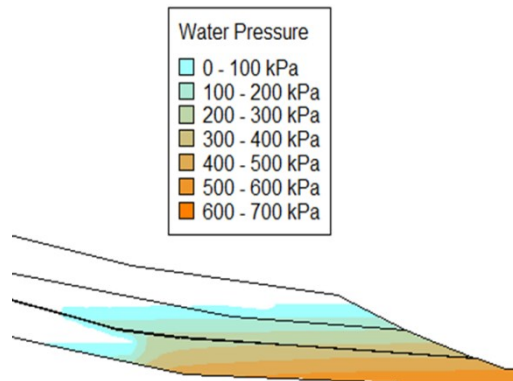


Figure 4-1-12 SEEP/W third step results (day19)

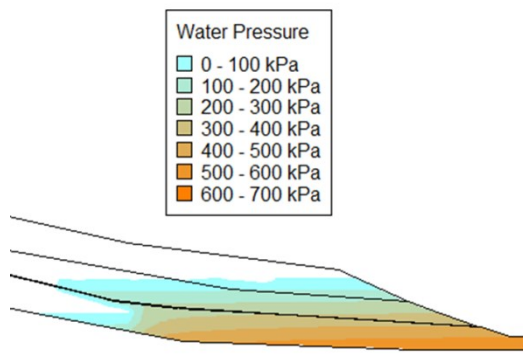


Figure 4-1-13 SEEP/W third step results (day20)

As the result of step one, it can be found that the groundwater level is almost horizontal. The result is almost the same as the result of the on-site investigation. Therefore, the simulation results are reasonable and can be used as initial conditions for the next few steps. After completing the first step, it may start to simulate the transient seepage field, which simulates the water level rising three meters per day, from 105 meters to 135 meters. In addition, the results of the first, third, fifth, seventh, ninth, and tenth days are listed. When the water level continues to rise, the water will slowly flow into the slope. From above, it can be easily observed that the groundwater level seems to slope downward. This is due to the low hydraulic conductivity of the slope. Therefore, the rate at which water penetrates the slope is much slower than the rate at which the water level rises, which causes this phenomenon. In step three analyses, the simulated water level was maintained at the final water level of the previous part for ten days. The results obtained can be used to compare with the previous part; the groundwater level gradually tends to be flat. The rate of change in the first few days will be greater than the rate of change in the following days. This is because the hydraulic gradient is reduced, so the water flows more slowly into the slope.

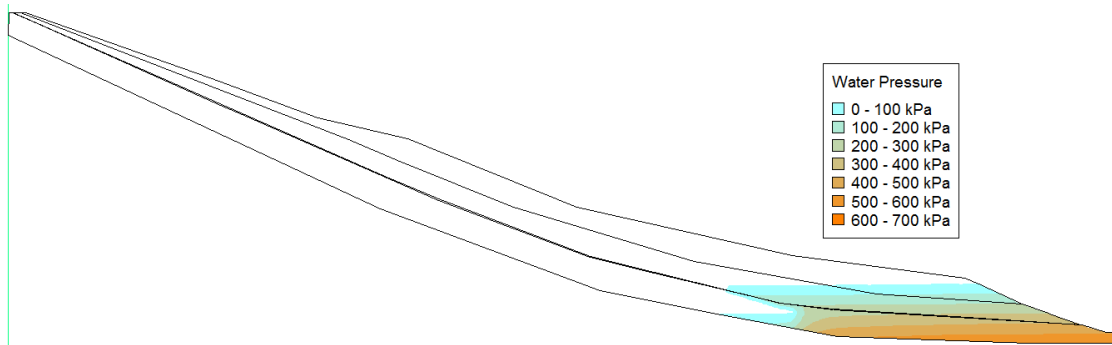


Figure 4-1-14 SEEP/W final step results (day21)

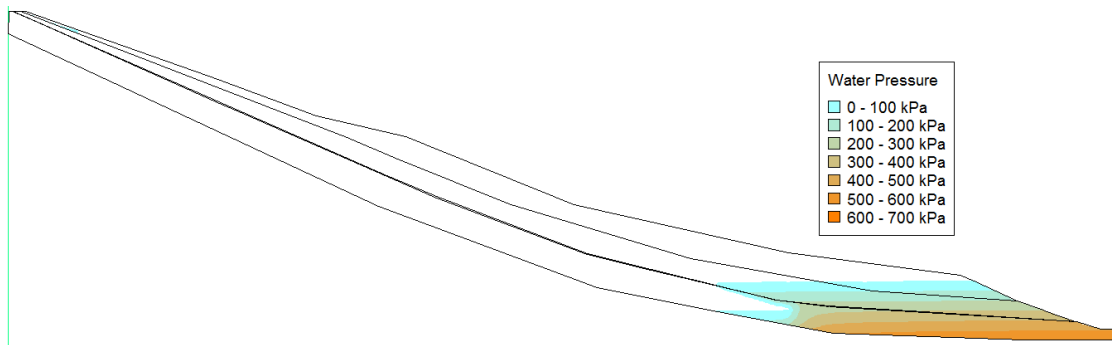


Figure 4-1-15 SEEP/W final step results (day23)

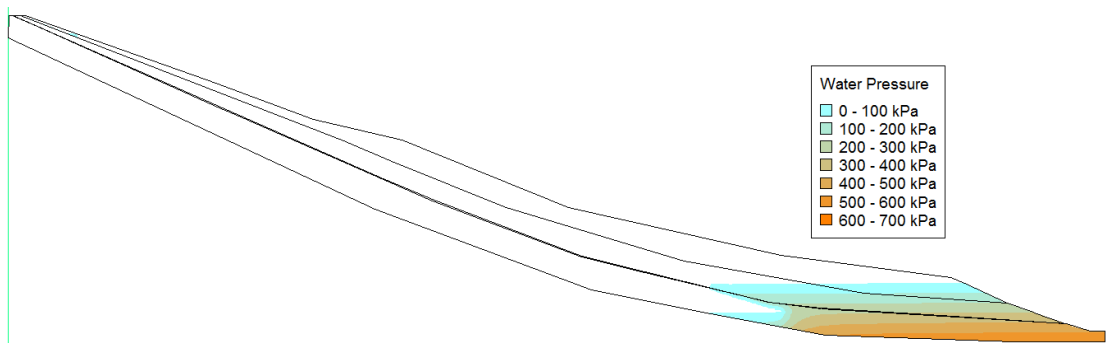


Figure 4-1-16 SEEP/W final step results (day25)

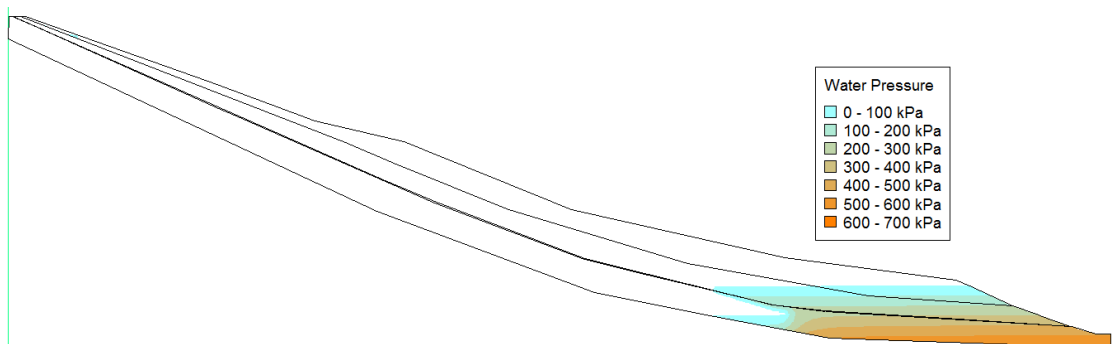


Figure 4-1-17 SEEP/W final step results (day27)

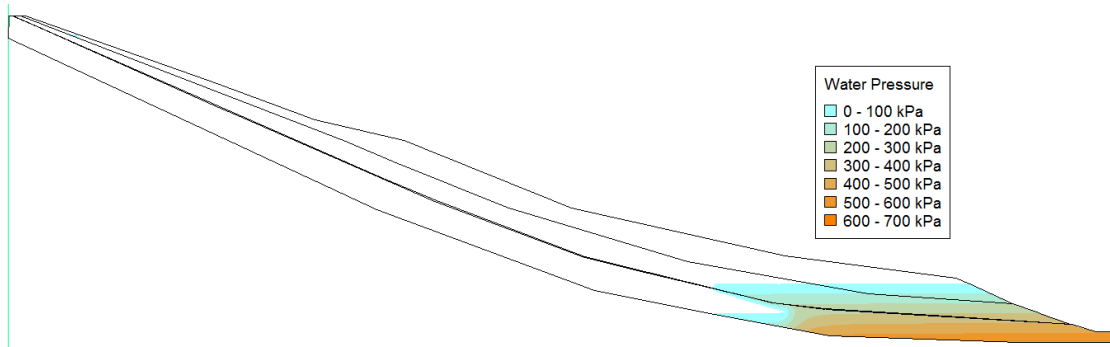


Figure 4-1-18 SEEP/W final step results (day29)

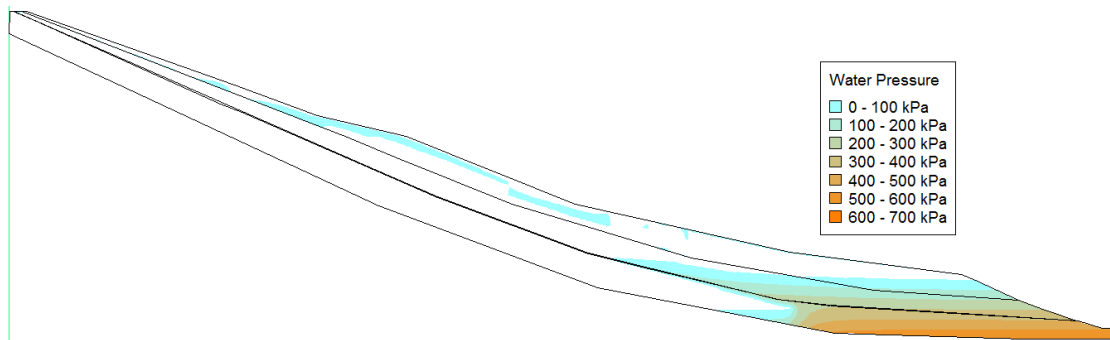


Figure 4-1-19 SEEP/W final step results (day31)

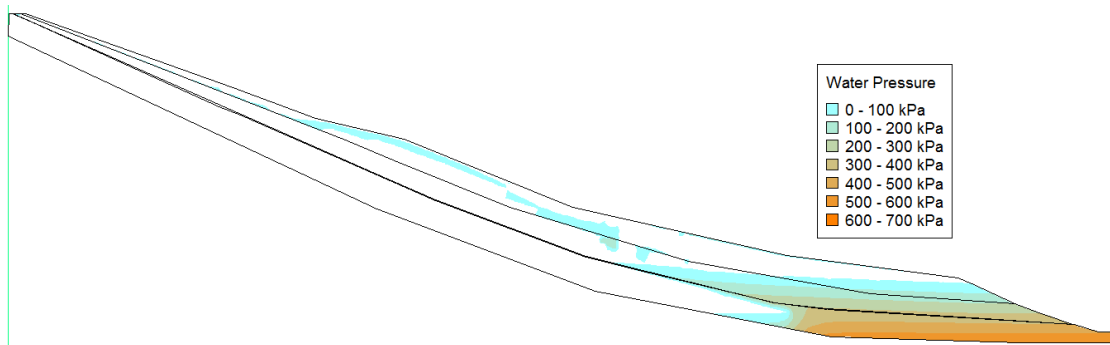


Figure 4-1-20 SEEP/W final step results (day33)

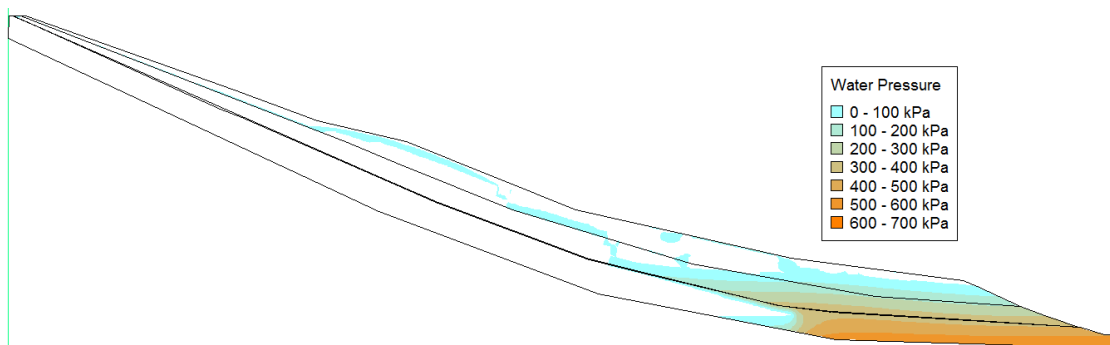


Figure 4-1-21 SEEP/W final step results (day35)

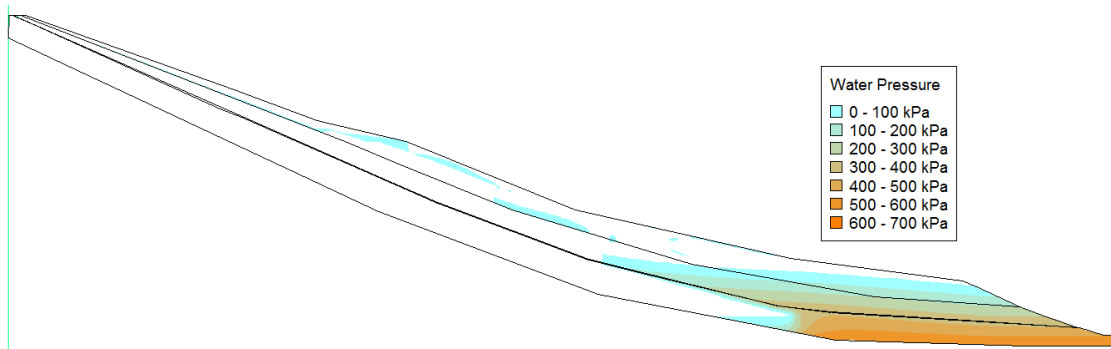


Figure 4-1-22 SEEP/W final step results (day37)

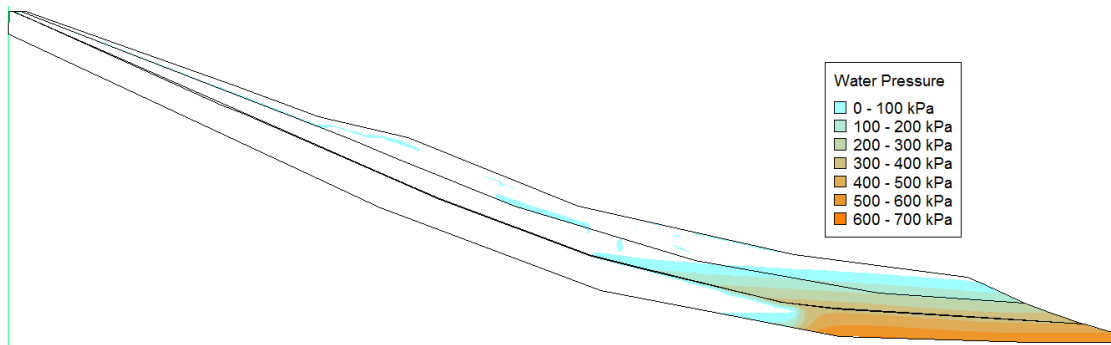


Figure 4-1-23 SEEP/W final step results (day39)

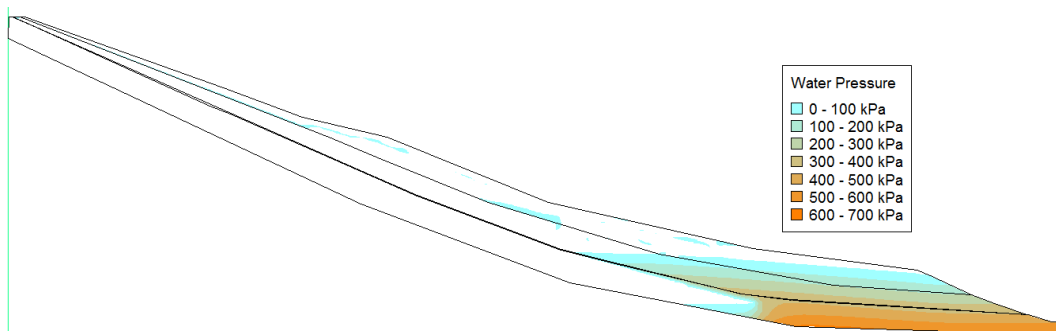


Figure 4-1-24 SEEP/W final step results (day41)

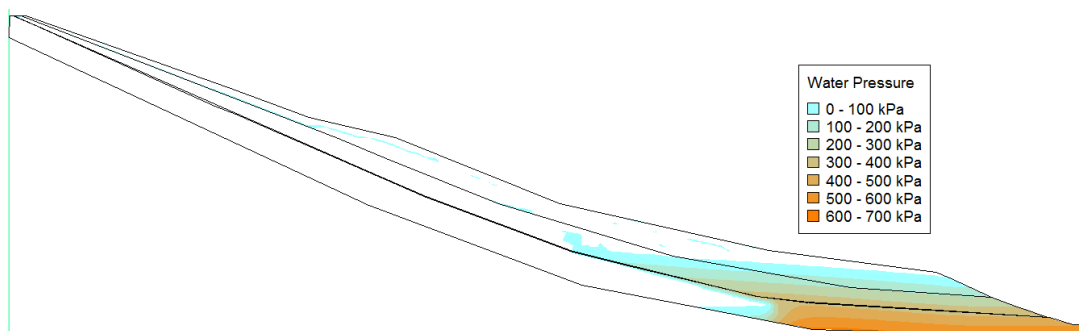


Figure 4-1-25 SEEP/W final step results (day43)

In the last step of the analysis, the results of a few days are listed. From the above results, it can be seen that in the days before the rainfall, there was little rainfall and a slow infiltration rate, so there was no obvious change in the slope. On the 27th day, it was gradually discovered that a small saturation zone appeared above the slope, but its area was small, and it was not easy to find. On the 31st day, a saturation zone was also formed on the slope surface. In the next few days, due to the continuous rainfall, the area of the saturation zone continued to increase and shifted to the lower part of the slope, while at the same time a small increase in the groundwater level was observed. Under the combined influence of these factors, the landslide finally occurred.

In the next section, the changes in pore water pressure monitored by points A, B, and C during the water level changes and rainfall periods will be listed. These data will be combined with the results of the subsequent slope stability analysis to determine whether the results of the analysis are reasonable.

4.1.1.1 SEEP/W result analysis

Since the pictures listed in the previous part can only show the approximate changes of the seepage field, some internal numerical changes cannot be drawn. Therefore, in order to have a deeper understanding of its internal numerical changes, it was mentioned at the end of Chapter 3 that in the analysis of SEEP/W, three points A, B, and C were added to monitor the numerical changes. Point A and C are mainly used to monitor the impact of water level changes (the first 20 days of analysis), while point B is mainly used to monitor the impact of rainfall (the 21st day to the end of the analysis). The following chart lists the change in water pressure from the beginning.

The initial value of all points is zero, and the meaning of the subsequent value is the amount of change from the initial state.

Table 4-2 Amount of PWP change detected by Point A

Day	Change in PWP (kPa)	Day	Change in PWP (kPa)
0	0	22	262.29093
1	0.00069	23	266.9671
2	0.00976	24	270.92764
3	0.08157	25	273.75362
4	0.41637	26	276.04673
5	1.44162	27	278.007
6	5.15961	28	279.68288
7	15.08632	29	281.16211
8	32.09902	30	284.06176
9	53.83249	31	289.17107
10	78.28583	32	296.17317
11	103.58949	33	304.11215
12	128.10676	34	313.63363
13	150.99406	35	327.32615
14	171.70022	36	341.72436
15	190.14468	37	353.84424
16	206.17694	38	362.81406
17	219.94415	39	368.94123
18	231.5403	40	373.89943
19	241.40476	41	378.15799
20	249.7881	42	381.42556
21	256.68196	43	383.76623

Table 4-3 Amount of PWP change detected by Point C

Day	Change in PWP (kPa)	Day	Change in PWP (kPa)
0	0	22	292.86771
1	5.42264	23	293.21079
2	17.07352	24	293.46059
3	34.10537	25	293.63008
4	54.98607	26	293.75382
5	78.65576	27	293.84727
6	104.23043	28	293.91825
7	131.09624	29	293.97426
8	158.85562	30	294.03789
9	187.24002	31	294.12518
10	216.0098	32	294.23949
11	238.87977	33	294.37342
12	255.47989	34	294.54621
13	267.15005	35	294.77224
14	275.2678	36	295.01792
15	280.90367	37	295.24924
16	284.8166	38	295.44426
17	287.54004	39	295.59659
18	289.44224	40	295.72147
19	290.77825	41	295.82386
20	291.72215	42	295.90388
21	292.39112	43	295.96449

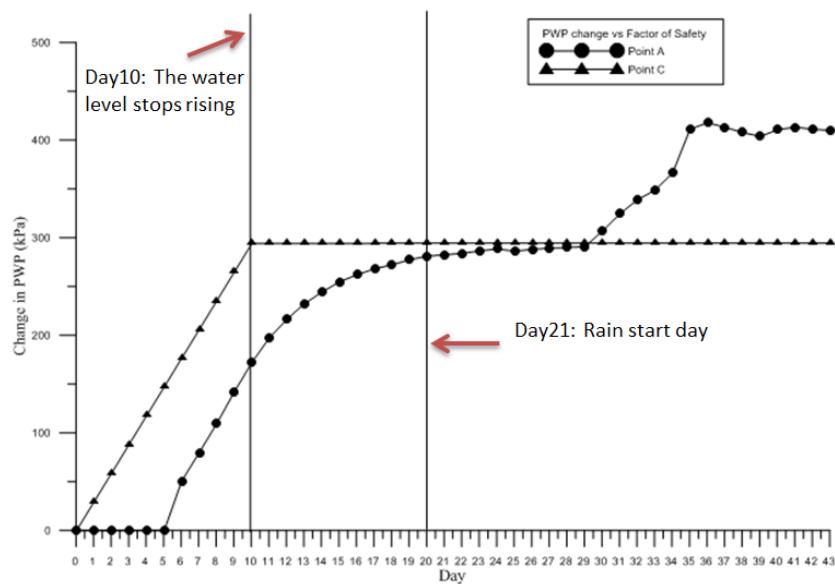


Figure 4-2 the change of PWP monitored by Point A and C over time

Since groundwater level has a certain impact on slope stability, it is necessary to discuss the impact of groundwater level. Figure 4-2 shows the change of PWP at points A and C over time. Combined with figures 4-1-2 to 4-1-7, it can be found that the PWP variation measured at point C will be greater than that at point A in the first ten days. It is because point C is closer to the water source. Therefore, when the water level continues to rise, the groundwater level will rise faster than point a, which is the reason why the PWP changes greatly. In addition, from the 11th day to the 20th day, since the water level was no longer rise, the water will slowly flow into the soil slope, and the groundwater level will gradually stabilize. Therefore, the groundwater level at point A has stabilized, while the groundwater level above point C will continue to rise. That's why the PWP of point a will change more than that of point C in the next ten days. From the 21st day to the end, rainfall will affect the groundwater level above point a, so PWP will continue to rise. On the contrary, the groundwater level above point C remains stable, so there will be no significant change.

Table 4-4 Amount of PWP change detected by Point B

Day	Change in PWP (kPa)	Day	Change in PWP (kPa)
0	0	22	197.68558
1	0	23	269.79201
2	0	24	277.53536
3	0	25	291.12598
4	0	26	299.40562
5	0	27	299.89416
6	0	28	300.37474
7	0	29	302.99125
8	0	30	309.00509
9	0	31	312.59448
10	0	32	312.91695
11	0	33	322.5374
12	0	34	428.138044
13	0	35	458.821352
14	0	36	452.858391
15	0	37	450.039608
16	0	38	447.951192
17	0	39	448.545002
18	0	40	454.564409
19	0	41	455.843015
20	0	42	456.35382
21	44.97985	43	457.12175

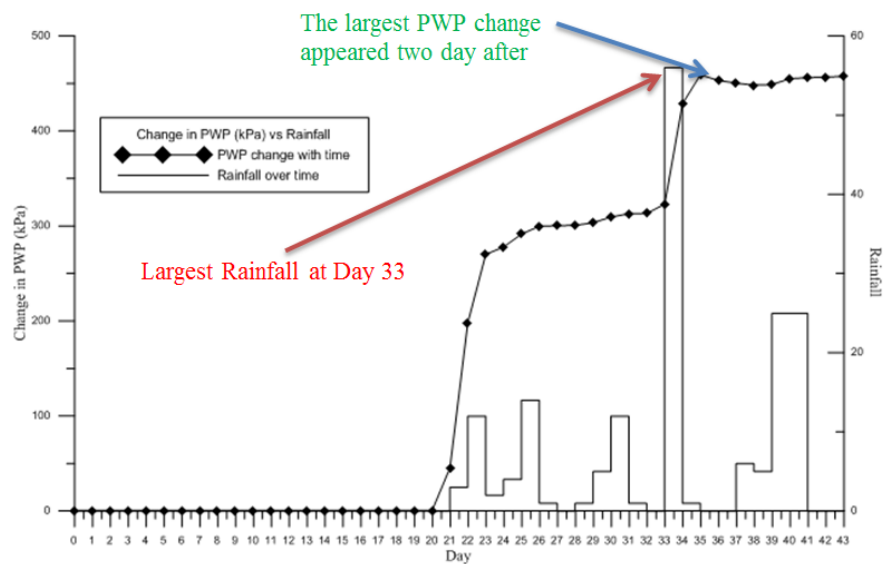


Figure 4-3 the change of PWP vs Rainfall (monitored by Point B)

Figure 4-3 lists the PWP changes from the beginning to the last day and puts the rainfall of each day for comparison. Since point B is located on the surface of the slope, as long as there is rainfall, the changes in PWP can be directly observed. It is worth mentioning that in the results of SEEP/W, there was no obvious change in the first few days of the rainfall. This is because the PWP at the beginning of the slope surface is negative (suction). With continuous rainfall, a more obvious saturated zone can be seen on day 31, but the locations of these saturated zones are not within the monitoring range of point B. This is why the saturation zone can be seen in figure 4-1-19, while the PWP in figure 4-3 does not change much on day 31. In addition, it can be seen from the figure that the largest rainfall occurred on day 33, while the largest change in PWP was on day 35, which proves that the impact of rainfall on slope stability is not immediate, but there will be a little delay.

4.1.2 Results from SLOPE/W

One of the advantages of using geo studio is that the analysis results of different modules can be transmitted to each other. By setting SEEP/W to parent analysis, the results of seepage analysis can be transmitted to SLOPE/W, so it is very convenient to analyze slope stability based on the SEEP/W seepage field. Since the failure surfaces are relatively similar, they will not be listed in this section. List only the last day of each step.

4.1.2.1 First step results of SLOPE/W analysis

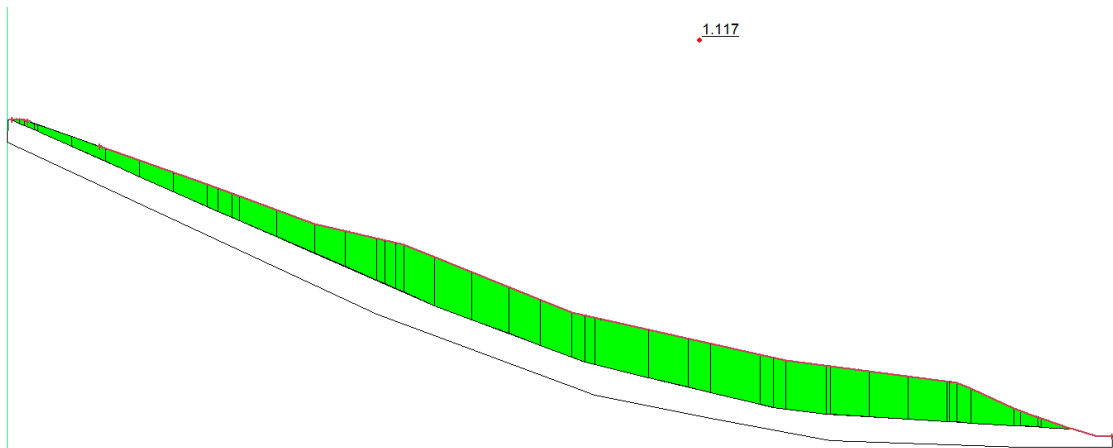


Figure 4-4 SLOPE/W first step results (Initial State)

In Figure 4-4, the FS of the slope in the initial state is 1.117. As mentioned in the previous chapter, the slope structure has some potential safety hazards. It can be seen from this value that its FS is not high. Therefore, it can be proved that the slope itself has some safety problems. This result will be used as the initial condition for other steps.

4.1.2.2 Second step results of SLOPE/W analysis

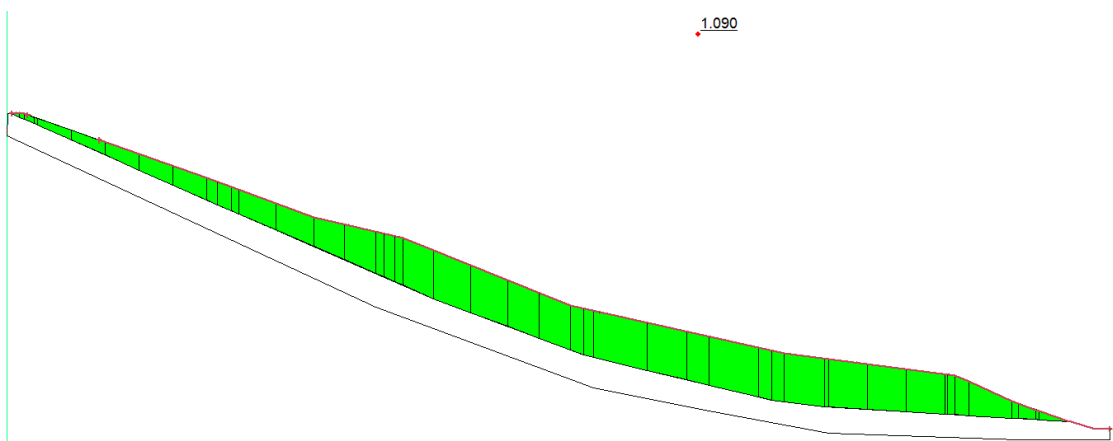


Figure 4-5 SLOPE/W second step results (day10)

Table 4-5 SLOPE/W second step results

Day	FS	Day	FS
1	1.116	6	1.102
2	1.115	7	1.099
3	1.113	8	1.096
4	1.11	9	1.094
5	1.106	10	1.09

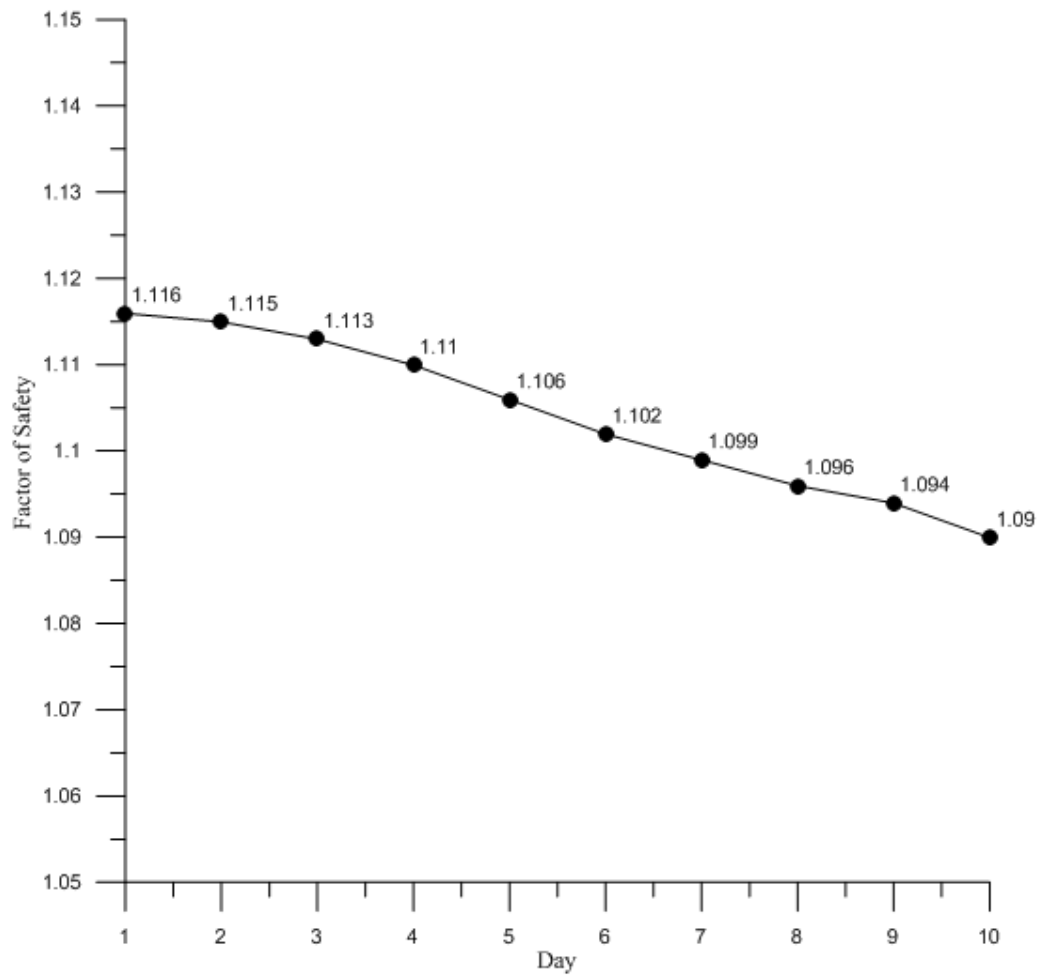


Figure 4-6 SLOPE/W second step results

It can be concluded from the above figure and table that due to the continuous rise of the water level, the factor of safety is continuously decreasing, starting from 1.116 and dropping to 1.09. Combined with the results of SEEP/W in the previous

part, the rise of the water level will affect the bottom of the slope, resulting in a decrease in its factor of safety.

4.1.2.3 Third step results of SLOPE/W analysis

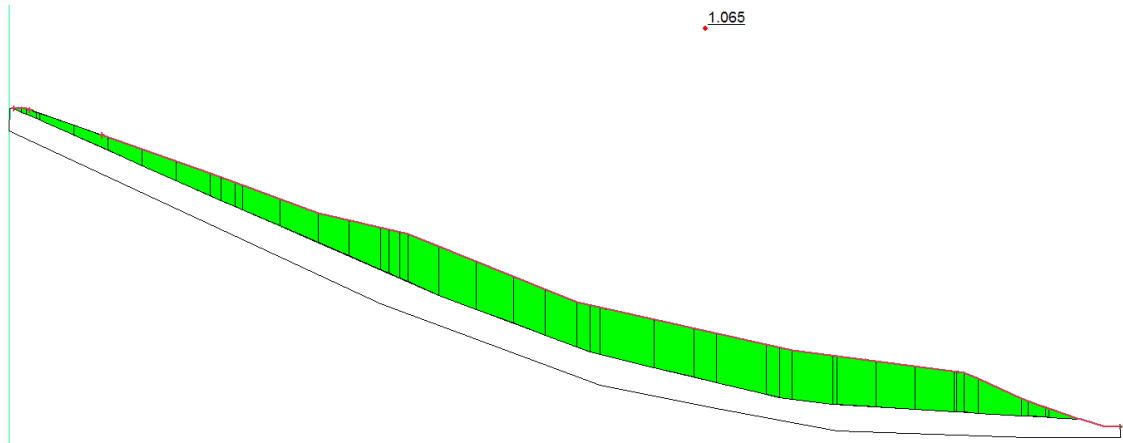


Figure 4-7 SLOPE/W third step results (day20)

Table 4-6 SLOPE/W third step results

Day	FS	Day	FS
11	1.085	16	1.07
12	1.081	17	1.068
13	1.078	18	1.067
14	1.074	19	1.066
15	1.071	20	1.065

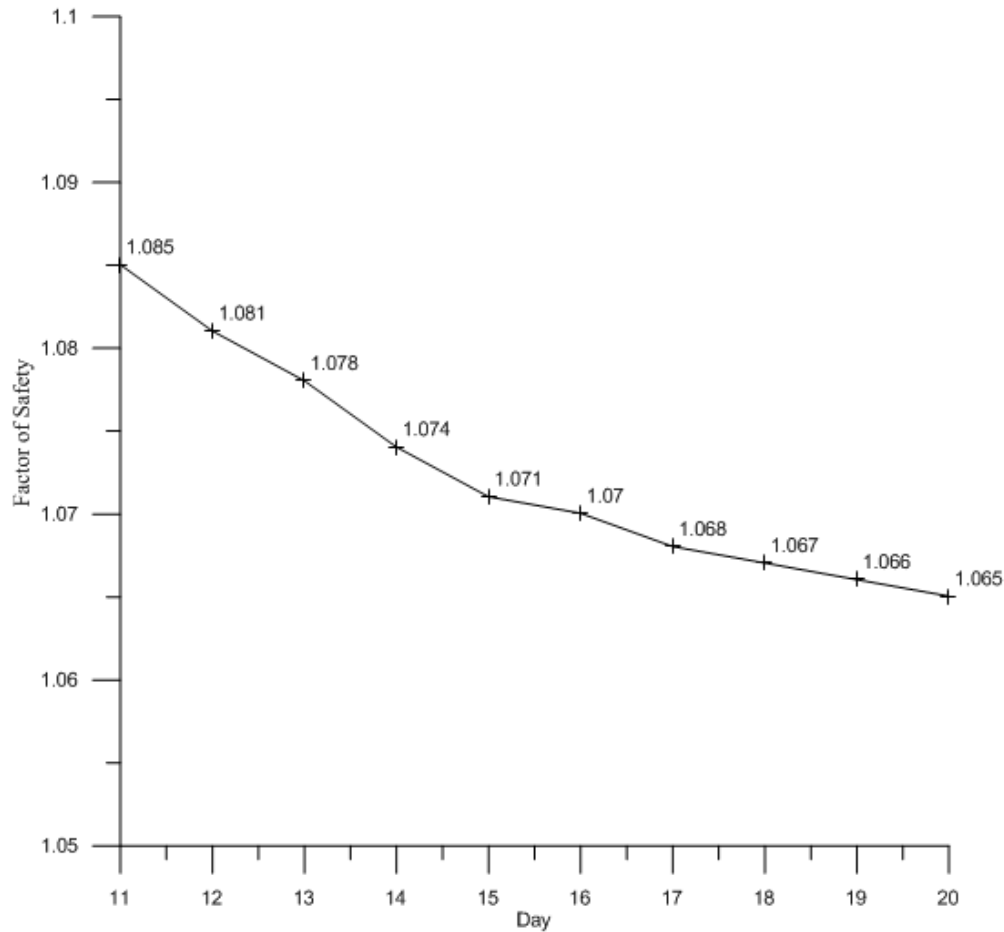


Figure 4-8 SLOPE/W third step results

From the above figure and table, it can be concluded that even if the water level stops rising, the factor of safety will continue to decrease, starting from 1.085 and gradually decreasing to 1.065. Combined with the results of SEEP/W, it can be concluded that water will continue to infiltrate into the slope. Therefore, it will continue to affect the safety of the bottom of the slope.

4.1.2.4 Final step results of SLOPE/W analysis

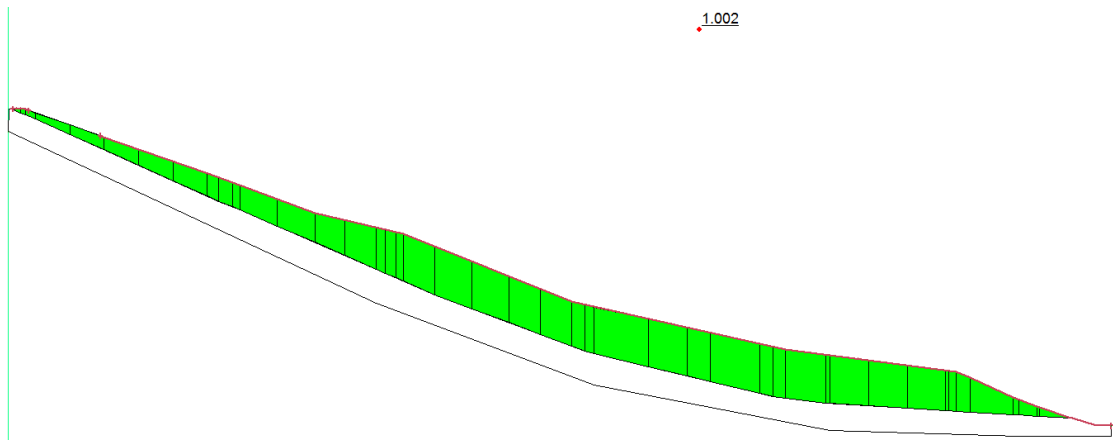


Figure 4-9 SLOPE/W final step results (day43)

Table 4-7 SLOPE/W final step results

Day	FS	Day	FS	Day	FS	Day	FS	Day	FS
21	1.065	26	1.062	31	1.059	36	1.021	41	1.004
22	1.064	27	1.062	32	1.057	37	1.019	42	1.003
23	1.064	28	1.062	33	1.055	38	1.016	43	1.002
24	1.063	29	1.062	34	1.049	39	1.016		
25	1.063	30	1.062	35	1.024	40	1.005		

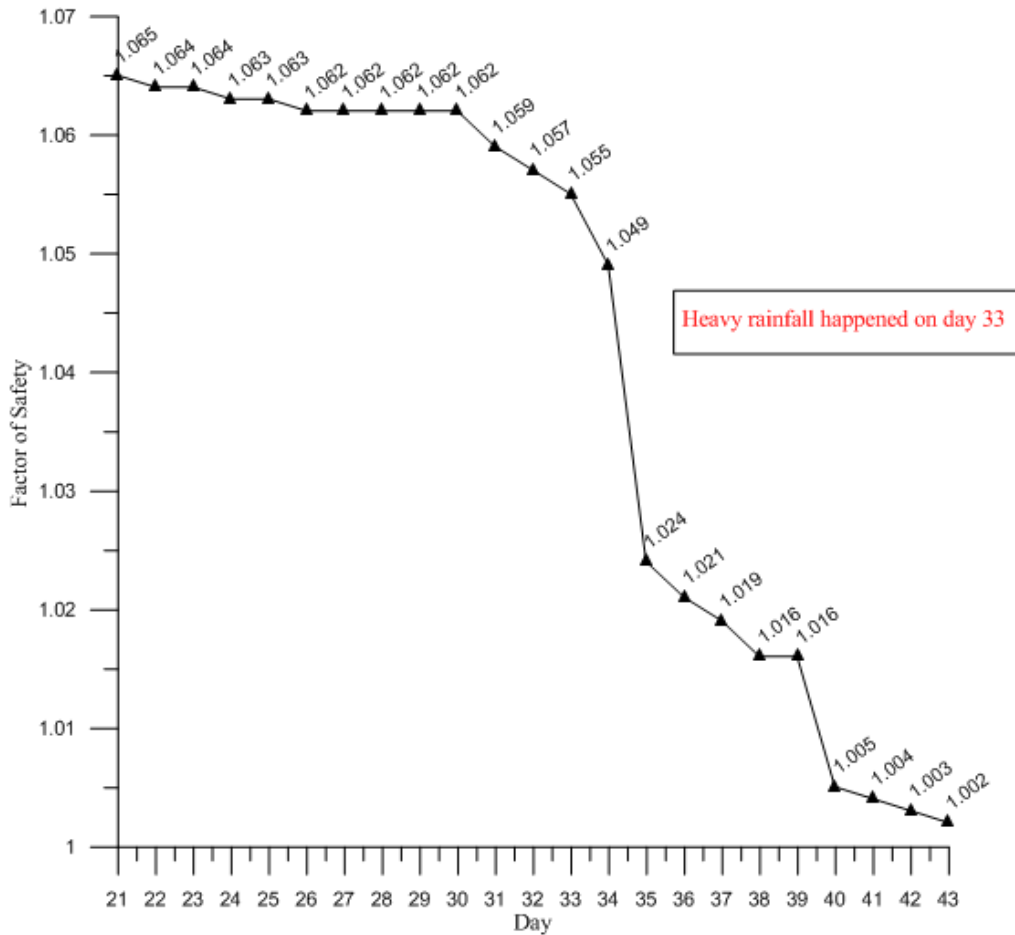


Figure 4-10 SLOPE/W final step results

The above figure and table list the daily factor of safety changes during the rainfall period. From the results, it can be found that the magnitude of its decline is greater. Therefore, it can be concluded that rainfall will have a greater impact on the FS of the slope. It can generate a certain range of saturation bands on the slope surface, and as the saturation band moves to the lower right, it will eventually reduce the FS to 1.002, leading to landslides. After completing the analysis of SEEP/W and SLOPE/W, the mechanism and process of its landslide were revealed. And to be able to check whether the settings of the model are correct, which helps in the next part of the analysis.

4.1.2.5 Summary for the results of SLOPE/W

Since the calculation of factor of safety considers the water pressure in SEEP / W, it can be concluded from the results of the numerical simulation that the change of pore water pressure will directly affect the slope stability, because the rise of pore water pressure will lead to the decrease of shear strength, which is the reason for the decrease of slope stability. In this study, the rise of pore water pressure is caused by two factors, including the rise of water level and continuous rainfall. The rise of reservoir water level controls the groundwater level in the lower part of the slope, while continuous rainfall affects the saturated zone on the surface of the shallow slope. Under the combined influence of the two factors, a landslide will eventually occur.

In slope / W analysis, the initial factor of safety of slope is calculated, which is 1.117. This is not a very safe value, because it is only an initial state and has not experienced the rise of water level and rainfall. Therefore, this reflects the safety problem of the slope itself. From the results of the second and third steps, it can be concluded that the FS is decreasing whether the water level continues to rise or remains constant. This is a reasonable result because the change of groundwater level will have a continuous impact on the bottom of the slope. In addition, the stability changes of the landslide in the next 23 days are listed. It can be seen that there is little change in the early stage, but with the emergence of the saturated zone, the FS begins to decrease. In the next few days, due to the heavy rain, the FS was greatly reduced. However, the water pressure may not be enough to cause sliding, so no landslide occurred. In addition, after a few days of rainfall, on the 43rd day, the FS dropped to the lowest, leading to the landslide. Compared with the actual situation, the simulation results are reasonable.

4.1.3 Discussion

In this part, some suggestions are given by combining the results of SEEP/W and SLOPE/W.

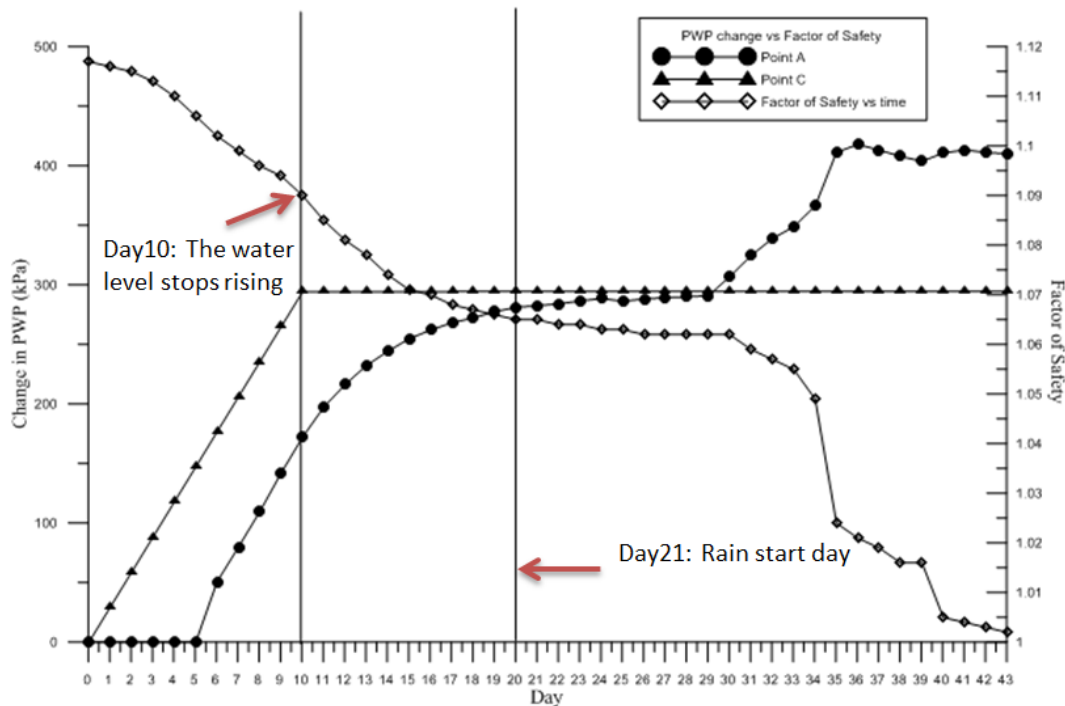


Figure 4-11 Amount of PWP change (Point A & C) vs Factor of safety

In the figure above, the PWP changes recorded by points A and C together with the factor of safety are listed. Through the integration of some data, it is concluded that the factor of safety decreased in the first ten days, which was mainly affected by the groundwater level above point C. As the water level rises, the PWP rate of change will be faster than that point A. In the following ten days, the factor of safety was affected by the slowly rising groundwater level above point A, which caused the PWP to increase at a faster rate. One suggestion that can be given in this section is that when carrying out the water storage work of the reservoir, it is not only necessary to pay attention to the PWP change of soil slope during the water storage period but also to pay attention to the change of the groundwater level after the water

storage work is completed. This is because the groundwater level far from the reservoir may still rise slowly.

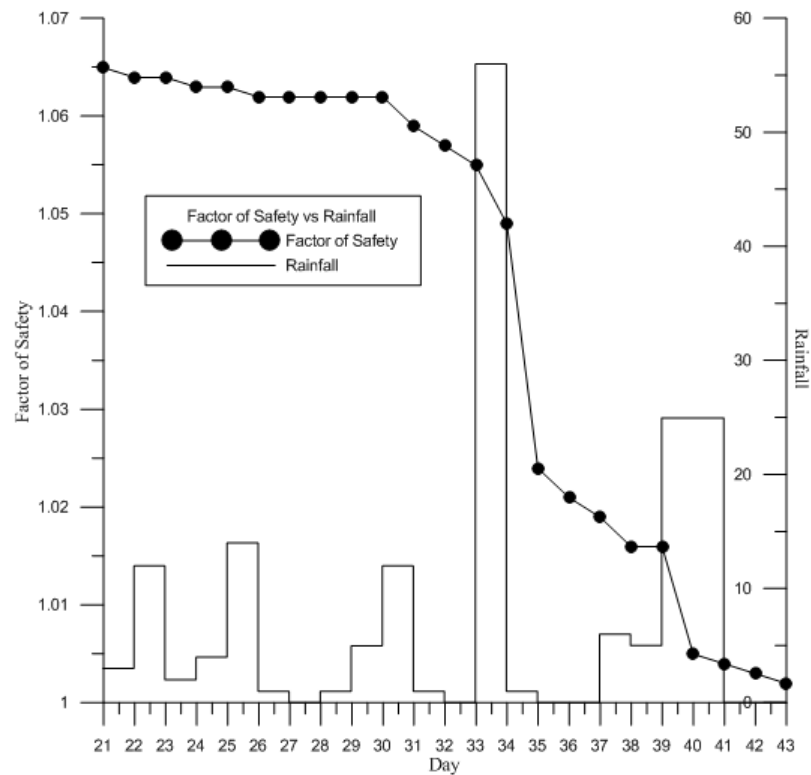


Figure 4-12 Rainfall vs Factor of safety over time

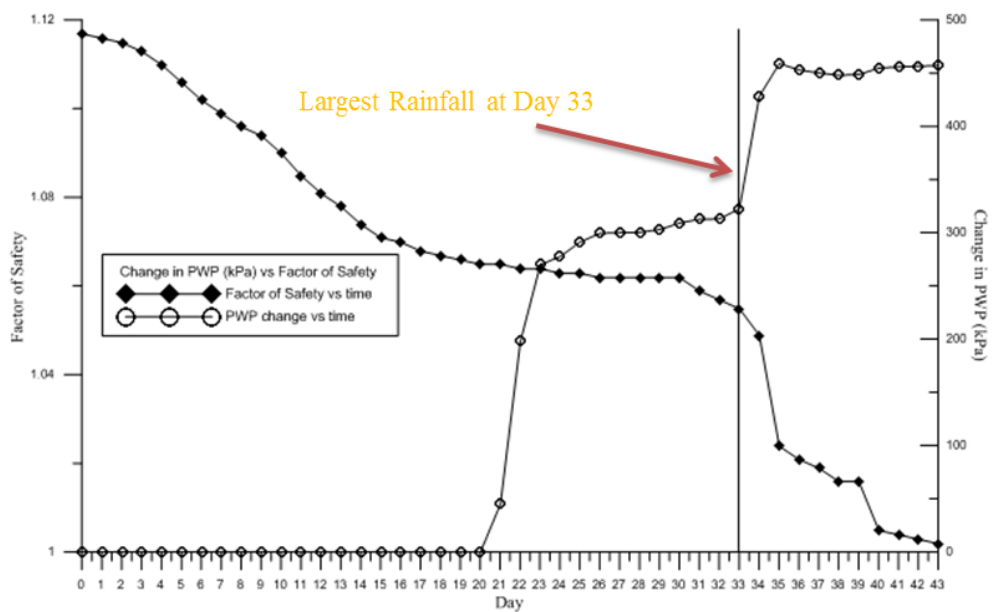


Figure 4-13 Amount of PWP change (Point B) vs Factor of safety over time

Two charts are listed above, namely the relationship between the factor of safety and amount of PWP change, and the relationship between the factor of safety and rainfall. The conclusion that can be drawn from these graphs is that on the day of heavy rainfall, the FS may not necessarily drop significantly. In this study, the significant drop in the FS occurred about two days after the occurrence of heavy rain. It can also be known from the analysis results of SEEP/W that after rainfall occurs, it takes time for rainwater to infiltrate into the soil, and the saturated zone formed by rainwater also takes some time to shift downwards. Therefore, in actual situations, when heavy rainfall occurs, it is necessary to pay close attention to the soil slope to avoid casualties caused by landslides.

4.2 Results for the second research purpose (rainfall patterns analysis)

In this chapter, the results of the second research objective will be listed, and it will be possible to know which of the four different rain patterns will have the greatest impact on Qianjiangping. The first three steps of the analysis process will be the same as the first part of the study, and only the fourth step will have a different rainfall situation. Due to the excessive number of results, only changes in accumulated rainfall and changes in FS will be listed. By comparing the differences between each set of data, summarize the impact of different rainfall patterns on slope stability.

4.2.1 Results for the pattern of “Delayed”

For the “Delayed” pattern, the value of rainfall will start from zero and the maximum value is 100mm. In this analysis, the duration of the study is nine days. Moreover, an additional 9 days will be used to monitor the change of the slope stability. As mentioned in Chapter 3, the first three steps remain unchanged. The

following figure will list the rainfall changes and accumulated rainfall of this pattern. And the results of SLOPE/W will be listed to observe the change of the factor of safety during the rainfall period so that the characteristics of this pattern can be summarized.

Table 4-8 Daily rainfall and accumulated rainfall for pattern “Delayed”

Day	Rainfall on that day (mm)	Accumulated rainfall(mm)
21	0	0
22	12.5	12.5
23	25	37.5
24	37.5	75
25	50	125
26	62.5	187.5
27	75	262.5
28	87.5	350
29	100	450

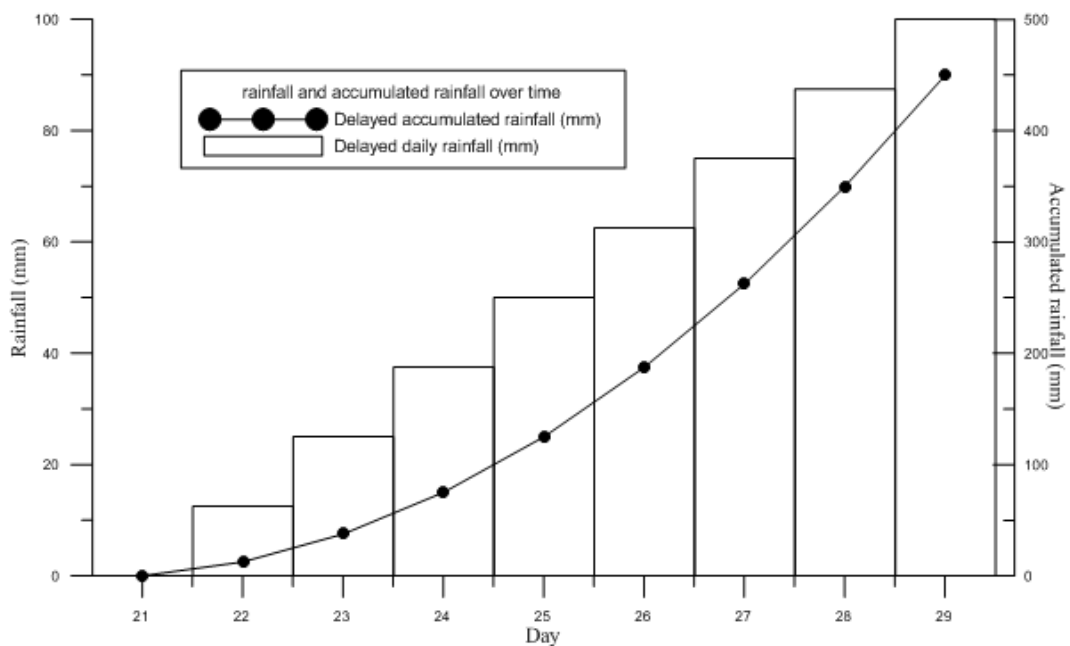


Figure 4-14 Daily rainfall and accumulated rainfall over time (Delayed)

Next, is the result of SLOPE/W:

Table 4-9 Factor of Safety results for rainfall pattern “Delayed”

DAY	FS	DAY	FS
21	1.065	30	1.01
22	1.06	31	0.999
23	1.059	32	0.991
24	1.058	33	0.988
25	1.055	34	0.985
26	1.037	35	0.986
27	1.033	36	0.987
28	1.03	37	0.989
29	1.023	38	0.99

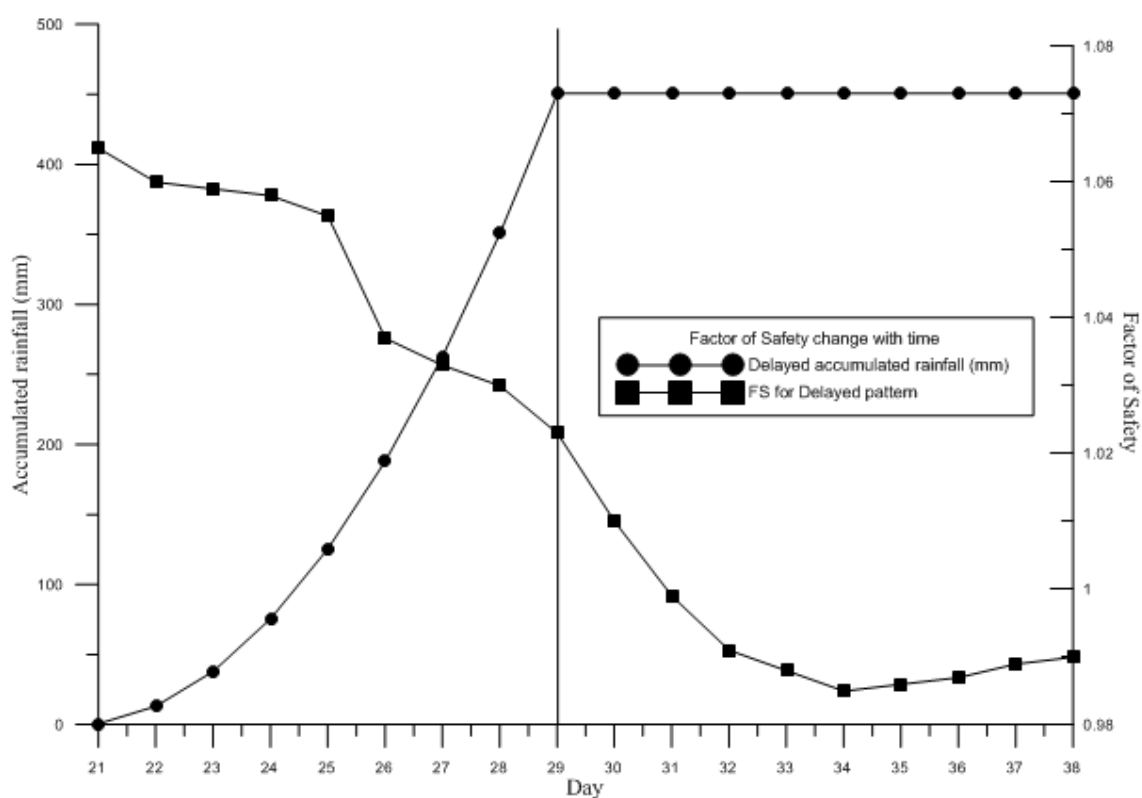


Figure 4-15 Accumulated rainfall verse factor of safety over time (Delayed)

Table 4-8 shows the daily rainfall and accumulated rainfall of the "delayed" pattern. From the results, the cumulative rainfall rate caused by this kind of rainfall

pattern is the slowest of the four, because the maximum rainfall occurs on the 29th day. Table 4-9 shows the results of the FS, which decreased from 1.065 to the lowest of 0.985. The results are also plotted in Figure 4-15. It can be concluded from the results that under the influence of this rainfall pattern, the slope will experience a landslide on the 31st day. The feature of this rainfall pattern is that the maximum rainfall occurs on the 29th day. As mentioned in the previous chapter, there is a delay in the effect of rainfall on slope stability. As a result, landslides occur two days after the end of heavy rainfall.

4.2.2 Results for the pattern of “Advanced”

For the "Advanced" pattern, the rainfall value will start from 100mm until it drops to zero. In this analysis, the duration of the study is nine days. After that, an additional 9 days will be used to observe the changes in the slope stability. As mentioned in Chapter 3, the first three steps remain unchanged. The following figure will list the rainfall changes and accumulated rainfall of this pattern. And the results of SLOPE/W will be listed to observe the change of the factor of safety during the rainfall period so that the characteristics of this pattern can be summarized.

Table 4-10 Daily rainfall and accumulated rainfall for pattern “Advanced”

Day	Rainfall on that day (mm)	Accumulated rainfall(mm)
21	100	100
22	87.5	187.500
23	75	262.500
24	62.5	325.000
25	50	375.000
26	37.5	412.500
27	25	437.500
28	12.5	450.000
29	0	450.000

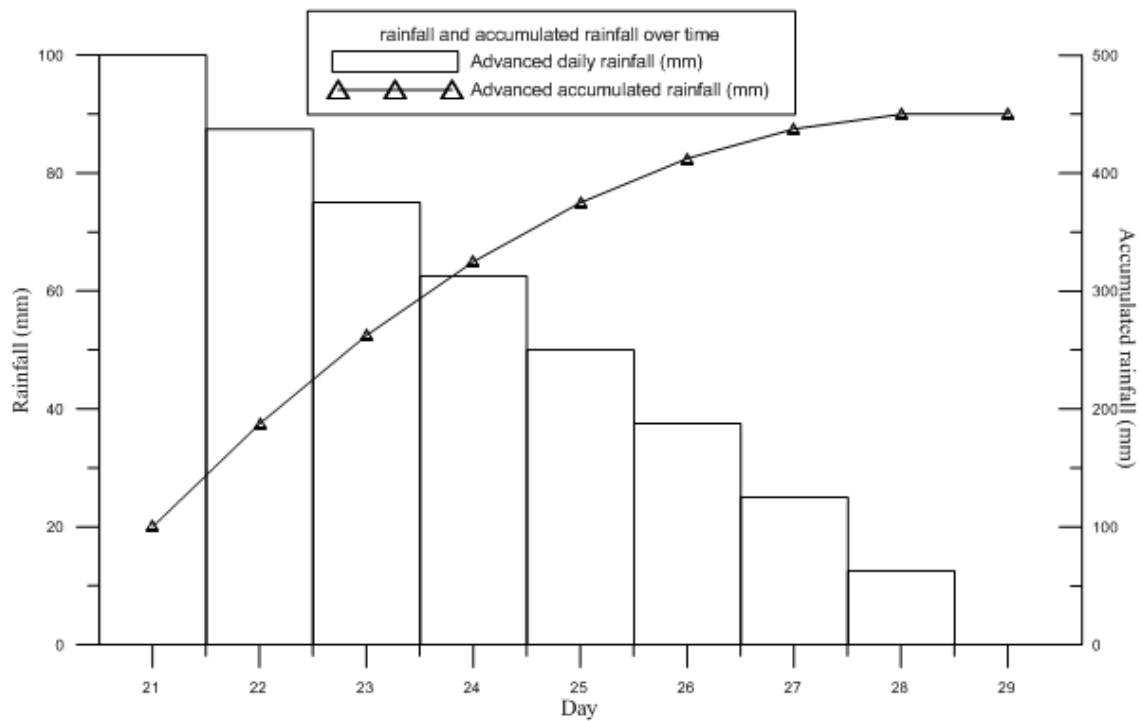


Figure 4-16 Daily rainfall and accumulated rainfall over time (Advanced)

Next, is the result of SLOPE/W:

Table 4-11 Factor of Safety results for rainfall pattern “Advanced”

DAY	FS	DAY	FS
21	1.065	30	0.999
22	1.043	31	1
23	1.022	32	1.001
24	1.01	33	1.001
25	0.998	34	1.002
26	0.993	35	1.002
27	0.992	36	1.002
28	0.993	37	1.003
29	0.998	38	1.003

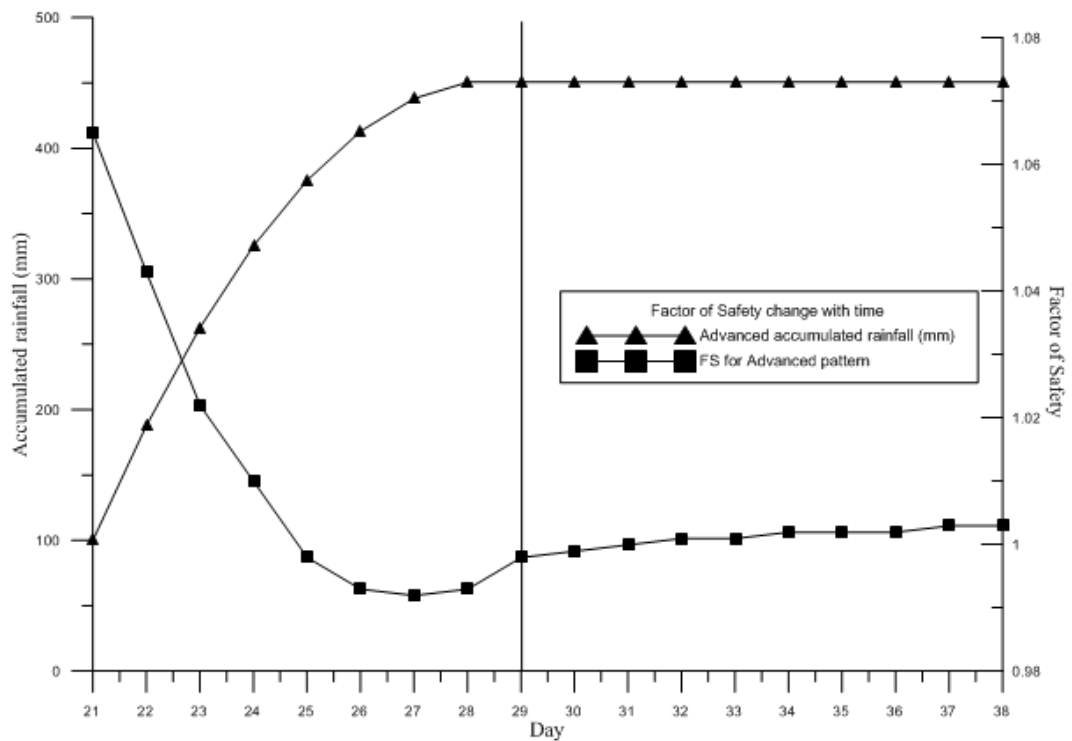


Figure 4-17 Accumulated rainfall verse factor of safety over time (Advanced)

Table 4-10 shows the daily rainfall and accumulated rainfall of the "advanced" pattern. From the results, the cumulative rainfall rate caused by this kind of rainfall pattern is the fastest of the four, because the largest rainfall occurs in the first few days. The results of the factor of safety are listed in Table 4-11. The coefficient decreases from 1.065 to the lowest of 0.992. The results are also plotted in Figure 4-17. It can be concluded from the results that under the influence of this rainfall pattern, the slope will experience a landslide on the 25th day. Because this rainfall pattern is characterized by the largest rainfall at the beginning, a large amount of rainfall will accumulate in the early stage, resulting in the rapid decline of FS.

4.2.3 Results for the pattern of “Uniform”

For the "Uniform" pattern, the rainfall value starts from the first day and will be 50mm until the end. In this analysis, the duration of the study is nine days. Moreover, an additional 9 days will be used to monitor the change of the slope stability. As mentioned in Chapter 3, the first three steps remain unchanged. The following figure will list the rainfall changes and accumulated rainfall of this pattern. And the results of SLOPE/W will be listed to observe the change of the factor of safety during the rainfall period so that the characteristics of this pattern can be summarized.

Table 4-12 Daily rainfall and accumulated rainfall for pattern “Uniform”

Day	Rainfall on that day (mm)	Accumulated rainfall(mm)
21	50	50
22	50	100
23	50	150
24	50	200
25	50	250
26	50	300
27	50	350
28	50	400
29	50	450

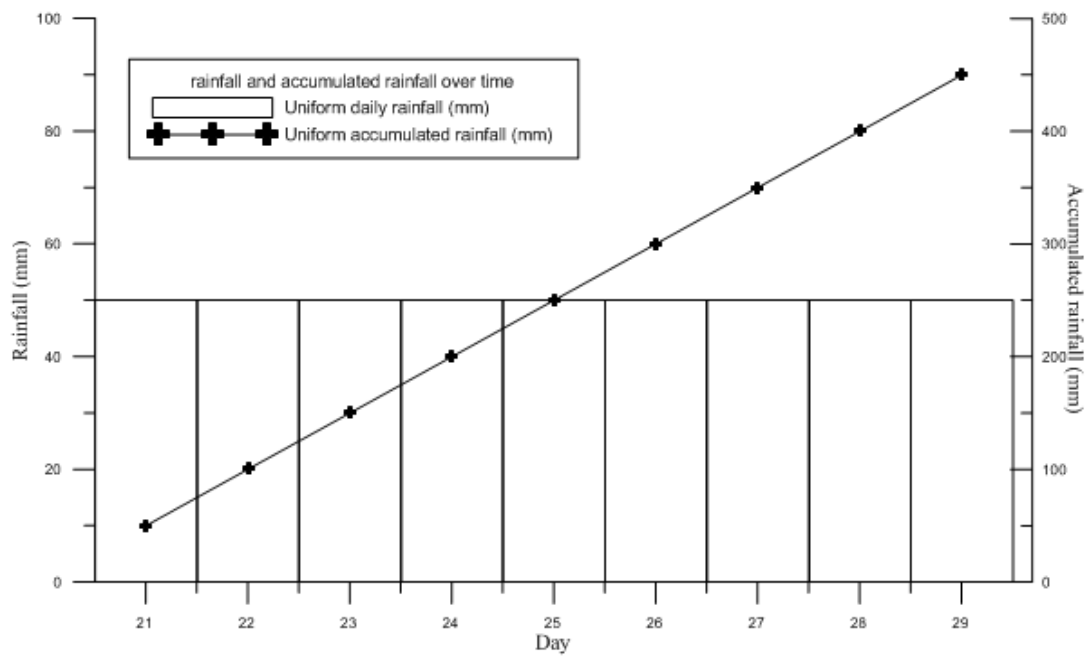


Figure 4-18 Daily rainfall and accumulated rainfall over time (Uniform)

Next, is the result of SLOPE/W:

Table 4-13 Factor of Safety results for rainfall pattern “Uniform”

DAY	FS	DAY	FS
21	1.065	30	0.988
22	1.05	31	0.988
23	1.039	32	0.991
24	1.023	33	0.993
25	1.01	34	0.995
26	1.004	35	0.995
27	0.998	36	0.998
28	0.992	37	0.998
29	0.99	38	0.999

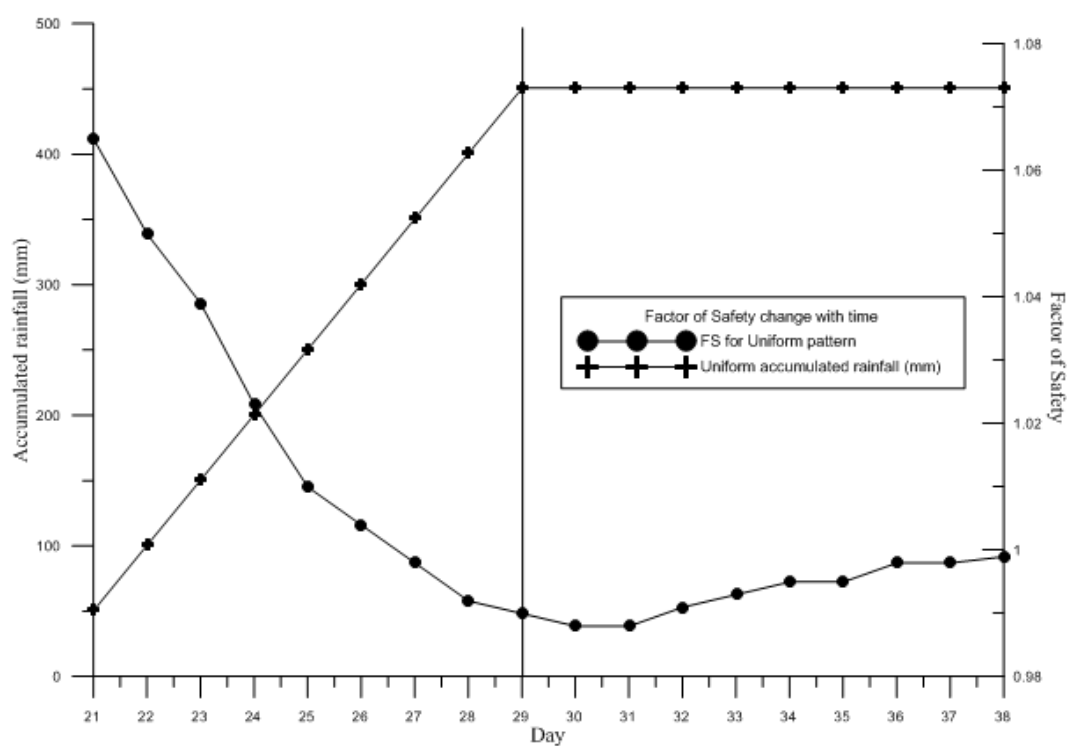


Figure 4-19 Accumulated rainfall verse factor of safety over time (Uniform)

Table 4-12 shows the daily rainfall and accumulated rainfall of the "uniform" pattern. From the results, the cumulative rainfall rate caused by this kind of rainfall pattern is the most average of the four, because the daily rainfall is the same. The results of the factor of safety are listed in Table 4-13. The coefficient decreases from 1.065 to the lowest of 0.988. The results are also plotted in Figure 4-19. Under the influence of this rainfall pattern, the slope will slide on the 27th day. Since this rainfall pattern is characterized by very average rainfall, the cumulative rainfall will increase linearly, and the factor of safety will decrease steadily.

4.2.4 Results for the pattern of “Normal”

For the "Normal" mode, the rainfall on the first day is 25mm, the rainfall on the last day is also 25mm, and the largest rainfall appears on the fifth day with a value of 100mm. In this analysis, the duration of the study is nine days. After that, an additional 9 days will be used to monitor the change of the slope stability. As mentioned in Chapter 3, the first three steps remain unchanged. The following figure will list the rainfall changes and accumulated rainfall of this pattern. And the results of SLOPE/W will be listed to observe the change of the factor of safety during the rainfall period so that the characteristics of this pattern can be summarized.

Table 4-14 Daily rainfall and accumulated rainfall for pattern “Normal”

Day	Rainfall on that day (mm)	Accumulated rainfall(mm)
21	25	25
22	25	50.000
23	50	100.000
24	75	175.000
25	100	275.000
26	75	350.000
27	50	400.000
28	25	425.000
29	25	450.000

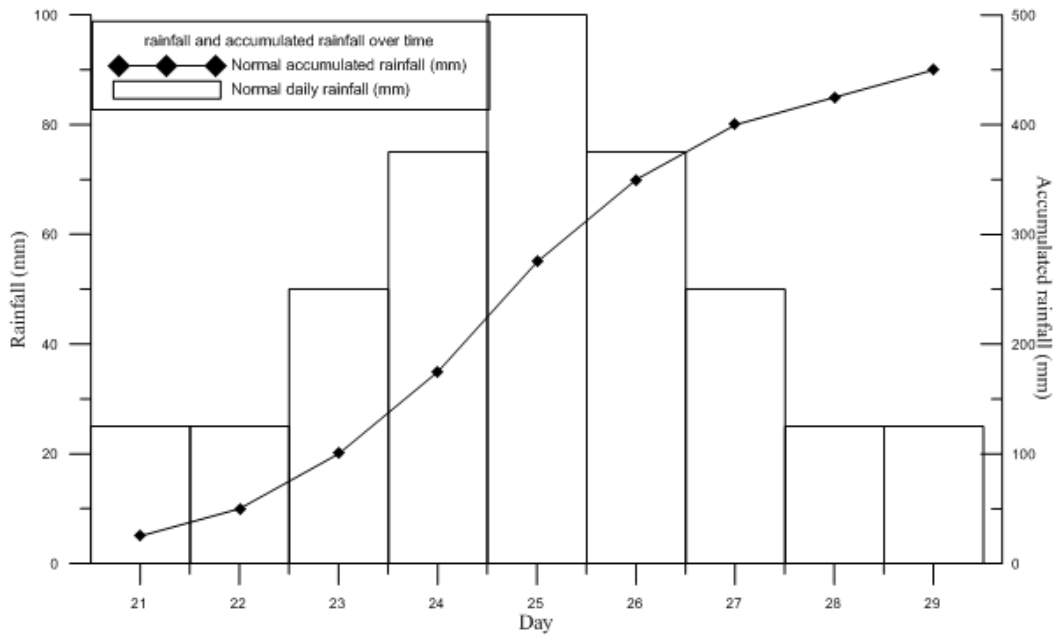


Figure 4-20 Daily rainfall and accumulated rainfall over time (Normal)

Next, is the result of SLOPE/W:

Table 4-15 Factor of Safety results for rainfall pattern “Normal”

DAY	FS	DAY	FS
21	1.065	30	0.984
22	1.06	31	0.984
23	1.06	32	0.985
24	1.023	33	0.987
25	1.012	34	0.99
26	1.006	35	0.991
27	0.999	36	0.993
28	0.99	37	0.993
29	0.985	38	0.995

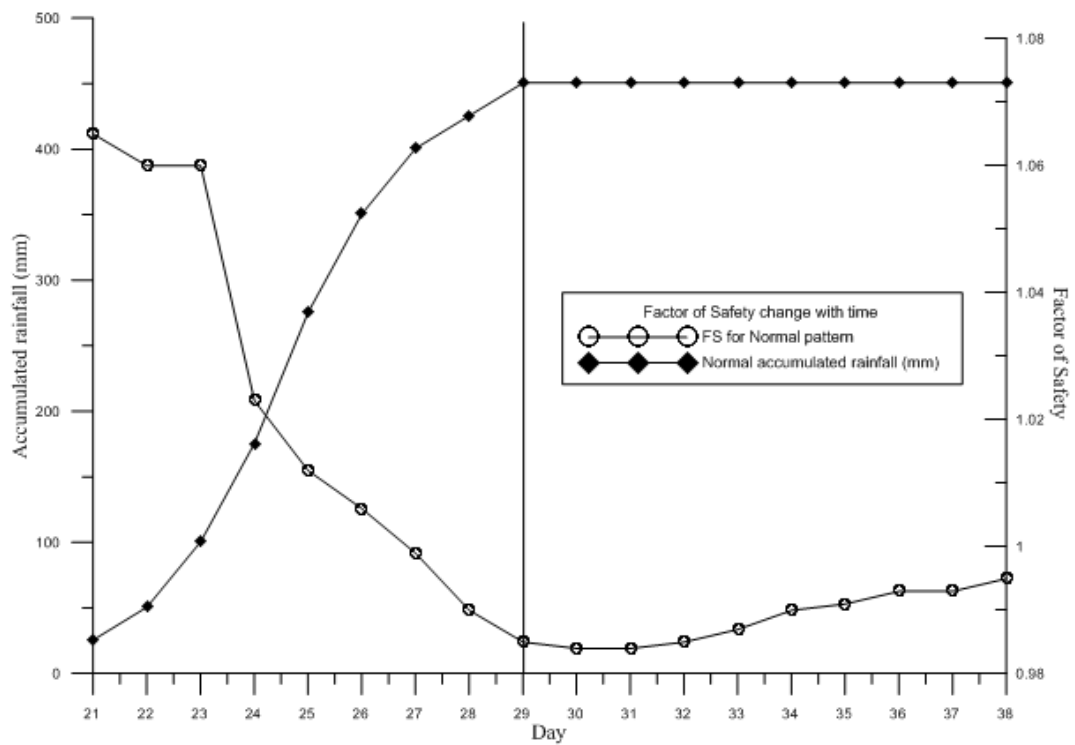


Figure 4-21 Accumulated rainfall verse factor of safety over time (Normal)

Table 4-14 shows the daily rainfall and accumulated rainfall of the "normal" pattern. From the results, the characteristic of this rainfall pattern is that the rainfall variation is very large. In addition to the beginning and end, the daily rainfall increment is the largest of the four rainfall patterns. The results of the factor of safety are listed in Table 4-15. The coefficient decreases from 1.065 to the lowest of 0.984. Under the influence of this rainfall pattern, the cumulative rainfall will increase in a curve. As a result, the factor of safety will vary greatly, and eventually, the slope will experience a landslide on day 27. This is a reasonable result because, after the 25th day, the soil slope can accumulate enough rainwater to cause a landslide.

4.2.5 Results summary

Table 4-16 Accumulated rainfall for four rainfall patterns

Day	Delayed	Advanced	Uniform	Normal
21	0	100	50	25
22	12.5	187.5	100	50
23	37.5	262.5	150	100
24	75	325	200	175
25	125	375	250	275
26	187.5	412.5	300	350
27	262.5	437.5	350	400
28	350	450	400	425
29	450	450	450	450

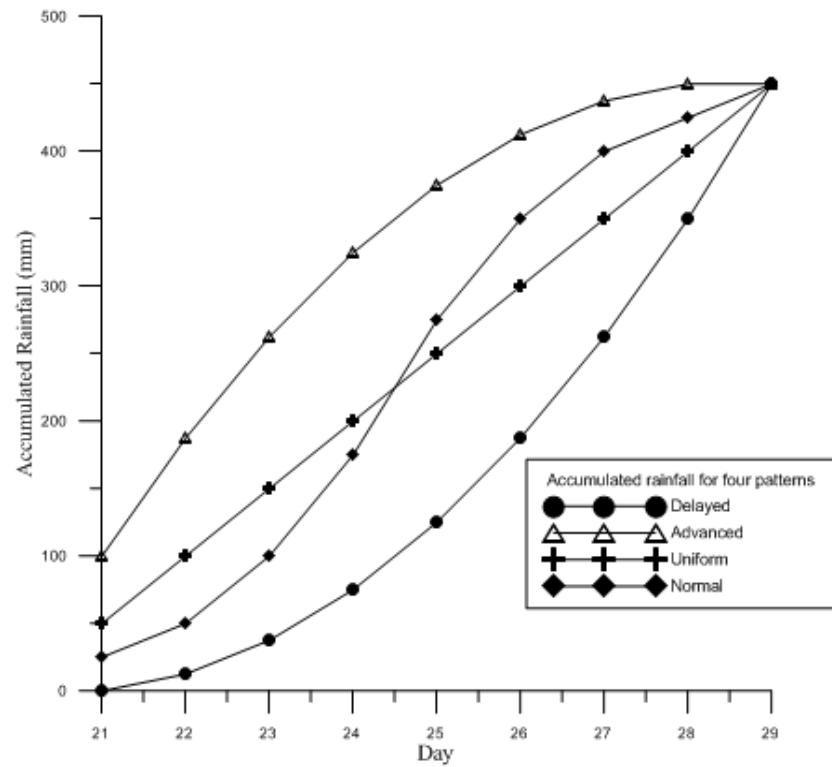


Figure 4-22 Accumulated rainfall for four patterns

Table 4-17 Factor of Safety results for four rainfall patterns

Day	Delayed	Advanced	Uniform	Normal
21	1.065	1.065	1.065	1.065
22	1.06	1.043	1.05	1.06
23	1.059	1.022	1.039	1.06
24	1.058	1.01	1.023	1.023
25	1.055	0.998	1.01	1.012
26	1.037	0.993	1.004	1.006
27	1.033	0.992	0.998	0.999
28	1.03	0.993	0.992	0.99
29	1.023	0.998	0.99	0.985
30	1.01	0.999	0.988	0.984
31	0.999	1	0.988	0.984
32	0.991	1.001	0.991	0.985
33	0.988	1.001	0.993	0.987
34	0.985	1.002	0.995	0.99
35	0.986	1.002	0.995	0.991
36	0.987	1.002	0.998	0.993
37	0.989	1.003	0.998	0.993
38	0.99	1.003	0.999	0.995

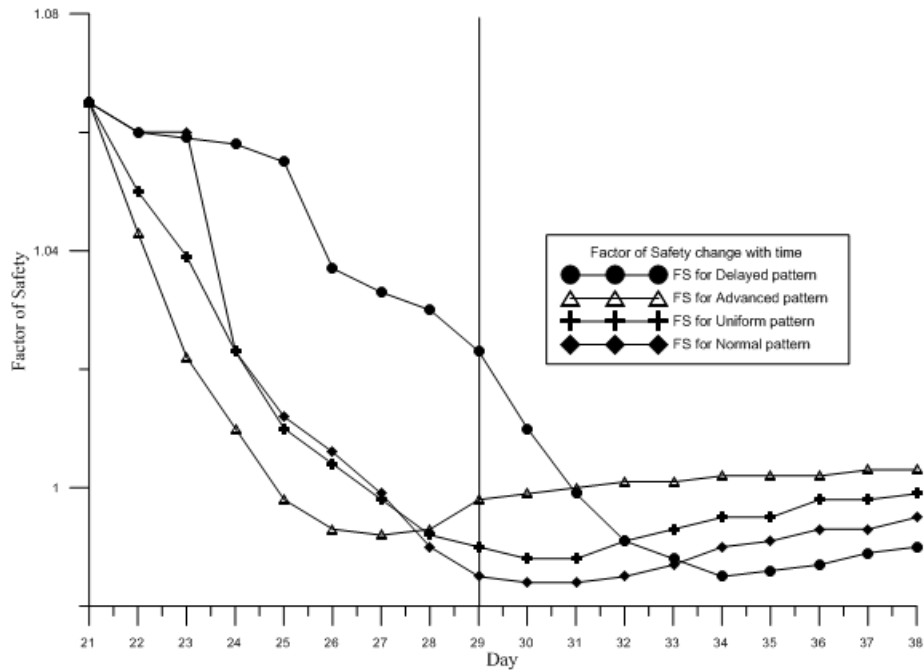


Figure 4-23 Factor of safety changes over time (for four rainfall patterns)

It can be seen from the above results that when the total amount of rainfall is the same, the simulation results of four different rainfall patterns will be very different. Because the characteristics of the four rainfall patterns are completely different, the increment of accumulated rainfall will be greatly different, although the final value is the same. For the "advanced" model, the factor of safety will be reduced more quickly due to the heavy rainfall accumulated in the early period. So, this is the fastest landslide of the four models. It can be expected that the rapid accumulation of rainfall will rapidly increase the pore water pressure, and the increase of pore water pressure will reduce the effective stress, thus reducing the shear strength. The "uniform" model and the "normal" model have a similar feature, and both will accumulate a larger amount of rainfall in the middle of the rainfall period. Therefore, the time of landslide is relatively close, and both occur in the later period of rainfall. For the "delayed" mode, this mode is more special among the four modes. This is the only rainfall pattern without landslide during rainfall, and the rainfall accumulation rate is the

slowest among the four rainfall patterns, which is the reason why landslide occurs after rainfall. Therefore, to sum up, even if the rainfall intensity is the same, different rainfall characteristics will bring different results.

4.3 Results for the third research purpose (rainfall intensity analysis)

In the above section, the effects of different rainfall patterns on slope stability are listed. These are based on the premise that the total amount of rainfall is equal so that their differences can be compared. The next thing to be studied is the influence of rainfall intensity on slope stability under the premise of a consistent rainfall pattern. In this study, the "Uniform" pattern is the subject of experimentation, because it is the most basic of all patterns and it is easier to control its changes. By increasing its daily rainfall from 50mm to 75mm and 100mm respectively, the difference between them can be compared. Similarly, after nine days of rainfall, nine more days will be added to observe the change. The following is the observation point D used in this section. The reason for choosing D is to observe the effect of increased rainfall. Since the rainfall intensity has increased by 50% and 100% respectively, the expected impact will be very obvious.

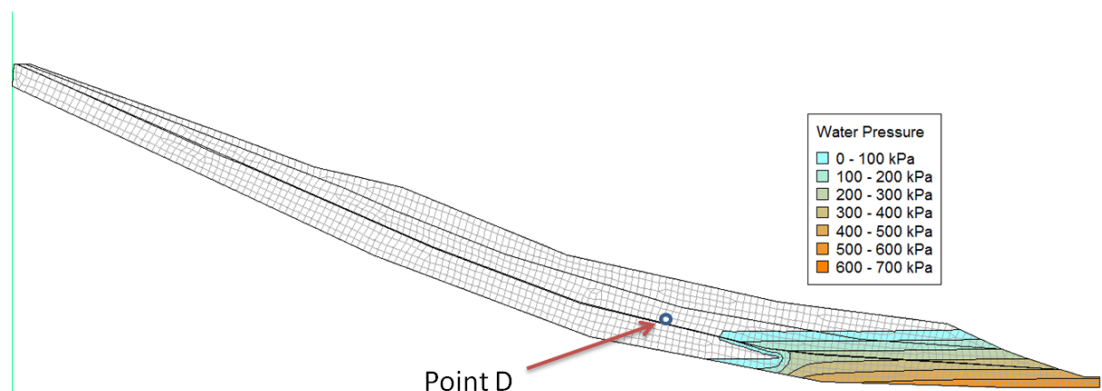


Figure 4-24 Location of observation points D

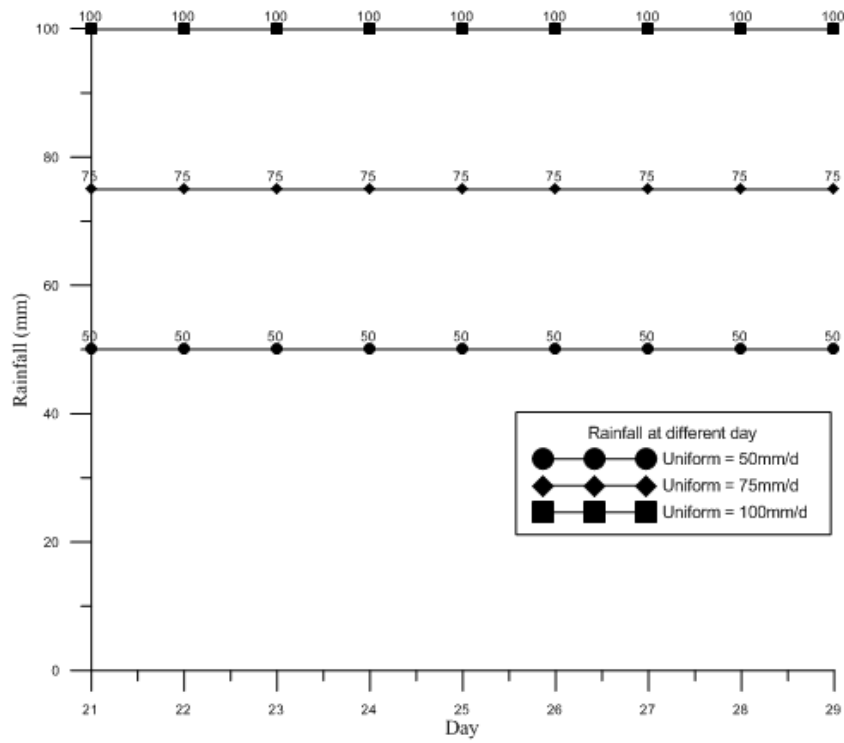


Figure 4-25 rainfall setting for rainfall intensity analysis

Results for rainfall intensity = 50mm/d:

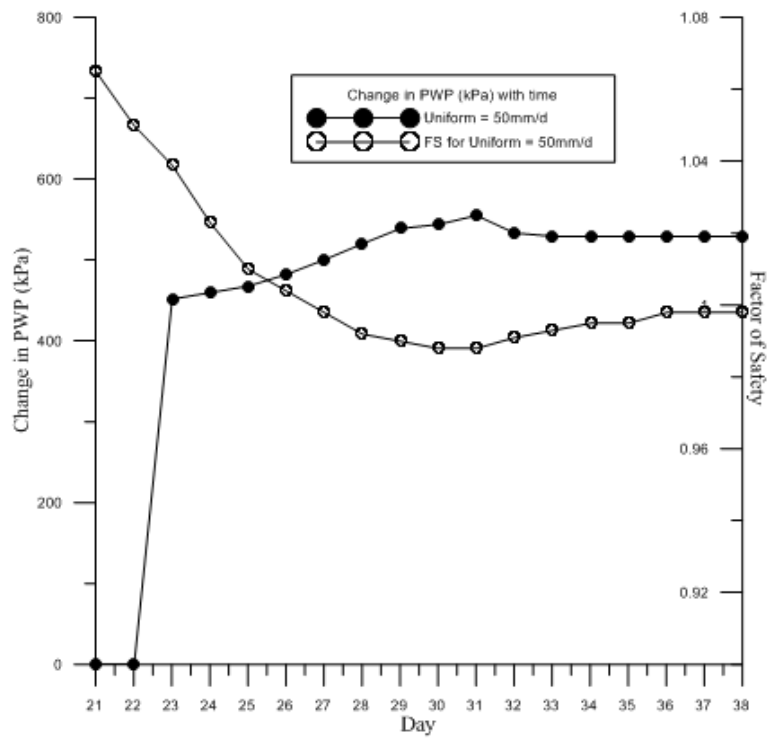


Figure 4-26 Amount of PWP change verse factor of safety for rainfall intensity = 50mm/d

Results for rainfall intensity = 75mm/d:

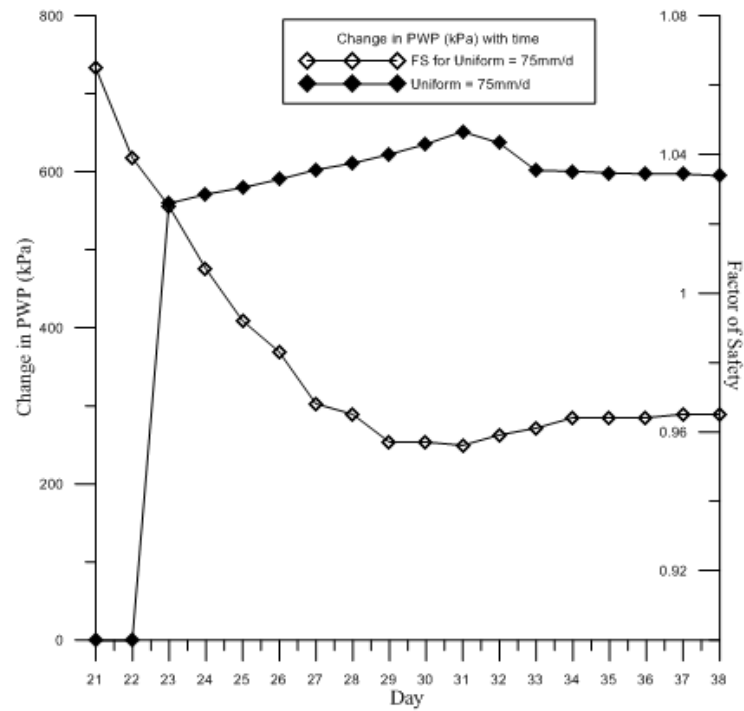


Figure 4-27 Amount of PWP change verse factor of safety for rainfall intensity = 75mm/d

Results for rainfall intensity = 100mm/d:

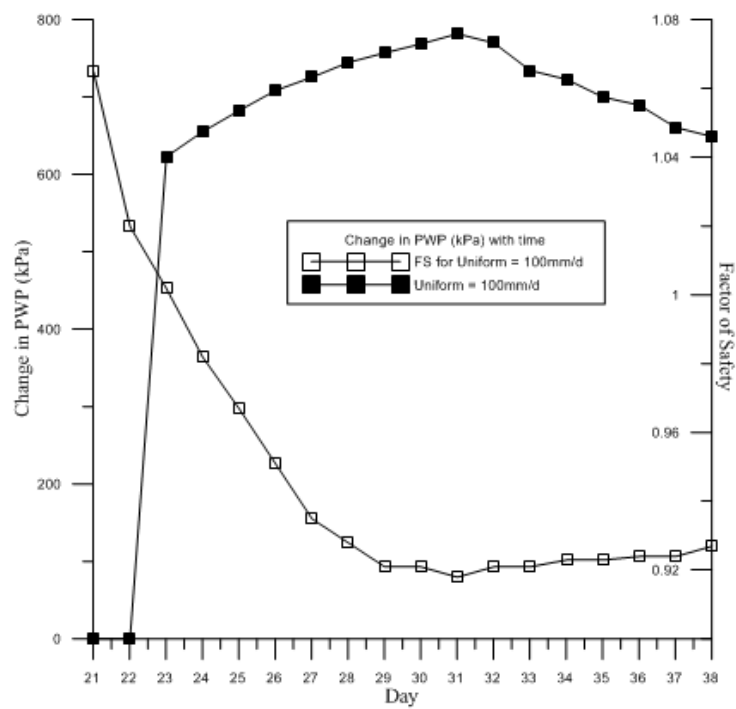


Figure 4-28 Amount of PWP change verse factor of safety for rainfall intensity = 100mm/d

From figure 4-26 to figure 4-28, it can be found that in addition to the increase of rainfall intensity, the upward trend of PWP will also increase, and the downward trend of factor of safety will also increase.

4.3.1 Results summary

Now let's integrate the data and results obtained in this section. The PWP changes brought by three different rainfall intensities will be combined to see the differences. Then there are the changes of factor of safety in three different situations.

Table 4-18 The PWP changes observed by point D for three rainfall conditions

Day	Uniform = 50mm	Uniform = 75mm	Uniform = 100mm
21	0	0	0
22	0	0	0
23	451.61034	560.5266	623.28703
24	459.465585	572.1643	655.72304
25	467.567848	580.638	682.88995
26	482.065161	591.3633	708.9005
27	500.1433465	603.5536	725.94556
28	519.814965	611.9657	745.15274
29	538.736781	623.3285	757.4361
30	543.698372	636.3484	769.17449
31	554.948271	652.54724	782.17516
32	533.167363	638.05369	770.42132
33	529.193931	602.72882	734.83695
34	528.799159	601.75198	723.27074
35	528.783577	599.54876	700.4439
36	528.778653	598.23692	689.9651
37	528.776782	598.21155	661.03648
38	528.776671	596.014459	649.37321

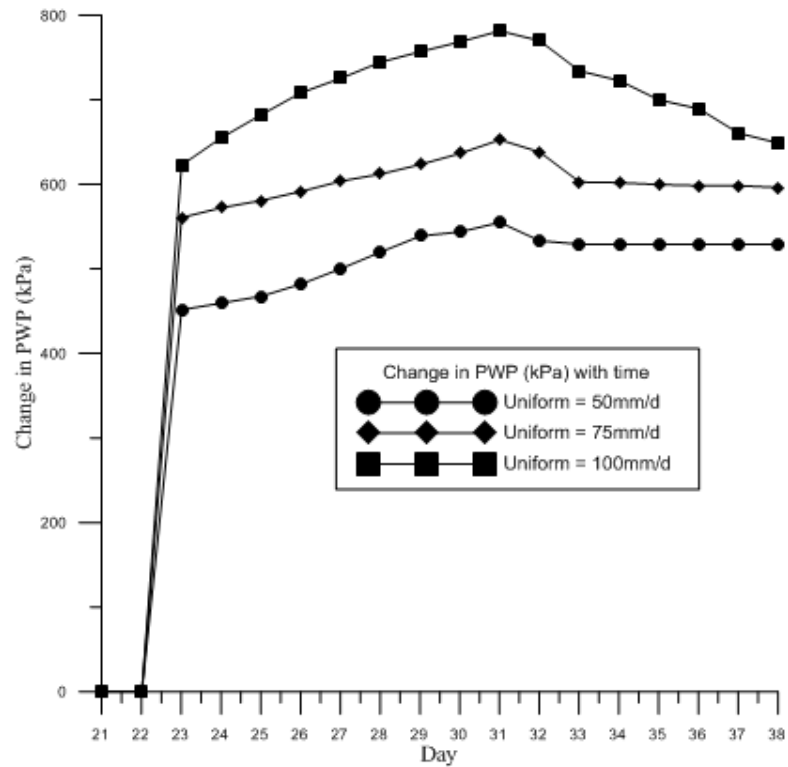


Figure 4-29 the change of PWP monitored by Point D over time

Table 4-19 Factor of Safety results for three rainfall conditions

Day	Uniform = 50mm	Uniform = 75mm	Uniform = 100mm
21	1.065	1.065	1.065
22	1.05	1.039	1.02
23	1.039	1.025	1.002
24	1.023	1.007	0.982
25	1.01	0.992	0.967
26	1.004	0.983	0.951
27	0.998	0.968	0.935
28	0.992	0.965	0.928
29	0.99	0.957	0.921
30	0.988	0.957	0.921
31	0.988	0.956	0.918
32	0.991	0.959	0.921
33	0.993	0.961	0.921
34	0.995	0.964	0.923
35	0.995	0.964	0.923
36	0.998	0.964	0.924
37	0.998	0.965	0.924
38	0.998	0.965	0.927

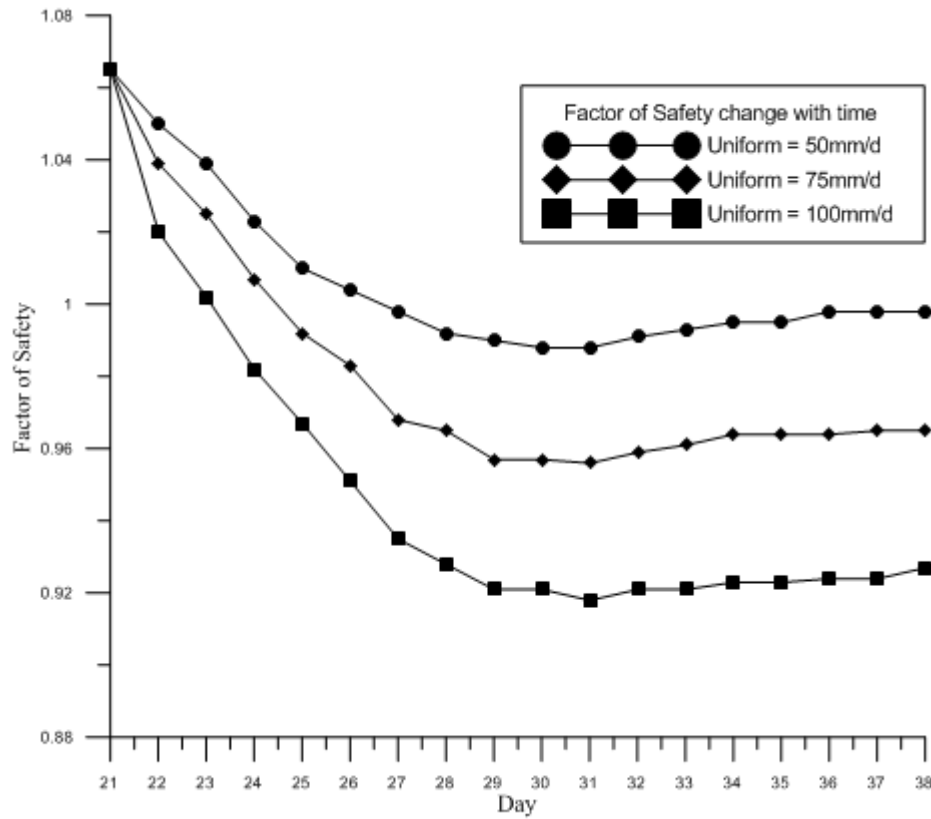


Figure 4-30 Factor of safety changes over time for three situations

The rainfall intensity has a significant impact on slope stability. In the three cases where the rainfall intensity is increasing, the result is that with the increase of the total amount of rainfall, the change of pore water pressure is also increasing. The rising trend of pore water pressure is very similar, but the rising range is different. This is a reasonable result because the increase in the amount of rainfall means that the amount of water infiltrated into the soil slope will increase. The rise of pore water pressure can directly affect the size of effective stress, and the size of effective stress can also control the shear strength of the soil. Therefore, the rise of pore water pressure means that slope stability is declining. Figure 4-30 summarizes the change of the factor of safety in three cases. It can be concluded that the greater the rainfall intensity, the greater the decline of the factor of safety.

It is worth mentioning that from Figure 4-29, it can be found that there is a very fast-rising trend of pore water pressure in the early stage of rainfall, which is a manifestation of the disappearance of suction. Because unsaturated soil is considered in the study, with the continuous infiltration of rainwater, the groundwater level will rise to the height of point D, and the matric suction at point D will disappear. Therefore, the rapid increase of pore water pressure in the early stage is caused by the disappearance of matric suction.

Chapter 5 CONCLUSION&FUTURE STUDY

5.1 Conclusion of this study

Through the simulation and analysis of Qianjiangping, it is verified that the landslide is mainly caused by the water storage of the Three Gorges Reservoir and continuous rainfall. The rise of the water level will increase the pore water pressure at the bottom of the slope. Theoretically, it will decrease the shear strength at the bottom of the slope, resulting in the decrease of the factor of safety.

The impact of rainfall can be divided into two parts: first, it will form a saturated zone on the slope surface; second, with the infiltration water slowly moving to the bottom of the slope, the groundwater level will rise. This process will increase the pore water pressure of the slope, and make the soil of slope surface gradually saturated, and the matric suction (negative pore water pressure) will also gradually decrease. Through this analysis also found that the impact of rainfall on slope stability is not immediate, because it takes some time for infiltration water to transfer to the bottom of the slope.

The results for four different rainfall patterns are also listed in Chapter 4.2. The characteristics of the four patterns are different, even under the same rainfall duration, rainfall intensity, and soil properties, the results are different. Since the accumulated rainfall of the "advanced" pattern is the fastest of the four patterns, it will be the fastest of the four patterns to landslide. For the "uniform" pattern and "normal" pattern, the cumulative rainfall rates of the two patterns are similar, but both are slightly slower than the "advanced" pattern. Therefore, the landslide time of the two rainfall patterns

will be slightly later. Finally, for the "delayed" pattern, the cumulative rainfall rate is the slowest of the four, so the time of landslide is also the latest.

Lastly, the study of rainfall intensity shows that rainfall intensity has an important influence on slope stability. The total amount of rainfall is directly proportional to the pore water pressure. In addition, higher rainfall will increase the decline of the factor of safety, because the increase of rainfall will increase the amount of water infiltrating into the soil slope, which will cause greater harm to the soil slope.

5.2 Future study

Due to the limited time, the analysis can only be done in this way, but I think it is very meaningful to carry out this type of analysis on the slope, which can give me a deeper understanding of the mechanism of landslide. If there is an opportunity to do this type of research in the future, I hope to collect more landslide data for analysis. Then, some mathematical methods (such as linear regression) can be used to establish a model to predict the occurrence of landslide. This type of research is very meaningful, because it can mathematically get the probability of landslide in a place and minimize the impact of landslide on people.

REFERENCES

- Atashband, S. (2015). Evaluate Reliability of Morgenstern–Price Method in Vertical Excavations. In S. Kadry & A. El Hami (Eds.), *Numerical Methods for Reliability and Safety Assessment: Multiscale and Multiphysics Systems* (pp. 529-547). Springer International Publishing.
https://doi.org/10.1007/978-3-319-07167-1_20
- Au, S. W. C. (1998). Rain-induced slope instability in Hong Kong. *Engineering Geology*, 51(1), 1-36.
[https://doi.org/https://doi.org/10.1016/S0013-7952\(98\)00038-6](https://doi.org/https://doi.org/10.1016/S0013-7952(98)00038-6)
- Chen, H., Lee, C. F., & Law, K. T. (2004). Causative Mechanisms of Rainfall-Induced Fill Slope Failures. *130*(6), 593-602.
[https://doi.org/doi:10.1061/\(ASCE\)1090-0241\(2004\)130:6\(593\)](https://doi.org/doi:10.1061/(ASCE)1090-0241(2004)130:6(593))
- Chen, R., Chen, H., Chen, K., & Zhung, H. J. E. g. (2009). Simulation of a slope failure induced by rainfall infiltration. *58*(5), 943-952.
- Collins, B. D., & Znidarcic, D. (2004). Stability Analyses of Rainfall Induced Landslides. *130*(4), 362-372.
[https://doi.org/doi:10.1061/\(ASCE\)1090-0241\(2004\)130:4\(362\)](https://doi.org/doi:10.1061/(ASCE)1090-0241(2004)130:4(362))
- Duncan, J. M. (1996). State of the Art: Limit Equilibrium and Finite-Element Analysis of Slopes. *122*(7), 577-596.
[https://doi.org/doi:10.1061/\(ASCE\)0733-9410\(1996\)122:7\(577\)](https://doi.org/doi:10.1061/(ASCE)0733-9410(1996)122:7(577))
- Duncan., J. M., Wright, S. G., & Brandon, T. L. (2014). *Soil Strength and Slope Stability*.
- Fredlund, D., & Xing, A. J. C. G. J. (1994). Equations for the soil-water characteristic curve. *31*, 521-532.
- Fredlund, D. G., & Rahardjo, H. (1993). *Soil mechanics for unsaturated soils*. John Wiley & Sons.
- Fredlund, D. G., Rahardjo, H., & Fredlund, M. D. (2012). Soil-Water Characteristic Curves for Unsaturated Soils. In *Unsaturated Soil Mechanics in Engineering Practice* (pp. 184-272).
<https://doi.org/https://doi.org/10.1002/9781118280492.ch5>

- Gerscovich, D. M. S., Vargas, E. A., & de Campos, T. M. P. (2006). On the evaluation of unsaturated flow in a natural slope in Rio de Janeiro, Brazil. *Engineering Geology*, 88(1-2), 23-40. <https://doi.org/10.1016/j.enggeo.2006.07.008>
- Griffiths, D. V., & Lane, P. A. (1999). Slope stability analysis by finite elements. 49(3), 387-403. <https://doi.org/10.1680/geot.1999.49.3.387>
- Hsu, Y.-C., & Liu, K.-F. (2019). Combining TRIGRS and DEBRIS-2D Models for the Simulation of a Rainfall Infiltration Induced Shallow Landslide and Subsequent Debris Flow. *Water*, 11(5). <https://doi.org/10.3390/w11050890>
- Jian, W., Xu, Q., Yang, H., & Wang, F. (2014). Mechanism and failure process of Qianjiangping landslide in the Three Gorges Reservoir, China. *Environmental Earth Sciences*, 72(8), 2999-3013. <https://doi.org/10.1007/s12665-014-3205-x>
- Jindal, P., Sharma, J., & Bashir, R. (2016). Effect of Pore-Water Surface Tension on Tensile Strength of Unsaturated Sand. *Indian Geotechnical Journal*, 46(3), 276-290. <https://doi.org/10.1007/s40098-016-0184-8>
- Krahn, J. (2003). The 2001 R.M. Hardy Lecture: The limits of limit equilibrium analyses. *Canadian Geotechnical Journal*, 40, 643-660. <https://doi.org/10.1139/t03-024>
- López-Acosta, N. P., & Mendoza-Promotor, J. A. (2016). Study of Unsaturated Soils by Coupled Numerical Analyses of Water Flow-Slope Stability.
- Li, N., Jiang, H., & Li, X. (2020). Behaviour of Capillary Barrier Covers Subjected to Rainfall with Different Patterns. 12(11), 3133. <https://www.mdpi.com/2073-4441/12/11/3133>
- Lim, T. T., Rahardjo, H., Chang, M. F., & Fredlund, D. G. (1996). Effect of rainfall on matric suctions in a residual soil slope. 33(4), 618-628. <https://doi.org/10.1139/t96-087>
- Mahmood, K., Kim, J. M., Ashraf, M., & Ziaurrehman. (2016). The effect of soil type on matric suction and stability of unsaturated slope under uniform rainfall. *KSCE Journal of Civil Engineering*, 20(4), 1294-1299. <https://doi.org/10.1007/s12205-015-0796-z>
- Mahmood, K., Ryu, J. H., & Kim, J. M. J. L. (2013). Effect of anisotropic conductivity on suction and reliability index of unsaturated slope exposed to uniform antecedent rainfall. 10(1), 15-22.

- Matsushi, Y., Hattanji, T., & Matsukura, Y. (2006). Mechanisms of shallow landslides on soil-mantled hillslopes with permeable and impermeable bedrocks in the Boso Peninsula, Japan. *Geomorphology*, 76(1), 92-108.
<https://doi.org/10.1016/j.geomorph.2005.10.003>
- Morgenstern, N. R., & Price, V. E. (1965). The Analysis of the Stability of General Slip Surfaces. *IS*(1), 79-93. <https://doi.org/10.1680/geot.1965.15.1.79>
- Ng, C. W. W., Shi, Q. J. C., & geotechnics. (1998). A numerical investigation of the stability of unsaturated soil slopes subjected to transient seepage. 22(1), 1-28.
- Potts, D. M., & Zdravković, L. (2001). *Finite Element Analysis in Geotechnical Engineering: Volume two - Application*. <https://doi.org/10.1680/feaigea.27831>
- Rahardjo, H., Kim, Y., & Satyanaga, A. (2019). Role of unsaturated soil mechanics in geotechnical engineering. *International Journal of Geo-Engineering*, 10(1), 8.
<https://doi.org/10.1186/s40703-019-0104-8>
- Rahardjo, H., Satyanaga, A., & Leong, E.-C. (2013). Effects of flux boundary conditions on pore-water pressure distribution in slope. *Engineering Geology*, 165, 133-142. <https://doi.org/10.1016/j.enggeo.2012.03.017>
- Richards, L. A. (1931). CAPILLARY CONDUCTION OF LIQUIDS THROUGH POROUS MEDIUMS. *I*(5), 318-333. <https://doi.org/10.1063/1.1745010>
- Sidle, R. C., Pearce, A. J., & O'Loughlin, C. L. (1985). *Hillslope stability and land use*. American geophysical union.
- Terzaghi, K. v. (1943). Stress Conditions for Failure in Soils. In *Theoretical Soil Mechanics* (pp. 7-25). <https://doi.org/10.1002/9780470172766.ch2>
- Terzaghi, K., Peck, R. B., & Mesri, G. (1996). *Soil mechanics in engineering practice*. John Wiley & Sons.
- Tsao, T. M., Wang, M. K., Chen, M. C., Takeuchi, Y., Matsuura, S., & Ochiai, H. (2005). A case study of the pore water pressure fluctuation on the slip surface using horizontal borehole works on drainage well. *Engineering Geology*, 78(1), 105-118. <https://doi.org/10.1016/j.enggeo.2004.11.002>
- Vanapalli, S. (2009). *Shear strength of unsaturated soils and its applications in geotechnical engineering practice*.
- Wang, F.-W., Zhang, Y.-M., Huo, Z.-T., Matsumoto, T., & Huang, B.-L. (2004). The July 14, 2003 Qianjiangping landslide, Three Gorges Reservoir, China. *Landslides*, 1(2), 157-162. <https://doi.org/10.1007/s10346-004-0020-6>

- Wang, F., Zhang, Y., Huo, Z., Peng, X., Wang, S., & Yamasaki, S. (2008). Mechanism for the rapid motion of the Qianjiangping landslide during reactivation by the first impoundment of the Three Gorges Dam reservoir, China. *Landslides*, 5, 379-386. <https://doi.org/10.1007/s10346-008-0130-7>
- Wu, L. Z., Xu, Q., & Zhu, J. D. (2017). Incorporating hydro-mechanical coupling in an analysis of the effects of rainfall patterns on unsaturated soil slope stability. *Arabian Journal of Geosciences*, 10(17), 386. <https://doi.org/10.1007/s12517-017-3147-1>
- Yeh, H.-F., Lee, C.-C., & Lee, C.-H. J. S. E. R. (2008). A rainfall-infiltration model for unsaturated soil slope stability. *18*(2), 271-278.
- Zhang, J., Li, J., & Lin, H. (2018). Models and influencing factors of the delay phenomenon for rainfall on slope stability. *European Journal of Environmental and Civil Engineering*, 22(1), 122-136. <https://doi.org/10.1080/19648189.2016.1179682>
- Zhang, L. L., Zhang, J., Zhang, L. M., & Tang, W. H. (2011). Stability analysis of rainfall-induced slope failure: a review. *164*(5), 299-316. <https://doi.org/10.1680/geng.2011.164.5.299>
- Zhang, M., Yin, Y., & Huang, B. (2015). Mechanisms of rainfall-induced landslides in gently inclined red beds in the eastern Sichuan Basin, SW China. *Landslides*, 12(5), 973-983. <https://doi.org/10.1007/s10346-015-0611-4>
- Zhu, J.-H., & Anderson, S. A. (1998). Determination of shear strength of Hawaiian residual soil subjected to rainfall-induced landslides. *48*(1), 73-82. <https://doi.org/10.1680/geot.1998.48.1.73>